Genetic Dissection of Flagellar Motility and Chemotaxis, and Their Roles in the Squid-Vibrio Symbiosis

By

Caitlin A. Brennan

A dissertation submitted in partial fulfillment

of the requirements for the degree of

Doctor of Philosophy

(Microbiology)

at the

University of Wisconsin-Madison

Spring 2013

Date of final oral examination: 12/13/12

The dissertation is approved by the following members of the Final Oral Committee:

Edward G. Ruby, Professor, Medical Microbiology and Immunology
Margaret J. McFall-Ngai, Professor, Medical Microbiology and Immunology
Rodney A. Welch, Professor, Medical Microbiology and Immunology
Heidi Goodrich-Blair, Professor, Bacteriology
Amy O. Charkowski, Associate Professor, Plant Pathology

Dedication

To the many people who helped me over the years, in ways both big and small- I could never name you all. While it is inconceivably rude to exclude any of you, I must especially dedicate this thesis to:

Ned,

and my family, though I'm still not convinced you know what I've spent all these years studying.

GENETIC DISSECTION OF FLAGELLAR MOTILITY AND CHEMOTAXIS, AND THEIR ROLES IN THE SQUID-VIBRIO SYMBIOSIS

Caitlin A. Brennan

Under the Supervision of Professor Edward G. Ruby

Vibrio fischeri is a Gram-negative, bioluminescent marine bacterium found both free-living and associated with the light organs of several species of fishes and squids. The symbiosis between *V. fischeri* and the Hawaiian bobtail squid, *Euprymna scolopes*, begins anew with each newly hatched juvenile squid. Symbionts from the surrounding seawater form mucus-bound aggregates on the light-organ surface, and then migrate to deep epithelium-lined crypts. Flagellar motility is essential for this symbiotic initiation, while chemotaxis mediates efficient colonization by *V. fischeri*. However, these important behaviors are poorly defined in *V. fischeri*. Using both forward and reverse genetic approaches, we first dissected the genetic basis of these behaviors, including the identification of novel motility-associated genes and the investigation of putative flagellar-gene paralogs. Using complementary genetic and imaging techniques, we then characterized the physical and chemical cues to which *V. fischeri* responds during migration into the light-organ crypts to understand the roles of both in symbiotic initiation. Models of natural initiation are under-represented in studies of host-microbe interactions, so the complexity observed during

initiation of the squid-vibrio symbiosis informs a greater understanding of the mechanisms by which microbes colonize a host.

To better grasp how *V. fischeri* senses and responds to the environment presented by the host, we sought to clarify the complex chemotactic repertoire of *V. fischeri*. We identified the ligands for two chemoreceptors: VfcA, which mediates chemotaxis towards amino acids; and VfcB, which senses several sugars, including chitobiose, a chitin-breakdown product found in the host environment. This study also defines a novel approach to determine the ligands sensed by chemoreceptors that can be applied across bacterial species.

The flagella of *V. fischeri*, as well as several important human pathogens, are encased in a membranous sheath of unknown function. Our work identified a novel role for the sheathed flagellum in the release of lipopolysaccharide, an immunogenic molecule, into the surrounding environment upon flagellar rotation. We demonstrated that this shed lipopolysaccharide was required for induction of host epithelial apoptosis. This phenomenon also informs the study of pathogenic bacteria with sheathed flagella, and opens new avenues of research into the biophysics of sheathed flagellar function.

Acknowledgments

This thesis would never have been possible without the contributions of a veritable army of people who have helped me both scientifically and personally. First of all, I thank Ned, who defies classification, for the innumerable roles he has assumed over the past years. As a mentor, he has served as a sounding board, an inspiration, and only an occasional damper, allowing me to explore topics as I saw fit. I can only hope to have lived up to his expectations. On a personal level, he has been everything from a 'landlord' to a (again, only occasional, I hope) shoulder to cry on.

Scientifically, I must thank my labmates, both past and present, who have shared this experience with me and always provided a lending hand or a listening ear when needed. I cannot name them individually, as every single person who has passed through both the Ruby and McFall-Ngai labs has left his mark on my work. I would also like to thank each of the members of my committee for helping to shape my scientific training. Several collaborators, including Sandy Parkinson and Run-zhi Lai at the University of Utah, Mike Apicella and Jason Hunt at the University of Utah, Morgan Beeby at Imperial College London, Shin-Ichi Aizawa at the Prefectural University of Hiroshima, and Cindy DeLoney-Marino at the University of Southern Indiana, were instrumental in the work performed as part of this thesis. None of the work could have been done without either the grants provided by the NIH and NSF or the administrative support of the MDTP and MMI offices. Many thanks to you all.

Personally, I must thank my family for their support and patience. I finally thank my friends, scientists and those with 'real jobs' alike, who have made the time fly, as much as 7+ years can. Regardless, it would not have been the same experience without any of them.

Table of Contents

List of Figures

Chapter 1

Chapter 2

Chapter 3

Chapter 4

Chapter 5

Chapter 6

Appendix B

List of Tables

Chapter 2

Chapter 3

Chapter 4

Chapter 1

General Introduction and Thesis Outline

PREFACE:

CAB formulated ideas and wrote the chapter.

"No man is an island,

Entire of itself.

Each is a piece of the continent,

A part of the main."

-John Donne, Meditation XVII, 1624

No known organisms exist in isolation. As used within this thesis and defined by Heinrich Anton de Bary in 1879, a symbiosis is an intimate association between two distinct organisms. The word implies neither negative nor positive effect on either partner and, instead, we view symbioses as falling along a continuum between purely parasitic and mutually beneficial associations. Microbial symbioses, in which the host is a eukaryotic organism and the symbiont is a microorganism, are ubiquitous in nature. While pathogenic associations are often given greater consideration by the scientific community and general populace alike, the importance of studying beneficial host-microbe interactions is rapidly being recognized, both for their ability to inform our understanding of pathogenesis and because of their biological importance in their own right.

SYMBIOTIC INITIATION:

The most important stage in any symbiotic association is symbiont acquisition, without which the host and microbe would be forced to exist as independent organisms. In the vast majority of microbial symbioses, horizontally-transmitted symbionts are taken up anew from the environment by each generation of host (Bright and Bulgheresi, 2010). While occurring in far fewer associations, symbionts can also be passed from parent to offspring via vertical transmission; as such, the symbiotic association is usually permanent within a familial line. Horizontal transmission is not only the predominant mode of symbiont acquisition across microbial symbioses, it is also the exclusive method used by human pathogens. Understanding how microbes initiate associations with eukaryotic hosts, therefore, is key to the study of symbiosis.

Mechanisms of natural initiation are best characterized in plant symbioses, such as the mutualism between legumes and nitrogen-fixing rhizobia. These symbioses serve as well-developed initiation models because of both the depth of research available on these long-studied associations and the relative ease of visualizing the site of symbiotic colonization. In fact, the rhizobium-legume symbiosis was the first host-microbe association in which fluorescently-labeled bacteria were used to directly observe symbiotic initiation (Gage *et al.*, 1996). These tools were used to characterize the early initiation events of this symbiosis, in which infection-thread entry serves as a bottleneck that limits the number of initiating bacterial cells (Gage, 2002). Beyond plant-microbes symbioses, models of symbiotic initiation have been largely informed by the characterization of invertebrate associations.

Like plant-microbe associations, many of these models are amenable to the visualization of symbiotic colonization with minimal disruption to the natural colonization route (Dulla *et al.*, 2012, Murfin *et al.*, 2012, Nyholm *et al.*, 2000). Indeed, such models have been successfully used to not only describe the route of symbiotic initiation, but also characterize the bacterial behaviors mediating distinct stages within this process.

While of greatest interest to human health, vertebrate models of initiation have proved difficult to characterize to the same level of detail as invertebrate and plant symbioses. There are two simple reasons for this discrepancy. First, and perhaps most obviously, these associations largely occur within the body cavity of opaque organisms. It would be unrealistic to expect to visualize colonization of the vertebrate gut tract through the body of a living mouse, for example, in the same manner as one could observe the gut tract of a nematode. However, techniques to circumvent this basic problem, such as whole body bioluminescence imaging in live mice (Baban *et al.*, 2012), are being developed. Second, many models of vertebrate-microbe symbiosis are experimentally initiated by methods that bypass the natural colonization route, instead opting for technically simpler and more reproducible approaches. For example, one of the models used in *Vibrio cholerae* research, the removable intestinal tie-adult rabbit diarrhea (RITARD) (Spira *et al.*, 1981), directly injects *V. cholerae* cells into a partially-resected section of the small intestine. Such an inoculation method likely masks the role that bacterial behaviors play in locating their symbiotic niche. Indeed, the impact of such behaviors, like motility, on symbiotic colonization varies greatly when assayed in models that utilize different inoculation methods (Richardson, 1991). This criticism is not to say these systems do not have merit in the study

of symbiosis; rather, that the acknowledgement of the strengths and limitations of different models best enables our understanding of symbiosis. As such, mechanisms of initiation in animal-microbe symbioses are currently best addressed using invertebrate models.

One of the first steps of symbiotic initiation is for the symbiont to correctly localize in the symbiotic niche, which is frequently distinct from the site of first contact between the host and symbiont. This localization can be largely passive by the symbiont, mediated by host behaviors such as gut peristalsis. Alternatively, bacterial symbionts can actively locate the site of symbiotic colonization using behaviors like flagellar motility, twitching motility, and chemotaxis (Dulla *et al.*, 2012). Upon arrival at the symbiotic niche, symbionts sense and respond to their new environment, undergoing transcriptional changes that are often mediated by two-component regulatory systems and quorum sensing (Fass and Groisman, 2009, Pirhonen *et al.*, 1993). Because of the intimate nature of symbiosis, symbionts usually physically interact with their partner by adhering to host surfaces. Frequently, this interaction is between the symbiont and the host extracellular matrix, but it can also occur directly between the bacterial and host cells. In the case of intracellular symbionts, adherence is followed by invasion of the host cell.

The behaviors of flagellar motility and chemotaxis are implicated in each of these themes underlying symbiotic initiation. Indeed, within the unique environments present in different host-microbe associations, both flagellar motility and the flagellum itself mediate symbiotic initiation by functioning in bacterial transit, effector secretion, biofilm formation, host recognition, and gene regulation (Butler and Camilli, 2004, Hayashi *et al.*, 2001, Lemon *et al.*, 2007, Liu *et al.*, 2008, Young *et al.*, 1999). The related behavior of chemotaxis also

plays a role in many host-microbe associations, both by enabling niche specificity and by preventing localization in harsh or otherwise undesirable tissue (Burall *et al.*, 2004, Butler *et al.*, 2006, Foynes *et al.*, 2000, Jones *et al.*, 1992, Stecher *et al.*, 2004). Flagellar motility and chemotaxis have been implicated, to different degrees, in myriad symbioses: the squid-vibrio mutualism (Graf *et al.*, 1994); *V. cholerae* pathogenesis (Richardson, 1991); uropathogenic *Escherichia coli* colonization of the bladder and kidneys (Lane *et al*., 2005, Wright *et al*., 2005); and the *Pseudomonas aeruginosa*-gnotobiotic zebrafish model (Rawls *et al.*, 2007), to name only a small number.

Despite the importance of these behaviors across symbioses, the specific stages at which chemotaxis and flagellar motility mediate colonization are not yet well characterized in any of these bacterium-animal interactions, because of the limitations of symbiotic initiation models discussed previously. As many of the mechanisms of symbiotic initiation are conserved both across model systems and between pathogenic and mutualistic associations, characterization of these behaviors in the squid-vibrio system would serve to inform general principles.

INITIATION OF THE SQUID-VIBRIO MUTUALISM:

Vibrio fischeri, a bioluminescent marine bacterium, is found both free-living and associated with the light-emitting organs of several species of fishes and squids. The best-characterized of these symbioses is its monospecific association with the Hawaiian bobtail squid, *Euprymna scolopes*. In this mutualism, *V. fischeri* colonizes a dedicated light organ in the squid (Figure 1-1A), where it is provided with nutrition in the form of amino acids, glycerol, and chitin sugars by the host, thereby enabling bacterial growth to densities much greater than those obtained in seawater (Graf and Ruby, 1998, Wier *et al.*, 2010). In exchange, the bioluminescence of the symbiont is harnessed by the host and used in counter-illumination, a camouflaging mechanism (Jones and Nishiguchi, 2004).

Colonization is a sequential process in which the bacteria initiate the association, accommodate to the light-organ environment, and persist for the lifetime of the squid. As a horizontally acquired symbiont, *V. fischeri* cells must be acquired from the surrounding seawater by each newly hatched juvenile squid. Ventilation of the squid mantle cavity passes *V. fischeri*-laden seawater across the light-organ surface, where bacteria aggregate in host-derived mucus suspended between the ciliated appendages (Figure 1-1B) (Nyholm *et al.*, 2002). After pausing in the mucus for approximately 2 hours, aggregates migrate to the pores of the light organ, through narrow ducts, and across antechambers, before finally accessing the deep crypts, where the cells will reside for the duration of the symbiosis (Nyholm *et al.*, 2000). Despite the short distance between the appendages and the deep crypts (less than 100 μm), this initiation process is both complex and highly specific. Initiation is restricted to

motile *V. fischeri* cells, at the exclusion of essentially all other species of bacteria (Nyholm *et al.*, 2000). Beyond niche localization, symbiotic initiation is also characterized by a complex molecular dialogue between *V. fischeri* and host cells. Recognition of bacterial products, such as lipopolysaccharide (LPS) and peptidoglycan (Foster *et al.*, 2000, Koropatnick *et al.*, 2004), by host cells modifies the light-organ environment, most notably by activating a morphogenetic program that results in regression of the ciliated light-organ appendages (Doino and McFall-Ngai, 1995, Montgomery and McFall-Ngai, 1994). This regression is posited to restrict secondary colonization.

Flagellar biosynthesis by *V. fischeri,* and its subsequent use for motility, are essential for the initiation process (Graf *et al.*, 1994, Millikan and Ruby, 2003) and implicated in migration from the mucus-bound aggregates to the pore (Nyholm *et al.*, 2000). Other studies have shown that alterations to motility, by both increasing and decreasing motility rates, result in defects in the initiation kinetics (Millikan and Ruby, 2002, Millikan and Ruby, 2004). While the role of chemotaxis in initiation is less characterized, a mutant disrupted in the chemotaxis response regulator CheY is defective in competition with wild-type *V. fischeri* (Hussa *et al.*, 2007). Over the course of my dissertation, two studies further elucidated the role of chemotaxis in initiation: chemotaxis provides a substantial advantage in competitive colonization and host-derived chitin breakdown products serve as a specific chemotactic signal during initiation (DeLoney-Marino and Visick, 2012, Mandel *et al*., 2012).

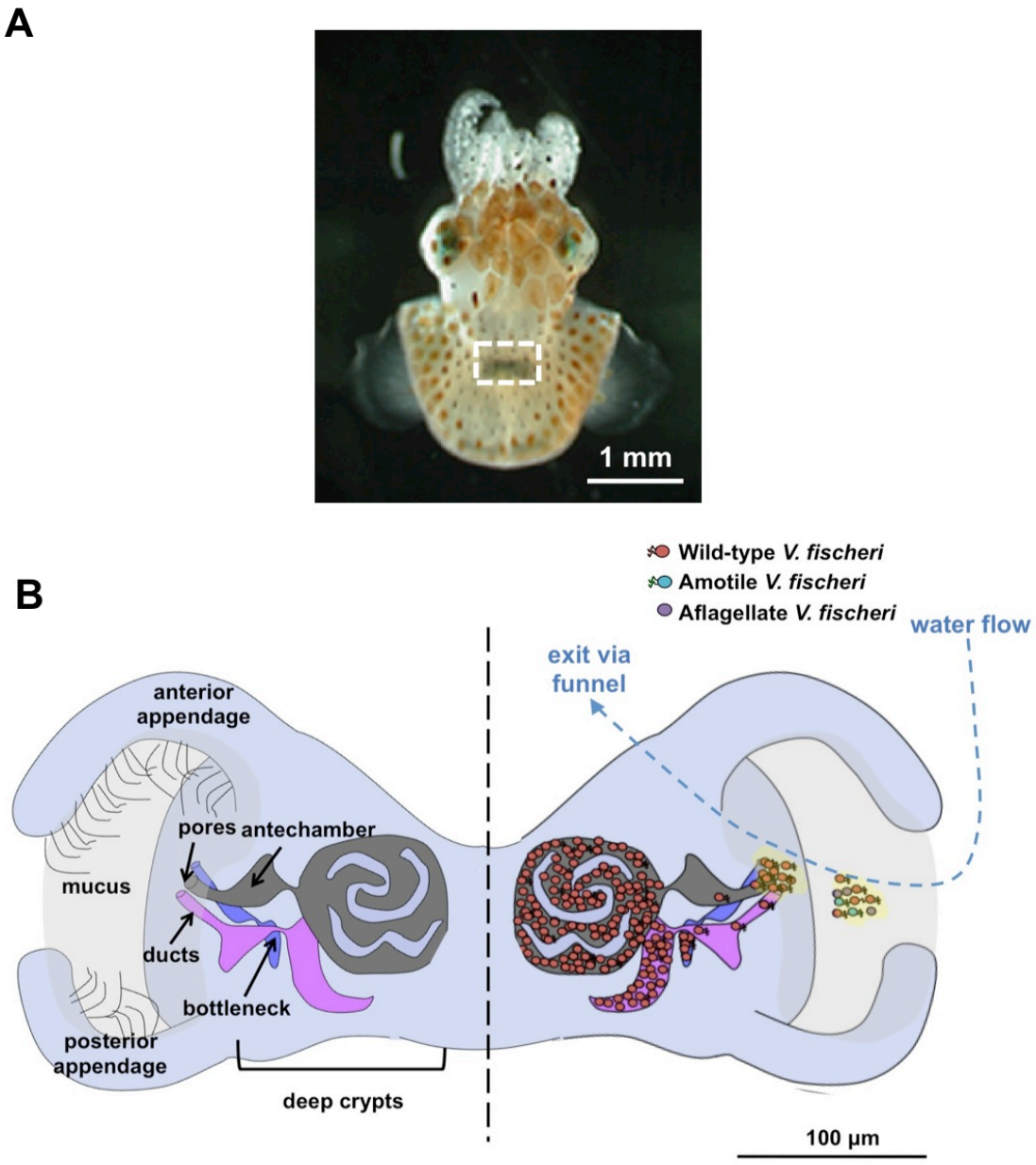

Figure 1-1. The juvenile light organ.

(A) A juvenile squid. White box indicates the location of the light organ.

(B) Cartoon of a juvenile light organ. The left lobe provides an orientation to the light organ. The right lobes models the path of symbiotic initiation, adapted from Nyholm and McFall Ngai, 2004, as understood at the beginning of my graduate tenure.

TOOLS TO STUDY FLAGELLAR MOTILITY IN THE SQUID-VIBRIO MUTUALISM:

Over the past 25 years, the squid-vibrio research community has generated many tools by which to study the roles of the flagellum and flagellar motility, both in culture and throughout the development and persistence of the symbiosis. Genomic tools are available for the study of both partners, including genome sequences for multiple *V. fischeri* strains and an expressed sequence tag (EST) database consisting of 14,000 unique open reading frames has been compiled from cDNA libraries of juvenile light-organ mRNA obtained under 5 distinct conditions (newly hatched, 12-h aposymbiotic and symbiotic, and 48-h aposymbiotic and symbiotic) (Chun *et al.*, 2006, Gyllborg *et al.*, 2012, Mandel *et al.*, 2008, Mandel *et al.*, 2009, Ruby *et al.*, 2005). Glass slide microarrays of squid open reading frames (Chun *et al.*, 2008)and Affymetrix chip arrays of the 3,800 genes of *V. fischeri* (Antunes *et al.*, 2007, Lupp and Ruby, 2005) enable transcriptional profiling of both partners. *V. fischeri* is also genetically tractable and plasmid-based constructs have been generated for a variety of uses (Dunn *et al.*, 2006). In culture, bacterial motility and its regulation can be addressed using many approaches, including transcriptional and western blotting analyses, negative-stain transmission electron microscopy, phase-contrast microscopy and soft-agar-based motility and chemotaxis assays.

To investigate the roles of flagellar motility and chemotaxis in symbiosis, we can use multiple assays that have been developed to study different aspects of the squid-vibrio mutualism. First, the standard assay through which the development of the squid-vibrio

association can be followed begins by exposing groups of symbiont-free juvenile squid to seawater containing wild-type or mutant strains of *V. fischeri*, either individually or in pairs. The luminescence of the squid, which can be continuously monitored, is an indication of the onset and level of colonization (Millikan and Ruby, 2002). The number of symbionts colonizing the squid can be determined directly by plating light-organ homogenates and counting the colonies that arise (Ruby and Asato, 1993). Multiple strains, differentiated by antibiotic resistance or another phenotypic characteristic, can be directly competed in this assay by adding more than one strain to the seawater with the aposymbiotic squid. Further, because candidate signal molecules or other agents added to seawater will diffuse through the light-organ pores and into the crypt spaces, the symbiosis is continuously accessible to experimental manipulation. To study chemotaxis, putative chemoattractants can be added to the seawater to block any gradient that may be sensed by the bacteria (Mandel *et al.*, 2012). The developmental stages of the symbiosis have been defined through anatomical, morphological, transcriptional and proteomic studies, identifying several aspects of host development under symbiont control (Foster *et al.*, 2000, Koropatnick *et al.*, 2004, Montgomery and McFall-Ngai, 1993). Confocal visualization both of colonizing fluorescently labeled bacteria and the host tissue enables real-time observation of bacterial movement at the single-cell level, a unique ability that greatly enables our ability to characterize the stage(s) in initiation that require flagellar motility and chemotaxis (Nyholm *et al.*, 2000). The squid-vibrio association is, therefore, an ideal model for understanding the complexity of flagellar motility in host-microbe interactions because of both the vast array of tools to study this behavior in culture and in symbiosis.

FLAGELLAR MOTILITY AND CHEMOTAXIS:

Flagellar motility is an environmentally-regulated behavior by which a bacterium propels itself through its surroundings. Composed of over 25 conserved proteins, the flagellum is a structural organelle that provides locomotive force to the cell, driven by either a proton or sodium motor force (Imae *et al.*, 1986, Manson *et al.*, 1977). Flagellar proteins and their assembly into a functional flagellum have been characterized in a detailed biochemical manner in *E. coli* and *Salmonella enterica* serovar *Typhimurium* (Kawagishi *et al.*, 1996, Macnab, 2003, Raha *et al.*, 1994, Schoenhals and Macnab, 1996). Broadly, the flagellar apparatus can be divided into structural, secretory, and motor/switch components (reviewed in Macnab, 2003). The flagellar structure includes the cytoplasmic and periplasmic hook-basal body complex, as well as extracellular filament composed of flagellin monomers. The secretory apparatus functions in flagellar assembly, while the motor and switch proteins serve to provide the locomotive force, as well as control rotational direction in response to the chemotaxis machinery.

Bacterial flagella are highly conserved at a structural level, but display diversity in morphology, number and subcellular localization. *V. fischeri* is motile by means of a unipolar tuft of approximately 2 to 9 sheathed flagella, rather than the lateral flagella of the model organisms *Escherichia coli* and *S. enterica* serovar *Typhimurium* in which the genetic basis of flagellar motility is best characterized (Allen and Baumann, 1971, Macnab, 2003). The use of multiple polar flagella in *V. fischeri* is unique even among the well-studied *Vibrio* species (McCarter, 2006): *V. cholerae* presents a single polar flagellum and *V. parahaemolyticus*

utilizes either a single polar flagellum or lateral flagella, depending on its environment (Freter *et al.*, 1981, McCarter and Silverman, 1990, Shinoda and Okamoto, 1977).

The polar flagella of the *Vibrionaceae* are distinct from the flagella of *E. coli* and *Salmonella* not only in their subcellular localization, but also in their encasement by a membranous sheath. Both lipopolysaccharide and membrane proteins are present in the flagellar sheath (Fuerst and Perry, 1988, Hranitzky *et al.*, 1980). As such, the sheath is considered to be an extension of the outer membrane, but it also has been shown to harbor sheath-specific protein antigens (Furuno *et al.*, 2000, Jones *et al.*, 1997, Luke and Penn, 1995). Sheathed flagella are found in other bacteria, such as *Helicobacter pylori* and *Brucella melitensis* (Ferooz and Letesson, 2010, Geis *et al.*, 1993). Neither a functional role, even as it relates to flagellar motility, nor a genetic basis for sheath biogenesis is known. It has recently been proposed that the sheath might serve to increase flagellar stability or mask the immunogenic flagellin subunits during host-microbe interactions (Yoon and Mekalanos, 2008).

Because of the high energetic cost of flagellar biogenesis, transcriptional regulation of flagellar motility is tightly regulated. In *V. cholerae*, the regulation of flagellar genes occurs in a four-step regulatory cascade controlled by the σ^{54}-dependent activator, FlrA, which activates the early flagellar gene, such as those involved in the basal body substructure (Klose *et al.*, 1998). Late flagellar genes, including those encoding hook and motor proteins, are expressed in a sequential manner by either the two-component regulator FlrC or FliA (σ^{28}) (Prouty *et al.*, 2001). In *V. fischeri*, mutations in *rpoN* (which encodes σ^{54}), *flrA* and *flrC* result in amotile cells, suggesting that flagellar regulation occurs through a similar regulatory

cascade (Hussa *et al.*, 2007, Millikan and Ruby, 2003, Wolfe *et al.*, 2004). In addition to flagellar genes, flagellar activators control both virulence and metabolic signatures in other bacteria (Kapatral *et al.*, 2004, Pruss *et al.*, 2003, Syed *et al.*, 2009) and have been similarly implicated in the modulation of unknown symbiotic factors in *V. fischeri* (Millikan and Ruby, 2003).

Migration to energetically-preferred environmental conditions is mediated by chemotaxis, which allows the bacterium to sense gradients stimuli such as amino acids, sugars, and oxygen (Adler, 1966, Henrichsen, 1972). Methyl-accepting chemotaxis proteins (MCPs) function as receptors that bind attractants or repellants, usually in the periplasm, and transduce a signal through the histidine kinase CheA. The consequence of CheA phosphorylation or dephosphorylation is signaling via phosphorelay that ends at FliM, a protein in the flagellar switch apparatus (Eisenbach, 1996, Stock, 1996). In one orientation (counter-clockwise, as viewed from behind the cell), the flagella rotate together as a bundle, leading to smooth swimming and prolonged motility in the same direction. When the switch at one of the flagella reverses orientation to clockwise, that flagellum leads to disruption of the bundle and the cell tumbles. By altering the tumbling frequency, chemotaxis directs an average change in the direction of travel for the bacteria.

While there is some diversity in their structure, MCPs typically consist of a periplasmic ligand binding domain and two cytoplasmic domains: the HAMP domain, which serves a regulatory function, and the MCP signaling domain (Lacal *et al.*, 2010). In *E. coli* K12, a total of five MCPs enable sensing of numerous attractants, including amino acids, peptides, galactose, ribose, and oxygen (Bibikov *et al.*, 1997, Hazelbauer *et al.*, 1969, Kondoh

et al., 1979, Manson *et al.*, 1986, Springer *et al.*, 1977). However, as more diverse bacterial species have been studied, we have learned that bacterial chemotaxis is frequently more complex than the *E. coli* paradigm (Porter *et al.*, 2008, Zusman *et al.*, 2007). Indeed, bioinformatics and increased genome sequence availability have revealed that the complexity of the MCP repertoires vary greatly among sequenced bacteria in both number and ligand binding domains (Krell *et al.*, 2011, Lacal *et al.*, 2010, Miller *et al.*, 2009). Within the *Vibrionaceae*, chemoreceptors-ligand interactions have not been well characterized. Even in the human pathogen *V. cholerae*, only three of up to 45 putative MCPs, mediating aerotaxis, amino acid chemotaxis, and chemotaxis towards chitin-derived sugars have been described (Boin and Hase, 2007, Meibom *et al.*, 2004, Nishiyama *et al.*, 2012).

Genome-scanning predicts that the genetic basis of flagellar motility and chemotaxis is complex in *V. fischeri*, as the genome encodes paralogs of multiple flagellar genes as well as 43 predicted chemoreceptors (McCarter, 2006, Ruby *et al.*, 2005). Novel motility and chemotaxis-associated genes continue to be discovered when these behaviors are examined in non-*E. coli* bacterial species (Cameron *et al.*, 2008, Correa *et al.*, 2005, Moisi *et al.*, 2009, Morris *et al.*, 2008). Thus, the characterization of the genetic basis flagellar motility and chemotaxis in *V. fischeri* will likely serve to inform our general understanding of these behaviors.

THESIS STRUCTURE:

In my dissertation, I sought to dissect the genetic basis of flagellar motility and chemotaxis in *V. fischeri* and to clarify the roles of these important behaviors in its symbiotic lifestyle. I also put an emphasis on tool generation during my thesis tenure, in an effort to develop *V. fischeri* as a model organism for the study of flagellar motility and chemotaxis. To that end, I attempted to characterize these behaviors at a genetic level from an unbiased place of observation, rather than asking highly-directed gene-product/function questions.

1. What is the genetic basis of flagellar motility in *V. fischeri*?

   In Chapter 2, we examine the genetic basis of swimming motility in *V. fischeri* using forward and reverse genetic techniques, phenotypics screening, and transcription profiling.

2. How are chemoeffectors sensed by *V. fischeri*?

   In Chapter 3, we examine mutants disrupted in 19 MCP-encoding genes to identify chemoreceptor-ligand pairs by traditional genetic techniques. In Chapter 4, in collaboration with Sandy Parkinson at the University of Utah, we develop and utilize a new approach to characterize the chemoeffectors sensed by chemoreceptor ligand-binding domains.

3. What is the function of the flagellar sheath?

   In Chapter 5, we consider the unknown function of the flagellar sheath and identify a new role for this uncommon adornment in the promotion of LPS release and activation of the host developmental program.

4. How do flagellar motility and chemotaxis mediate symbiotic initiation?

   In Appendix B, we characterize the roles of these behaviors in the initiation of the squid-vibrio symbiosis by coupling genetic and imaging techniques.

REFERENCES:

Adler, J. (1966) Chemotaxis in bacteria. *Science* **153**(3737): p. 708-16.

Allen, R.D. and Baumann, P. (1971) Structure and arrangement of flagella in species of the genus *Beneckea* and *Photobacterium fischeri*. *J Bacteriol* **107**(1): p. 295-302.

Antunes, L.C., Schaefer, A.L., Ferreira, R.B., Qin, N., Stevens, A.M., Ruby, E.G., and Greenberg, E.P. (2007) A transcriptome analysis of the *Vibrio fischeri* LuxR-LuxI regulon. *J Bacteriol* **189**(22): p. 8387-91.

Baban, C.K., Cronin, M., Akin, A.R., O'Brien, A., Gao, X., Tabirca, S., Francis, K.P., and Tangney, M. (2012) Bioluminescent bacterial imaging *in vivo*. *J Vis Exp* (69).

Bibikov, S.I., Biran, R., Rudd, K.E., and Parkinson, J.S. (1997) A signal transducer for aerotaxis in *Escherichia coli*. *J Bacteriol* **179**(12): p. 4075-9.

Boin, M.A. and Hase, C.C. (2007) Characterization of *Vibrio cholerae* aerotaxis. *FEMS Microbiol Lett* **276**(2): p. 193-201.

Bright, M. and Bulgheresi, S. (2010) A complex journey: transmission of microbial symbionts. *Nat Rev Microbiol* **8**(3): p. 218-30.

Burall, L.S., Harro, J.M., Li, X., Lockatell, C.V., Himpsl, S.D., Hebel, J.R., Johnson, D.E., and Mobley, H.L. (2004) *Proteus mirabilis* genes that contribute to pathogenesis of urinary tract infection: identification of 25 signature-tagged mutants attenuated at least 100-fold. *Infect Immun* **72**(5): p. 2922-38.

Butler, S.M. and Camilli, A. (2004) Both chemotaxis and net motility greatly influence the infectivity of *Vibrio cholerae*. *Proc Natl Acad Sci U S A* **101**(14): p. 5018-23.

Butler, S.M., Nelson, E.J., Chowdhury, N., Faruque, S.M., Calderwood, S.B., and Camilli, A. (2006) Cholera stool bacteria repress chemotaxis to increase infectivity. *Mol Microbiol* **60**(2): p. 417-26.

Cameron, D.E., Urbach, J.M., and Mekalanos, J.J. (2008) A defined transposon mutant library and its use in identifying motility genes in *Vibrio cholerae*. *Proc Natl Acad Sci U S A* **105**(25): p. 8736-41.

Chun, C.K., Scheetz, T.E., Bonaldo Mde, F., Brown, B., Clemens, A., Crookes-Goodson, W.J., Crouch, K., DeMartini, T., Eyestone, M., Goodson, M.S., Janssens, B., Kimbell, J.L., Koropatnick, T.A., Kucaba, T., Smith, C., Stewart, J.J., Tong, D., Troll, J.V., Webster, S., Winhall-Rice, J., Yap, C., Casavant, T.L., McFall-Ngai, M.J., and Soares, M.B. (2006) An annotated cDNA library of juvenile *Euprymna scolopes* with and without colonization by the symbiont *Vibrio fischeri*. *BMC Genomics* **7**: p. 154.

Chun, C.K., Troll, J.V., Koroleva, I., Brown, B., Manzella, L., Snir, E., Almabrazi, H., Scheetz, T.E., Bonaldo Mde, F., Casavant, T.L., Soares, M.B., Ruby, E.G., and McFall-Ngai, M.J. (2008) Effects of colonization, luminescence, and autoinducer on host transcription during development of the squid-vibrio association. *Proc Natl Acad Sci U S A* **105**(32): p. 11323-8.

Correa, N.E., Peng, F., and Klose, K.E. (2005) Roles of the regulatory proteins FlhF and FlhG in the *Vibrio cholerae* flagellar transcription hierarchy. *J Bacteriol* **187**(18): p. 6324-32.

DeLoney-Marino, C.R. and Visick, K.L. (2012) Role for *cheR* of *Vibrio fischeri* in the *Vibrio*-squid symbiosis. *Can J Microbiol* **58**(1): p. 29-38.

Doino, J.A. and McFall-Ngai, M.J. (1995) A transient exposure to symbiosis-competent bacteria induces light organ morphogenesis in the host squid. *Biol Bull* **189**(3): p. 347-355.

Dulla, G.F., Go, R.A., Stahl, D.A., and Davidson, S.K. (2012) *Verminephrobacter eiseniae* type IV pili and flagella are required to colonize earthworm nephridia. *ISME J* **6**(6): p. 1166-75.

Dunn, A.K., Millikan, D.S., Adin, D.M., Bose, J.L., and Stabb, E.V. (2006) New rfp- and pES213-derived tools for analyzing symbiotic *Vibrio fischeri* reveal patterns of infection and *lux* expression in situ. *Appl Environ Microbiol* **72**(1): p. 802-10.

Eisenbach, M. (1996) Control of bacterial chemotaxis. *Mol Microbiol* **20**(5): p. 903-10.

Fass, E. and Groisman, E.A. (2009) Control of *Salmonella* pathogenicity island-2 gene expression. *Curr Opin Microbiol* **12**(2): p. 199-204.

Ferooz, J. and Letesson, J.J. (2010) Morphological analysis of the sheathed flagellum of *Brucella melitensis*. *BMC Res Notes* **3**: p. 333.

Foster, J.S., Apicella, M.A., and McFall-Ngai, M.J. (2000) *Vibrio fischeri* lipopolysaccharide induces developmental apoptosis, but not complete morphogenesis, of the *Euprymna scolopes* symbiotic light organ. *Dev Biol* **226**(2): p. 242-54.

Foynes, S., Dorrell, N., Ward, S.J., Stabler, R.A., McColm, A.A., Rycroft, A.N., and Wren, B.W. (2000) *Helicobacter pylori* possesses two CheY response regulators and a histidine kinase sensor, CheA, which are essential for chemotaxis and colonization of the gastric mucosa. *Infect Immun* **68**(4): p. 2016-23.

Freter, R., Allweiss, B., O'Brien, P.C., Halstead, S.A., and Macsai, M.S. (1981) Role of chemotaxis in the association of motile bacteria with intestinal mucosa: in vitro studies. *Infect Immun* **34**(1): p. 241-9.

Fuerst, J.A. and Perry, J.W. (1988) Demonstration of lipopolysaccharide on sheathed flagella of *Vibrio cholerae* O:1 by protein A-gold immunoelectron microscopy. *J Bacteriol* **170**(4): p. 1488-94.

Furuno, M., Sato, K., Kawagishi, I., and Homma, M. (2000) Characterization of a flagellar sheath component, PF60, and its structural gene in marine *Vibrio*. *J Biochem* **127**(1): p. 29-36.

Gage, D.J. (2002) Analysis of infection thread development using Gfp- and DsRed-expressing *Sinorhizobium meliloti*. *J Bacteriol* **184**(24): p. 7042-6.

Gage, D.J., Bobo, T., and Long, S.R. (1996) Use of green fluorescent protein to visualize the early events of symbiosis between *Rhizobium meliloti* and alfalfa (*Medicago sativa*). *J Bacteriol* **178**(24): p. 7159-66.

Geis, G., Suerbaum, S., Forsthoff, B., Leying, H., and Opferkuch, W. (1993) Ultrastructure and biochemical studies of the flagellar sheath of *Helicobacter pylori*. *J Med Microbiol* **38**(5): p. 371-7.

Graf, J., Dunlap, P.V., and Ruby, E.G. (1994) Effect of transposon-induced motility mutations on colonization of the host light organ by *Vibrio fischeri*. *J Bacteriol* **176**(22): p. 6986-91.

Graf, J. and Ruby, E.G. (1998) Host-derived amino acids support the proliferation of symbiotic bacteria. *Proc Natl Acad Sci U S A* **95**(4): p. 1818-22.

Gyllborg, M.C., Sahl, J.W., Cronin, D.C., 3rd, Rasko, D.A., and Mandel, M.J. (2012) Draft genome sequence of *Vibrio fischeri* SR5, a strain isolated from the light organ of the Mediterranean squid *Sepiola robusta*. *J Bacteriol* **194**(6): p. 1639.

Hayashi, F., Smith, K.D., Ozinsky, A., Hawn, T.R., Yi, E.C., Goodlett, D.R., Eng, J.K., Akira, S., Underhill, D.M., and Aderem, A. (2001) The innate immune response to bacterial flagellin is mediated by Toll-like receptor 5. *Nature* **410**(6832): p. 1099-103.

Hazelbauer, G.L., Mesibov, R.E., and Adler, J. (1969) *Escherichia coli* mutants defective in chemotaxis toward specific chemicals. *Proc Natl Acad Sci U S A* **64**(4): p. 1300-7.

Henrichsen, J. (1972) Bacterial surface translocation: a survey and a classification. *Bacteriol Rev* **36**(4): p. 478-503.

Hranitzky, K.W., Mulholland, A., Larson, A.D., Eubanks, E.R., and Hart, L.T. (1980) Characterization of a flagellar sheath protein of *Vibrio cholerae*. *Infect Immun* **27**(2): p. 597-603.

Hussa, E.A., O'Shea, T.M., Darnell, C.L., Ruby, E.G., and Visick, K.L. (2007) Two-component response regulators of *Vibrio fischeri*: identification, mutagenesis, and characterization. *J Bacteriol* **189**(16): p. 5825-38.

Imae, Y., Matsukura, H., and Kobayasi, S. (1986) Sodium-driven flagellar motors of alkalophilic *Bacillus*. *Methods Enzymol* **125**: p. 582-92.

Jones, A.C., Logan, R.P., Foynes, S., Cockayne, A., Wren, B.W., and Penn, C.W. (1997) A flagellar sheath protein of *Helicobacter pylori* is identical to HpaA, a putative N-acetylneuraminyllactose-binding hemagglutinin, but is not an adhesin for AGS cells. *J Bacteriol* **179**(17): p. 5643-7.

Jones, B.D., Lee, C.A., and Falkow, S. (1992) Invasion by *Salmonella typhimurium* is affected by the direction of flagellar rotation. *Infect Immun* **60**(6): p. 2475-80.

Jones, B.W. and Nishiguchi, M.K. (2004) Counterillumination in the hawaiian bobtail squid, *Euprymna scolopes* Berry (Mollusca : Cephalopoda). *Marine Biology* **144**(6): p. 1151-1155.

Kapatral, V., Campbell, J.W., Minnich, S.A., Thomson, N.R., Matsumura, P., and Pruss, B.M. (2004) Gene array analysis of *Yersinia enterocolitica* FlhD and FlhC: regulation of enzymes affecting synthesis and degradation of carbamoylphosphate. *Microbiology* **150**(Pt 7): p. 2289-300.

Kawagishi, I., Imagawa, M., Imae, Y., McCarter, L., and Homma, M. (1996) The sodium-driven polar flagellar motor of marine *Vibrio* as the mechanosensor that regulates lateral flagellar expression. *Mol Microbiol* **20**(4): p. 693-9.

Klose, K.E., Novik, V., and Mekalanos, J.J. (1998) Identification of multiple sigma54-dependent transcriptional activators in *Vibrio cholerae*. *J Bacteriol* **180**(19): p. 5256-9.

Kondoh, H., Ball, C.B., and Adler, J. (1979) Identification of a methyl-accepting chemotaxis protein for the ribose and galactose chemoreceptors of *Escherichia coli*. *Proc Natl Acad Sci U S A* **76**(1): p. 260-4.

Koropatnick, T.A., Engle, J.T., Apicella, M.A., Stabb, E.V., Goldman, W.E., and McFall-Ngai, M.J. (2004) Microbial factor-mediated development in a host-bacterial mutualism. *Science* **306**(5699): p. 1186-8.

Krell, T., Lacal, J., Munoz-Martinez, F., Reyes-Darias, J.A., Cadirci, B.H., Garcia-Fontana, C., and Ramos, J.L. (2011) Diversity at its best: bacterial taxis. *Environ Microbiol* **13**(5): p. 1115-24.

Lacal, J., Garcia-Fontana, C., Munoz-Martinez, F., Ramos, J.L., and Krell, T. (2010) Sensing of environmental signals: classification of chemoreceptors according to the size of their ligand binding regions. *Environ Microbiol* **12**(11): p. 2873-84.

Lemon, K.P., Higgins, D.E., and Kolter, R. (2007) Flagellar motility is critical for *Listeria monocytogenes* biofilm formation. *J Bacteriol* **189**(12): p. 4418-24.

Liu, Z., Miyashiro, T., Tsou, A., Hsiao, A., Goulian, M., and Zhu, J. (2008) Mucosal penetration primes *Vibrio cholerae* for host colonization by repressing quorum sensing. *Proc Natl Acad Sci U S A* **105**(28): p. 9769-74.

Luke, C.J. and Penn, C.W. (1995) Identification of a 29 kDa flagellar sheath protein in *Helicobacter pylori* using a murine monoclonal antibody. *Microbiology* **141 (Pt 3)**: p. 597-604.

Lupp, C. and Ruby, E.G. (2005) *Vibrio fischeri* uses two quorum-sensing systems for the regulation of early and late colonization factors. *J Bacteriol* **187**(11): p. 3620-9.

Macnab, R.M. (2003) How bacteria assemble flagella. *Annu Rev Microbiol* **57**: p. 77-100.

Mandel, M.J., Schaefer, A.L., Brennan, C.A., Heath-Heckman, E.A., Deloney-Marino, C.R., McFall-Ngai, M.J., and Ruby, E.G. (2012) Squid-derived chitin oligosaccharides are a chemotactic signal during colonization by *Vibrio fischeri*. *Appl Environ Microbiol* **78**(13): p. 4620-6.

Mandel, M.J., Stabb, E.V., and Ruby, E.G. (2008) Comparative genomics-based investigation of resequencing targets in *Vibrio fischeri*: focus on point miscalls and artefactual expansions. *BMC Genomics* **9**: p. 138.

Mandel, M.J., Wollenberg, M.S., Stabb, E.V., Visick, K.L., and Ruby, E.G. (2009) A single regulatory gene is sufficient to alter bacterial host range. *Nature* **458**(7235): p. 215-8.

Manson, M.D., Blank, V., Brade, G., and Higgins, C.F. (1986) Peptide chemotaxis in *E. coli* involves the Tap signal transducer and the dipeptide permease. *Nature* **321**(6067): p. 253-6.

Manson, M.D., Tedesco, P., Berg, H.C., Harold, F.M., and Van der Drift, C. (1977) A protonmotive force drives bacterial flagella. *Proc Natl Acad Sci U S A* **74**(7): p. 3060-4.

McCarter, L., *Motility and Chemotaxis* in *The Biology of Vibrios*, F.L. Thompson, B. Austin, and J. Swings, Editors. 2006, ASM Press: Washington, D.C. p. 115-132.

McCarter, L. and Silverman, M. (1990) Surface-induced swarmer cell differentiation of *Vibrio parahaemolyticus*. *Mol Microbiol* **4**(7): p. 1057-62.

Meibom, K.L., Li, X.B., Nielsen, A.T., Wu, C.Y., Roseman, S., and Schoolnik, G.K. (2004) The *Vibrio cholerae* chitin utilization program. *Proc Natl Acad Sci U S A* **101**(8): p. 2524-9.

Miller, L.D., Russell, M.H., and Alexandre, G. (2009) Diversity in bacterial chemotactic responses and niche adaptation. *Adv Appl Microbiol* **66**: p. 53-75.

Millikan, D.S. and Ruby, E.G. (2002) Alterations in *Vibrio fischeri* motility correlate with a delay in symbiosis initiation and are associated with additional symbiotic colonization defects. *Appl Environ Microbiol* **68**(5): p. 2519-28.

Millikan, D.S. and Ruby, E.G. (2003) FlrA, a σ^{54}-dependent transcriptional activator in *Vibrio fischeri*, is required for motility and symbiotic light-organ colonization. *J Bacteriol* **185**(12): p. 3547-57.

Millikan, D.S. and Ruby, E.G. (2004) *Vibrio fischeri* flagellin A is essential for normal motility and for symbiotic competence during initial squid light organ colonization. *J Bacteriol* **186**(13): p. 4315-25.

Moisi, M., Jenul, C., Butler, S.M., New, A., Tutz, S., Reidl, J., Klose, K.E., Camilli, A., and Schild, S. (2009) A novel regulatory protein involved in motility of *Vibrio cholerae*. *J Bacteriol* **191**(22): p. 7027-38.

Montgomery, M.K. and McFall-Ngai, M. (1994) Bacterial symbionts induce host organ morphogenesis during early postembryonic development of the squid *Euprymna scolopes*. *Development* **120**(7): p. 1719-29.

Montgomery, M.K. and McFall-Ngai, M.J. (1993) Embryonic development of the light organ of the sepiolid squid *Euprymna scolopes* Berry. *Biol Bull* **184**: p. 296-308.

Morris, D.C., Peng, F., Barker, J.R., and Klose, K.E. (2008) Lipidation of an FlrC-dependent protein is required for enhanced intestinal colonization by *Vibrio cholerae*. *J Bacteriol* **190**(1): p. 231-9.

Murfin, K.E., Chaston, J., and Goodrich-Blair, H. (2012) Visualizing bacteria in nematodes using fluorescent microscopy. *J Vis Exp* (68).

Nishiyama, S., Suzuki, D., Itoh, Y., Suzuki, K., Tajima, H., Hyakutake, A., Homma, M., Butler-Wu, S.M., Camilli, A., and Kawagishi, I. (2012) Mlp24 (McpX) of *Vibrio cholerae* implicated in pathogenicity functions as a chemoreceptor for multiple amino acids. *Infect Immun* **80**(9): p. 3170-8.

Nyholm, S.V., Deplancke, B., Gaskins, H.R., Apicella, M.A., and McFall-Ngai, M.J. (2002) Roles of *Vibrio fischeri* and nonsymbiotic bacteria in the dynamics of mucus secretion during symbiont colonization of the *Euprymna scolopes* light organ. *Appl Environ Microbiol* **68**(10): p. 5113-22.

Nyholm, S.V., Stabb, E.V., Ruby, E.G., and McFall-Ngai, M.J. (2000) Establishment of an animal-bacterial association: recruiting symbiotic vibrios from the environment. *Proc Natl Acad Sci U S A* **97**(18): p. 10231-5.

Pirhonen, M., Flego, D., Heikinheimo, R., and Palva, E.T. (1993) A small diffusible signal molecule is responsible for the global control of virulence and exoenzyme production in the plant pathogen *Erwinia carotovora*. *EMBO J* **12**(6): p. 2467-76.

Porter, S.L., Wadhams, G.H., and Armitage, J.P. (2008) Rhodobacter sphaeroides: complexity in chemotactic signalling. *Trends Microbiol* **16**(6): p. 251-60.

Prouty, M.G., Correa, N.E., and Klose, K.E. (2001) The novel σ^{54}- and σ^{28}-dependent flagellar gene transcription hierarchy of *Vibrio cholerae*. *Mol Microbiol* **39**(6): p. 1595-609.

Pruss, B.M., Campbell, J.W., Van Dyk, T.K., Zhu, C., Kogan, Y., and Matsumura, P. (2003) FlhD/FlhC is a regulator of anaerobic respiration and the Entner-Doudoroff pathway

through induction of the methyl-accepting chemotaxis protein Aer. *J Bacteriol* **185**(2): p. 534-43.

Raha, M., Sockett, H., and Macnab, R.M. (1994) Characterization of the *fliL* gene in the flagellar regulon of *Escherichia coli* and *Salmonella typhimurium*. *J Bacteriol* **176**(8): p. 2308-11.

Rawls, J.F., Mahowald, M.A., Goodman, A.L., Trent, C.M., and Gordon, J.I. (2007) *In vivo* imaging and genetic analysis link bacterial motility and symbiosis in the zebrafish gut. *Proc Natl Acad Sci U S A* **104**(18): p. 7622-7.

Richardson, K. (1991) Roles of motility and flagellar structure in pathogenicity of *Vibrio cholerae*: analysis of motility mutants in three animal models. *Infect Immun* **59**(8): p. 2727-36.

Ruby, E.G. and Asato, L.M. (1993) Growth and flagellation of *Vibrio fischeri* during initiation of the sepiolid squid light organ symbiosis. *Arch Microbiol* **159**(2): p. 160-7.

Ruby, E.G., Urbanowski, M., Campbell, J., Dunn, A., Faini, M., Gunsalus, R., Lostroh, P., Lupp, C., McCann, J., Millikan, D., Schaefer, A., Stabb, E., Stevens, A., Visick, K., Whistler, C., and Greenberg, E.P. (2005) Complete genome sequence of *Vibrio fischeri*: a symbiotic bacterium with pathogenic congeners. *Proc Natl Acad Sci U S A* **102**(8): p. 3004-9.

Schoenhals, G.J. and Macnab, R.M. (1996) Physiological and biochemical analyses of FlgH, a lipoprotein forming the outer membrane L ring of the flagellar basal body of *Salmonella typhimurium*. *J Bacteriol* **178**(14): p. 4200-7.

Shinoda, S. and Okamoto, K. (1977) Formation and function of *Vibrio parahaemolyticus* lateral flagella. *J Bacteriol* **129**(3): p. 1266-71.

Spira, W.M., Sack, R.B., and Froehlich, J.L. (1981) Simple adult rabbit model for V*ibrio cholerae* and enterotoxigenic *Escherichia coli* diarrhea. *Infect Immun* **32**(2): p. 739-47.

Springer, M.S., Goy, M.F., and Adler, J. (1977) Sensory transduction in *Escherichia coli*: two complementary pathways of information processing that involve methylated proteins. *Proc Natl Acad Sci U S A* **74**(8): p. 3312-6.

Stecher, B., Hapfelmeier, S., Muller, C., Kremer, M., Stallmach, T., and Hardt, W.D. (2004) Flagella and chemotaxis are required for efficient induction of *Salmonella enterica* serovar *Typhimurium* colitis in streptomycin-pretreated mice. *Infect Immun* **72**(7): p. 4138-50.

Stock, J.B., and M. G. Surette, *Chemotaxis, p. 1103-1129.* , in *Escherichia coli and Salmonella, 2nd ed.*, R.C.I. F. C. Neidhart, J. I. Ingraham, E. C. C. Lin, K. B. Low, B. Magasanik, W. S. Reznikoff, M. Riley, M. Schaechter, and H. E. Umbarger, Editor 1996, ASM Press: Washington, DC.

Syed, K.A., Beyhan, S., Correa, N., Queen, J., Liu, J., Peng, F., Satchell, K.J., Yildiz, F., and Klose, K.E. (2009) The *Vibrio cholerae* flagellar regulatory hierarchy controls expression of virulence factors. *J Bacteriol* **191**(21): p. 6555-70.

Wier, A.M., Nyholm, S.V., Mandel, M.J., Massengo-Tiasse, R.P., Schaefer, A.L., Koroleva, I., Splinter-Bondurant, S., Brown, B., Manzella, L., Snir, E., Almabrazi, H., Scheetz, T.E., Bonaldo Mde, F., Casavant, T.L., Soares, M.B., Cronan, J.E., Reed, J.L., Ruby, E.G., and McFall-Ngai, M.J. (2010) Transcriptional patterns in both host and

bacterium underlie a daily rhythm of anatomical and metabolic change in a beneficial symbiosis. *Proc Natl Acad Sci U S A* **107**(5): p. 2259-64.

Wolfe, A.J., Millikan, D.S., Campbell, J.M., and Visick, K.L. (2004) *Vibrio fischeri* σ^{54} controls motility, biofilm formation, luminescence, and colonization. *Appl Environ Microbiol* **70**(4): p. 2520-4.

Yoon, S.S. and Mekalanos, J.J. (2008) Decreased potency of the *Vibrio cholerae* sheathed flagellum to trigger host innate immunity. *Infect Immun* **76**(3): p. 1282-8.

Young, G.M., Schmiel, D.H., and Miller, V.L. (1999) A new pathway for the secretion of virulence factors by bacteria: the flagellar export apparatus functions as a protein-secretion system. *Proc Natl Acad Sci U S A* **96**(11): p. 6456-61.

Zusman, D.R., Scott, A.E., Yang, Z., and Kirby, J.R. (2007) Chemosensory pathways, motility and development in *Myxococcus xanthus*. *Nat Rev Microbiol* **5**(11): p. 862-72.

Chapter 2

Genetic Determinants of Swimming Motility in the Squid Light-Organ Symbiont *Vibrio fischeri*

PREFACE:

Submitted to *Molecular Microbiology* in December 2012 as:

Brennan CA, Mandel MJ, Gyllborg MC, Thomasgard KA, and Ruby EG. "Genetic Determinants of Swimming Motility in the Squid Light-Organ Symbiont *Vibrio fischeri*."

CAB, EGR, and MJM formulated ideas and planned experiments. CAB, MJM, MCG, and KAT performed experiments. CAB, MJM, and EGR wrote and edited the chapter.

ABSTRACT:

Bacterial flagellar motility is a complex cellular behavior required for the colonization of the light-emitting organ of the Hawaiian bobtail squid, *Euprymna scolopes*, by the beneficial bioluminescent symbiont *Vibrio fischeri*. We characterized the basis of this behavior by performing (i) a forward-genetic screen to identify mutants defective in soft-agar motility, as well as (ii) a transcriptional analysis to determine the genes that are expressed downstream of the flagellar master regulator FlrA. Mutants with severe defects in soft-agar motility were identified due to insertions in genes with putative roles in flagellar motility and in genes that were unexpected, including those predicted to encode hypothetical proteins and cell division-related proteins. Analysis of mutants for their ability to enter into a productive symbiosis indicated that flagellar motility mutants are deficient, while chemotaxis mutants are able to colonize a subset of juvenile squid to light-producing levels. Thirty-three genes required for normal motility in soft agar were also down-regulated in the absence of FlrA, suggesting they belong to the flagellar regulon of *V. fischeri*. Mutagenesis of putative paralogs of the flagellar motility genes *motA*, *motB* and *fliL* revealed that *motA1*, *motB1*, and both *fliL1* and *fliL2*, but not *motA2* and *motB2*, likely contribute to soft-agar motility. Using these complementary approaches, we have characterized the genetic basis of flagellar motility in *V. fischeri* and furthered our understanding of the roles of flagellar motility and chemotaxis in colonization of the juvenile squid, including identifying eleven novel mutants unable to enter into a productive light-organ symbiosis.

INTRODUCTION:

Flagellar motility is an environmentally regulated behavior by which a bacterium propels itself through its surroundings, directed by behavior-modifying machinery such as the chemotaxis system (Adler, 1966, Henrichsen, 1972). Within the unique environments present in different host-microbe associations, both flagellar motility and the flagellum itself can play important roles in bacterial transit, niche specificity, effector secretion, biofilm formation, host recognition, and gene regulation (Butler and Camilli, 2004, Hayashi *et al.*, 2001, Lemon *et al.*, 2007, Liu *et al.*, 2008, Young *et al.*, 1999). While the process of flagellar motility is difficult to study in most host-microbe interactions, the symbiosis between the bioluminescent, gram-negative bacterium *Vibrio fischeri* and its host the Hawaiian bobtail squid, *Euprymna scolopes,* is an ideal model in which to study how this critical behavior mediates symbiotic initiation. The squid-vibrio mutualism provides a vast array of tools to study the roles of the flagellum and flagellar motility both in culture and throughout the development and persistence of the symbiosis (DeLoney-Marino *et al.*, 2003, Mandel *et al.*, 2012, Nyholm *et al.*, 2000).

The association between *V. fischeri* and *E. scolopes* begins as soon as the juvenile squid hatches in seawater containing the symbiont. Colonization is a sequential process in which the bacteria initiate the association, accommodate to the light-organ environment, and persist in epithelium-lined crypts for the lifetime of the squid (Nyholm and McFall-Ngai, 2004). The steps mediating symbiotic initiation involve a complex exchange of signals and responses between *V. fischeri* and the juvenile squid (Mandel *et al.*, 2012, Nyholm and

McFall-Ngai, 2004, Visick and Ruby, 2006). To enter into the symbiosis, *V. fischeri* cells must migrate from external aggregates, through mucus to the pores of the light organ, and finally into crypts deep within the tissue. Remarkably, essentially all other species of bacteria are excluded from completing this path. Flagellar biosynthesis by *V. fischeri,* and its subsequent use for motility, are essential for the initiation process (Graf *et al.*, 1994, Millikan and Ruby, 2003). While the role of chemotaxis in initiation is less well characterized, a mutant disrupted in the chemotaxis response regulator CheY is defective in competition with wild-type *V. fischeri* (Hussa *et al.*, 2007). Other studies have shown that alterations to motility -- both increasing and decreasing motility rates -- result in defects in the initiation kinetics (Millikan and Ruby, 2002, Millikan and Ruby, 2004).

V. fischeri is motile by means of a unipolar tuft of approximately 2 to 7 sheathed flagella, rather than by the peritrichous flagella of the model organisms *Escherichia coli* and *Salmonella enterica* serovar Typhimurium (Allen and Baumann, 1971, Macnab, 2003). The use of multiple polar flagella in *V. fischeri* is unique even among the well-studied *Vibrio* species (McCarter, 2006): *V. cholerae* bears a single polar flagellum and *V. parahaemolyticus* presents either a single sheathed polar flagellum or multiple unsheathed lateral flagella, depending on its environment (Freter *et al.*, 1981, McCarter and Silverman, 1990, Shinoda and Okamoto, 1977). These structural differences suggest that flagellar biosynthesis is carefully and specifically controlled in this genus. Within Gram-negative bacteria, the complex regulation of genes involved in flagellar motility occurs through a multiple-tiered cascade of events. In *E. coli*, early flagellar genes are activated in a σ^{70}-dependent manner by the master regulator FlhDC. Late flagellar genes are then activated under the control of FliA

(σ^{28}) (Arnosti and Chamberlin, 1989, Iino *et al.*, 1988). In contrast, the regulation of flagellar genes by *V. cholerae* occurs in a four-tiered regulatory cascade controlled by the σ^{54}-dependent activator, FlrA, which activates the early flagellar genes, such as those involved in the MS ring structure (Klose and Mekalanos, 1998). Late flagellar genes, including those encoding hook and motor proteins, are expressed in a sequential manner by either the two-component regulator FlrC or the FliA sigma factor (Prouty *et al.*, 2001). In *V. fischeri*, amotile cells are observed in strains encoding single mutations in the genes *rpoN* (which encodes σ^{54}), *flrA* or *flrC*, suggesting that flagellar regulation occurs through a regulatory cascade that is similar to its congener (Hussa *et al.*, 2007, Millikan and Ruby, 2003, Wolfe *et al.*, 2004). Flagellar activators do not exclusively regulate flagellar gene products; instead, they control both virulence and metabolic signatures in other bacteria (Kapatral *et al.*, 2004, Pruss *et al.*, 2003, Syed *et al.*, 2009) and have been similarly implicated in the modulation of unknown symbiotic factors in *V. fischeri* (Millikan and Ruby, 2003).

Genome-scanning predicts that the genetic basis of flagellar motility and chemotaxis is complex in *V. fischeri*, as this organism's two chromosomes encode paralogs of multiple *E. coli* flagellar genes as well as 43 predicted methyl-accepting chemotaxis proteins (MCPs) (Mandel *et al.*, 2008, McCarter, 2006, Ruby *et al.*, 2005). Similarly large numbers of MCPs have been observed in other sequenced microbes not in the *Enterobacteriaceae*, but their function(s) remains poorly described (Miller *et al.*, 2009). Several genetic studies have identified the genes involved in proper flagellar elaboration in bacteria with polar flagellar systems (Kim and McCarter, 2000, Overhage *et al.*, 2007). In these bacteria, additional proteins are important for motility, including the regulators FlhF and FlhG, which control

flagellar number in *V. cholerae* (Correa *et al.*, 2005, Klose and Mekalanos, 1998). The continuing discovery of new polar flagellum-specific genes (Cameron *et al.*, 2008, Moisi *et al.*, 2009, Morris *et al.*, 2008). as well as differences in flagellar structure, suggest there exist additional novel structural components and/or regulatory factors that are critical for flagellar motility of *V. fischeri*.

In the work described here, we sought to understand the genetic basis of flagellar motility, an essential cellular behavior for the host-associated life-style of *V. fischeri*. We performed both forward and reverse genetic analyses, coupled with transcriptional profiling, to identify the genes that contribute to normal motility during symbiosis.

MATERIALS AND METHODS:

Bacterial strains and media

Strains and plasmids used in this work are listed in Table 2-1. *V. fischeri* strains are derived from the squid isolate ES114 (Boettcher and Ruby, 1990) and were grown at 28°C in either Luria-Bertani salt (LBS) medium (per liter, 10 g Bacto-tryptone, 5 g yeast extract and 20 g NaCl, 50 mL 1M Tris buffer, pH 7.5, in distilled water) or seawater-based tryptone (SWT) medium (per liter, 5 g Bacto-tryptone, 3 g yeast extract, 3 mL glycerol, 700 mL Instant Ocean [Aquarium Systems, Inc, Mentor, OH] at a salinity of 33-35 ppt, and 300 ml distilled water). When used to support overnight growth, SWT was supplemented with 50 mM Tris buffer, pH 7.5. *E. coli* strains, as used for cloning, were grown at 37°C in Luria-Bertani medium or brain heart infusion medium (BD, Sparks, MD). When appropriate, antibiotics were added to media at the following concentrations: erythromycin (erm), 5 μg/ml for *V. fischeri* and 150 μg/ml for *E. coli*; kanamycin (kan), 100 μg/ml for *V. fischeri* and 50 μg/ml for *E. coli*; and chloramphenicol (cam), 2.5 μg/ml for *V. fischeri* and 25 μg/ml for *E. coli*. Growth media were solidified with 1.5% agar as needed.

Construction and motility screening of an arrayed transposon mutant collection

To investigate the genetic basis of flagellar motility, we conducted random mutagenesis with pMJM10 a conjugatable plasmid that encodes an erythromycin-resistant transposon. Plasmid pMJM10 is a derivative of pEVS170 (Lyell *et al.*, 2008) that includes outward-facing T7 promoters on the transposon and MseI/Tsp509I sites in the vector

Table 2-1. Strains and plasmids used in this study

Strain or Plasmid	Description	Reference or source
Strains		
V. fischeri		
MJM1100	ES114, sequenced wild-type light organ isolate	(Boettcher and Ruby, 1990)
DM159	Δ*flrA::kan*	(Millikan and Ruby, 2003)
CAB1625	*fliL1*::pCAB50 Campbell mutant	This work
CAB1626	*fliL2*::pCAB51 Campbell mutant	This work
CAB1627	*motA1*::pCAB52 Campbell mutant	This work
CAB1628	*motA2*::pCAB53 Campbell mutant	This work
CAB1629	*motB2*::pCAB54 Campbell mutant	This work
CAB1630	*motB1*::pCAB55 Campbell mutant	This work
MB06265	*flgP*::Tn*erm*	This work
MB06357	*motB1*::Tn*erm*	This work
MB06428	*cheY*::Tn*erm*	This work
MB08164	*flgI*::Tn*erm*	This work
MB08359	*VF_0171*::Tn*erm*	This work
MB08380	*rfbX*::Tn*erm*	This work
MB08627	*VF_2581*::Tn*erm*	This work
MB08701	*cheA*::Tn*erm*	This work
MB08705	*VF_0173*::Tn*erm*	This work
MB08726	ig*VF_0135*::Tn*erm*	This work
MB08840	*flhA*::Tn*erm*	This work
MB08886	*flrC*::Tn*erm*	This work
MB08888	*fliI*::Tn*erm*	This work
MB09672	*mutS*::Tn*erm*	This work
MB09956	*flgH*::Tn*erm*	This work
MB10022	23s rRNA::Tn*erm*	This work
MB11332	*VF_1697*::Tn*erm*	This work
MB12230	*fliM*::Tn*erm*	This work
MB12341	*flgK*::Tn*erm*	This work
MB12561	*motX*::Tn*erm*	This work
MB13452	*rffH*::Tn*erm*	This work
MB14051	*VF_0172*::Tn*erm*	This work
MB14478	*flgT*::Tn*erm*	This work
MB14580	*flgE*::Tn*erm*	This work
MB14746	*rmlB*::Tn*erm*	This work
MB15443	*flhG*::Tn*erm*	This work
MB15490	*VF_0192*::Tn*erm*	This work
MB15821	*fliA::tn (VF_1834)*	This work
MB16040	23s rRNA::Tn*erm*	This work
MB16329	*flgL*::Tn*erm*	This work
MB16504	*flaA*::Tn*erm*	This work
MB16653	*VF_0077*::Tn*erm*	This work
MB18981	*fliG*::Tn*erm*	This work
MB19388	*flhF*::Tn*erm*	This work
MB19520	*fliL1*::Tn*erm*	This work
MB19624	*cheW*::Tn*erm*	This work
MB20044	*VF_A0058*::Tn*erm*	This work

MB20794	*fliN*::Tn*erm*	This work
MB20979	*cheZ*::Tn*erm*	This work
MB21386	*flgO*::Tn*erm*	This work
MB21407	*flrA*::Tn*erm*	This work
MB21447	*fliR*::Tn*erm*	This work
MB21566	*flgN*::Tn*erm*	This work
MB22953	*fliF*::Tn*erm*	This work
MB23025	*flgF*::Tn*erm*	This work
MB23130	*mshB*::Tn*erm*	This work
MB23533	*flgG*::Tn*erm*	This work
MB23837	*cheB::*Tn*erm*	This work
MB24277	*VF_1491*::Tn*erm*	This work
MB24439	*flaD*::Tn*erm*	This work
MB24714	*flrB*::Tn*erm*	This work
MB25656	16s rRNA::Tn*erm*	This work
MB26712	*motY*::Tn*erm*	This work
MB26857	16s rRNA::Tn*erm*	This work
MB27080	*fliD*::Tn*erm*	This work
MB28068	ig*VF_1874*::Tn*erm*	This work
MB28468	*flgD*::Tn*erm*	This work
MB28617	23s rRNA::Tn*erm*	This work
MB28641	*motA1*::Tn*erm*	This work
MB29802	*fliK*::Tn*erm*	This work
MB30445	*rpoN*::Tn*erm*	This work
MB30578	*fliH*::Tn*erm*	This work
MB31054	ig*VF_1837*::Tn*erm*	This work
MB31274	*mukF*::Tn*erm*	This work
MB32667	*can*::Tn*erm*	This work
MB32946	*amiB*::Tn*erm*	This work
MB33180	16s rRNA::Tn*erm*	This work
MB33191	*VF_0189*::Tn*erm*	This work
MB33314	*mukB*::Tn*erm*	This work
MB33650	*VF_0174*::Tn*erm*	This work
E. coli		
DH5*α*-*λ*pir	Cloning vector	(Hanahan, 1983)
Plasmids		
pMJM10	Plasmid used for Tn*erm* transposition, kan^R	This work
pEVS122	*oriR6K*-based suicide vector, erm^R	(Dunn *et al*., 2005)
pVSV105	pES213-based plasmid used for complementation, cam^R	(Dunn *et al*., 2006)
pAKD701	pES213-based plasmid used for reporter fusions, kan^R	(Dunn and Stabb, 2008)
pEVS104	conjugative helper plasmid, kan^R	(Stabb and Ruby, 2002)
pCAB52	pEVS122 containing a fragment of *motA1* ORF	This work
pCAB55	pEVS122 containing a fragment of *motB1* ORF	This work
pCAB53	pEVS122 containing a fragment of *motA2* ORF	This work
pCAB54	pEVS122 containing a fragment of *motB2* ORF	This work
pCAB50	pEVS122 containing a fragment of *fliL1* ORF	This work
pCAB51	pEVS122 containing a fragment of *fliL2* ORF	This work
pCAB11	pVSV105 with the *flgOP* complementing fragment	This work

pCAB12	pVSV105 with the *flgP* complementing fragment	This work
pCAB60	pVSV105 with the *flgT* complementing fragment	This work
pCAB58	pVSV105 with the *VF_1491* complementing fragment	This work
pCAB59	pVSV105 with the *amiB* complementing fragment	This work
pCAB66	pVSV105 with the *mukB* complementing fragment	This work
pCAB65	pVSV105 with the *mutS* complementing fragment	This work
pCAB56	pVSV105 with the *fliL2* complementing fragment	This work
pCAB36	pAKD701 with the *fliE* promoter	This work
pCAB37	pAKD701 with the *flhA* promoter	This work
pCAB38	pAKD701 with the *flrB* promoter	This work
pCAB39	pAKD701 with the *fliK* promoter	This work
pCAB47	pAKD701 with the *flgA* promoter	This work
pCAB40	pAKD701 with the *flgB* promoter	This work
pCAB44	pAKD701 with the *flaD* promoter	This work
pCAB41	pAKD701 with the *motX* promoter	This work
pCAB46	pAKD701 with the *motA1* promoter	This work
pCAB48	pAKD701 with the *flgO* promoter	This work
pCAB49	pAKD701 with the *flgT* promoter	This work

backbone outside of the transposon. The tranpsoson was built as an optimized vector to conduct TraSH analysis (Sassetti *et al.*, 2001) in *V. fischeri* and it performs comparable to pEVS170 for traditional forward genetic analysis. The plasmid backbone encodes a Tn*5* transposase, kanamycin-resistance, and an R6Kγ (pi-dependent) origin of replication that does not replicate in *V. fischeri*. In 10-15% of instances the plasmid backbone is retained in *V. fischeri* illegitimately (Lyell *et al.*, 2008); these isolates are identified by their kanamycin resistance and removed from the study.

Construction from pEVS170 was accomplished as follows. First, oligonucleotides T7US-F2 and T7US-R2 (Table 2-2) were 5'-phosphorylated with T4 polynucleotide kinase (Promega, Madison WI) and then annealed. The resulting heteroduplex was introduced into the SpeI and Bme1580I sites of pEVS170. The resulting plasmid was named pMJM8 (contains a single outward-facing T7 promoter at the upstream end of the transposon, relative to the orientation of the *erm* cassette). Second, vector sequence adjacent to the transposon upstream end was modified to introduce MseI and Tsp509I sites by site-directed mutagenesis. The QuikChange II Kit (Stratagene, La Jolla, CA) was used according to the manufacturer's instructions, and mutation of the hexanucleotide GGGGGG to TTAATT with oligonucleotides MseTspUS-F and MseTspUS-R introduced the new restriction endonuclease cleavage sites, for the resulting plasmid pMJM9. Finally, the downstream T7 promoter and MseI/Tsp509I sites were introduced in a single step. pMJM9 served the template for a PCR reaction in which T7DS-pcrF2 and T7DS-pcrR amplified most of the plasmid, introducing the changes. The resulting PCR product was digested with KpnI (sites were included in the primers) and DpnI (to digest the template DNA), then self-ligated to generate pMJM10. The

Table 2-2. Primers used in this study

Primer name	Sequence (5'-3')
T7US-F2	CTAGATAATACGACTCACTATAGGGCGGCC
T7US-R2	GCCCTATAGTGAGTCGTATTAT
MseTspUS-F	GAGACAGGTCGACCTGCAGGGTTAATTGGGAAAGCCACGTTGTGTCTC
MseTspUS-R	GAGACACAACGTGGCTTTCCCAATTAACCCTGCAGGTCGACCTGTCTC
T7DS-pcrF2	GAGGATGTCGGTACCCCCTATAGTGAGTCGTATTAGTACAACTGAG
T7DS-pcrR	GTGACGTCAGGTACCAGATGTGTATAAGAGACAGAATTAATCCGTAGCGTCC TGAACGG
170Int2	AGCTTGCTCAATCAATCACC
ARB1	GGCCACGCGTCGACTAGTACNNNNNNNNNNGATAT
170Ext3	GCAGTTCAACCTGTTGATAGTACG
ARB2	GGCCACGCGTCGACTAGTAC
170Int3	CAAAGCAATTTTGAGTGACACAGG
170Seq1	AACACTTAACGGCTGACA
fliL1_campbellF	GCCCCGGGTGCCGCTTTAGAAGCGAATATGCC
fliL1_campbellR	GCGCATGCTTCGGCCACGTGGTTCTCTTAACT
fliL2_campbellF	GCCCCGGGAGAAGTCGCACCTCAAATGGGCTA
fliL2_campbellR	GCGCATGCTCTTATTTCTTCACGACCCGCCAG
motA1_campbellF	GCCCCGGGCAATGGTACTGGCTGGTGGTATA
motA1_campbellR	GCGCATGCCTTTACGAGCCGCATCAGCCATTT
motB1_campbellF	GCCCCGGGATTGATGGAGAATCGGATCGTGCTG
motB1_campbellR	GCGCATGCCACTAATCTCGCGCTCTAGTGCTT
motA2_campbellF	GCCCCGGGCGGCTTATTGATGGCGTTTGGTGT
motA2_campbellR	GCGCATGCTCGTCACGTTTGTCTCGTCAAGCA
motB2_campbellF	GCCCCGGGAAAGTGGTTGATACGTCGGCTCAC
motB2_campbellR	GCGCATGCCGACCTCTTTCATCGCTTCTGAA
flgO_compF	GCTCTAGAACTTAAGATCCTTTAGGCGGC
flgP_compR	GCTCTAGACTAACACACAGGAAACAGCTATGAAACATTGGTTTTTATTA
flgP_compF	GCGGTACCACCGAGGGCAATAGCATTATGTCG
flgT_compF	GCTCTAGATGGCAATTGGTGAACGAGCA
flgT_compR	GCGGTACCAACAACACGCTAGGCACTGT
1491_compF	GCTCTAGAGCAGTCGATGATACATTCAAACTGTG
1491_compR	GCGAGCTCTCCACAGTGGTGTTCCTGTT
amiB_compF	GCTCTAGACTAACACACAGGAAACAGCTGTGTTAATCGGTAAATATTTTCGA
amiB_compR	GCGGTACCTTGGTTGGCTAATCGTGCTGGT
mukB_compF	CCTAACACACAGGAAACAGCTATGATTGAACGTGGTAAATA
mukB_compR	ACGCATTCCGCTTCTGTTGT
mutS_compF	AACTTCTTCACTAACCGCGCCA
mutS_compR	TGGCTGATTCATGGCTGCAT
fliL2_compF	GCTCTAGAACCCACGATTGCTGATCACCTT
fliL2_compR	GCGGTACCACAGCGCATTTAGCAGGCTT
fliE_fusionF	GCCCTAGGACCAGAGCAACAAGTACCGT
fliE_fusionR	GCGTCGACTTAGGCTTTCGCAAACATTGCA

flhA_fusionF	GCCCTAGGGACGCGACTACCAATATCCA
flhA_fusionR	GCGTCGACTTACGGTATGGGTAAAATTACCA
flrB_fusionF	GCCCTAGGTCGAATGATTTACCAGAAGA
flrB_fusionR	GCGTCGACTTACTTGTGTATCAAGTAAAATAACA
fliK_fusionF	GCCCTAGGTCACAAGTGGATAATTGCCA
fliK_fusionR	GCGTCGACTTACTCTTTTAGCTCTTCAATAAAGCCT
flgA_fusionF	GCCCTAGGAGAAACCTTGAATTGTACGGT
flgA_fusionR	GCGTCGACTTAGAAACTTATAAATAGGCCGA
flgB_fusionF	GCCCTAGGTGAAATCTCAAGTGTTAAATCA
flgB_fusionR	GCGTCGACTTATGCTTTATAGCGAGGAGT
flaD_fusionF	GCCCTAGGACTATGCCAAAGCCGGGGCT
flaD_fusionR	GCGTCGACTTAACTGTTAATTTTAAGACCTGA
motX_fusionF	GCCCTAGGTGAAGATCTAACAGGCGTGCCA
motX_fusionR	GCGTCGACTTAAAACAGTCGAAATAATTGGT
motA1_fusionF	GCCCTAGGTTGATTGACGACAGAATCCA
motA1_fusionR	GCGTCGACTTAACCAACTACGATTAAAACCGA
flgO_fusionF	GCCCTAGGTATCGGCCCCAGAAAACAGCA
flgO_fusionR	GCGTCGACTTAGCGTGGGGTATCAGCCAGCA
flgT_fusionF	GCCCTAGGGTCGTATTCGATGTTACAAACTGTTCA
flgT_fusionR	GCGTCGACTTATGCCGCATCTTTACTGGTTAAGA

transposon sequence and its immediate flanking DNA were confirmed by DNA sequencing at the University of Wisconsin Biotechnology Center.

The construction of the MB mutant collection is illustrated in detail in Figure 2-1. Briefly, we mutagenized *V. fischeri* ES114 by Tn*erm* transposition and arrayed mutants into 96-well trays for individual analysis. We screened the arrayed mutants for strains that contained a transposon insertion (erythromycin-resistant), but that additionally did not retain the donor plasmid (kanamycin-sensitive). These strains were rearrayed, frozen as glycerol stocks, and saved for further analysis.

For soft-agar motility screening, strains were inoculated from the rearrayed cultures into 100 μL SWT buffered with 50 mM HEPES and grown overnight. Omnitrays (Nunc, Rochester, NY) containing SWT 0.3% agar were inoculated, in duplicate, with 1 μL of each overnight culture using a 96-pin replicator (V&P Scientific, San Diego, CA). Soft-agar plates were then incubated at 28°C for 4-6 h and examined for alterations in swim colony morphology.

The final library contains 23,906 mutant strains, and is termed the MB Collection. This collection contains only trays that, upon screening for motility phenotypes, provided reproducible phenotypes across the entire agar tray during the motility screen. We observed a correlation between aberrant motility screen results and subsequent inability to regrow strains from plate freezer stocks. We attributed such results to harsh growth conditions during passage of the strains (*e.g.*, inadvertent heat shock). In this manner, motility screening provided a quality control step for the entire collection. Trays that did not pass this step were not included in the final collection or in the screen results.

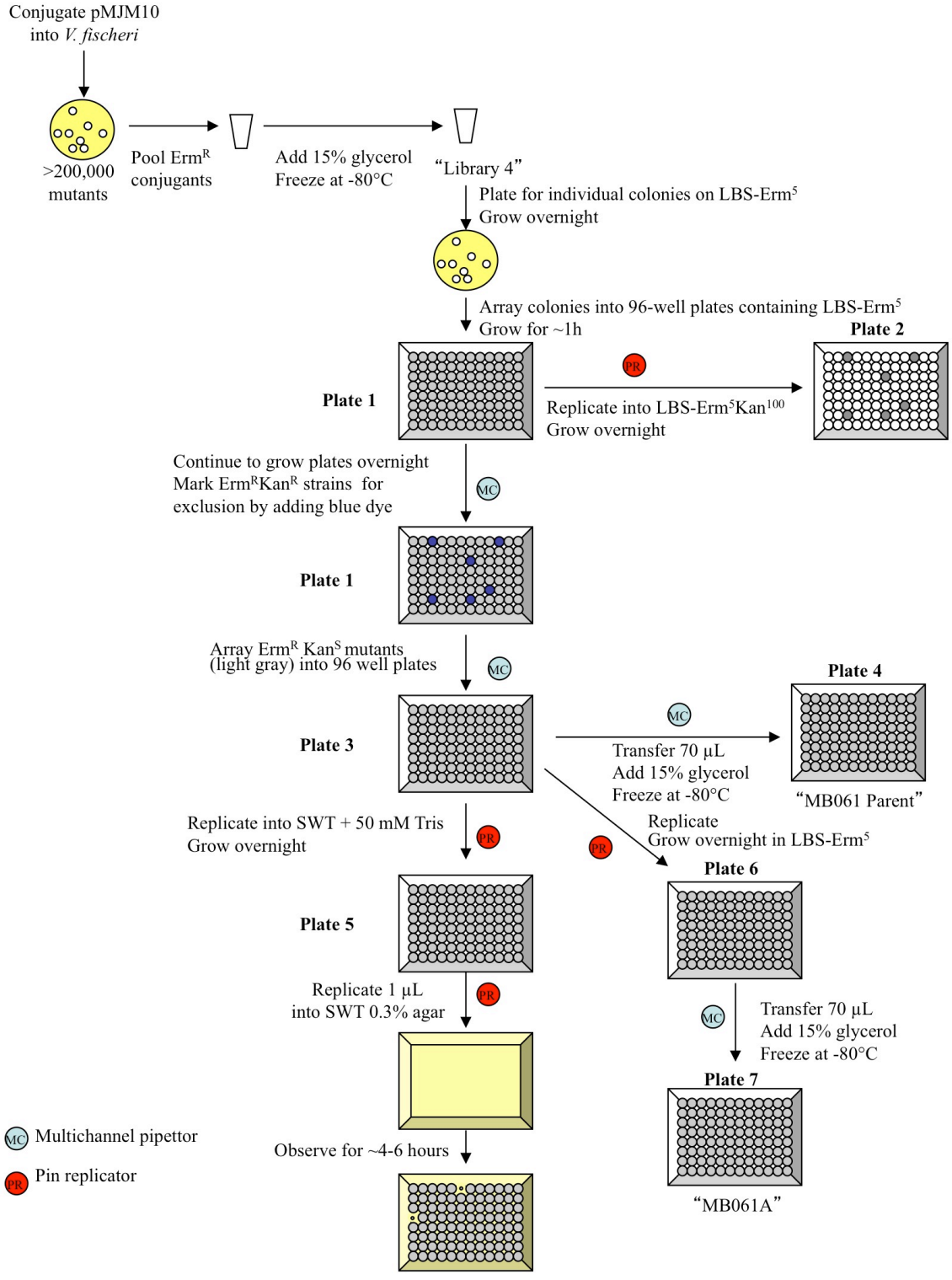
Conjugate pMJM10
into V. fischeri
>200,000
mutants
Pool Erm^R
conjugants
Add 15% glycerol
Freeze at -80°C
"Library 4"
Plate for individual colonies on LBS-Erm^5
Grow overnight
Array colonies into 96-well plates containing LBS-Erm^5
Grow for ~1h
Plate 1
Plate 2
PR
Replicate into LBS-Erm^5Kan^100
Grow overnight
Continue to grow plates overnight
Mark Erm^RKan^R strains for
exclusion by adding blue dye
MC
Plate 1
Array Erm^R Kan^S mutants
(light gray) into 96 well plates
MC
Plate 4
Plate 3
MC
Transfer 70 µL
Add 15% glycerol
Freeze at -80°C
"MB061 Parent"
Replicate into SWT + 50 mM Tris
Grow overnight
PR
PR
Replicate
Grow overnight in LBS-Erm^5
Plate 6
Plate 5
Replicate 1 µL
into SWT 0.3% agar
PR
MC
Transfer 70 µL
Add 15% glycerol
Freeze at -80°C
Plate 7
Observe for ~4-6 hours
"MB061A"
MC Multichannel pipettor
PR Pin replicator

Figure 2-1. Construction and soft-agar motility screening of a *V. fischeri* transposon-mutant collection. A schematic diagram demonstrating the method of library construction and motility screening utilized in this work.

The insertion site of the candidate amotile mutants were identified using arbitrarily-primed PCR as previously described (Caetano-Anolles, 1993, O'Toole *et al.*, 1999). Briefly, the transposon junction site was amplified from a diluted overnight culture in two successive rounds of PCR using primer sets ARB1/170Ext3, followed by ARB2/170Int3 (Table 2-2). The sample was submitted for sequencing to the DNA Sequencing Center at the University of Wisconsin Biotech Center (Madison, WI) with primer 170Seq1. In the event that this method did not yield a high quality sequence, arbitrarily primed PCR was repeated on purified genomic DNA collected using the Wizard SV Genomic DNA Purification kit (Promega, Madison, WI).

Motility studies

For individual soft-agar motility assays, cells were grown to an OD_{600} of ~0.3-0.4. Cultures were then normalized to an OD_{600} of 0.3, and 2 µl of each strain were inoculated into plates containing SWT supplemented with 0.3% agar. Plates were grown at 28°C for approximately 10-12 h, at which point the diameter of each swim colony was measured and plates were photographed, if desired.

In preparation for all microscopy, cells were grown in SWT broth with shaking at 28°C to an OD_{600} of ~0.3. For liquid motility and cell morphology studies, live cells were applied to a slide and examined by phase-contrast microscopy under a 40x objective. For examination of flagellar structures, cells were applied to Formvar-coated copper grids (Ted Pella Co., Tustin, CA) for 5 min, washed with sterile water for 30 s and negatively stained for 1 min with NanoW (Nanoprobes, Yaphank, NY). Grids were immediately examined using a

Philips CM120 transmission electron microscope (University of Wisconsin Medical School Electron Microscope Facility, Madison, WI).

Molecular cloning:

Campbell-type (insertion-duplication) mutagenesis using the suicide vector pEVS122 (Dunn *et al.*, 2005) was performed to generate disruptions in *motA1*, *motB1*, *motA2*, *motB2*, *fliL1*, *and fliL2*. Using the following primer pairs, ~200 bp of homology near the 5' end of each open reading frame (ORF) was amplified for each gene by PCR: *motA1*, motA1_campbellF and motA1_campbellR; *motB1*, motB1_campbellF and motB1_campbellR; *motA2*, motA2_campbellF and motA2_campbellR; *motB2*, motB2_campbellF and motB2_campbellR; *fliL1*, fliL1_campbellF and fliL1_campbellR; and *fliL2*, fliL2_campbellF and fliL2_campbellR (Table 2-2). The primer pairs also added XmaI and SphI restriction enzyme sites, which were used to clone the amplified products into the XmaI/SphI-digested pEVS122 using standard techniques. The resulting constructs were conjugated into *V. fischeri* ES114 (MJM1100 isolate) as previously described (Stabb *et al.*, 2002).

Complementation constructs were generated using the pES213-derived pVSV105 (Dunn *et al.*, 2006). For *flgOP*, *flgT*, *VF_1491*, *mutS*, and *fliL2*, each ORF and 350 bp upstream was amplified by PCR using the following primer pairs: *flgOP*, flgO_compF and flgP_compR; *flgT*, flgT_compF and flgT_compR; *VF_1491*, 1491_compF and 1491_compR; *mutS*, mutS_compF and mutS_compR; and *fliL2*, fliL2_compF and fliL2_compR. For *flgP* (primer pair flgP_compF and flgP_compR), *amiB* (primer pair amiB_compF and

amiB_compR), and *mukB* (primer pair mukB_compF and mukB_compR), which are located within predicted operons, amplification introduced a ribosome site, such that gene expression is driven by the *lacZα* promoter. The amplified products were directionally cloned into the multiple cloning site of pVSV105 (Dunn *et al.*, 2006), using standard molecular techniques. Both the complementation construct and vector control were conjugated into wild-type *V. fischeri* and the relevant mutant by triparental mating (Stabb *et al.*, 2002).

LacZ transcriptional fusions were constructed by amplification of the promoter region and subsequent cloning into SalI/AvrII-digested pAKD701, upstream of a promoterless *lacZ* (Dunn and Stabb, 2008). The primer pairs were designed to amplify ~350 bp upstream of the start codon and the first 120 bp of the ORF, as well as introduce SalI and AvrII restriction enzyme sites into the product. Primer pairs are as follows: *fliEp*, fliE_fusionF and fliE_fusionR; *flhAp*, flhA_fusionF and flhA_fusionR; *flrBp*, flrB_fusionF and flrB_fusionR; *fliKp*, fliK_fusionF and fliK_fusionR; *fliKp*, fliK_fusionF and fliK_fusionR; *flgAp*, flgA_fusionF and flgA_fusionR; *flgBp*, flgB_fusionF and flgB_fusionR; *flaDp*, flaD_fusionF and flaD_fusionR; *motXp*, motX_fusionF and motX_fusionR; *motA1p*, motA1_fusionF and motA1_fusionR; *flgOp*, flgO_fusionF and flgO_fusionR; and *flgTp*, flgT_fusionF and flgT_fusionR. Reporter constructs were introduced to wild-type *V. fischeri* and the *flrA*::Tn*erm* mutant by tri-parental mating.

Transcriptional studies

For microarray analysis, wild-type and Δ*flrA* cells were grown in SWT with shaking at 28 °C with an OD_{600} of ~0.5. RNA from two biological replicates was harvested, labeled

and hybridized to the *V. fischeri* Affymetrix chip, as previously described (Wang *et al.*, 2010, Wier *et al.*, 2010). In β-galactosidase assay studies, wild type or the *flrA*::Tn*erm* mutant harboring reporter constructs were similarly cultured in SWT medium with shaking at 28 °C to an OD_{600} of ~0.5. β-galactosidase activity was measured from four biological replicates, using a modified microtiter dish method (Slauch and Silhavy, 1991, Studer *et al.*, 2008). The relative units of β-galactosidase activity were calculated using the following formula: $(V_{max})/(OD_{600}) \times$ volume [ml]).

Bioinformatic analyses

Microarray analysis was performed with Cyber-T software (Baldi and Long, 2001), using a cut-off of at least a two-fold change and a p-value < 0.01. The Database of prOkaryotic OpeRons (DOOR) was used to analysis of the *V. fischeri* ES114 genome and predict operon structure (Dam *et al.*, 2007). Functional classes, as listed in Figure 2-5, were informed, in part, by the cellular role categorization provided by the J. Craig Venter Institute Comprehensive Microbial Resource (Peterson *et al.*, 2001).

Squid experiments

Newly hatched squid were colonized using standard methods (Naughton and Mandel, 2012), except that the final culturing was done in SWT broth, and as described in individual experiments. The inoculation time was listed for each experiment. At the end of each experiment, the luminescence of individual squid was measured using a TD-20/20 luminometer (Turner Biosystems, Sunnyvale, CA). Squid were considered colonized to

luminous levels if the reading was above 10 relative light units (RLUs); background readings were usually less than 2 RLUs. For experiments in which bacterial load was determined, squid were surface-sterilized by storage at -80°C. Individual squid were then homogenized, and each homogenate was diluted and plated for colony forming units (CFU) on LBS agar.

RESULTS:

Construction and soft-agar motility screening of a *V. fischeri* transposon mutant collection

To investigate the genetic basis of flagellar motility, we randomly mutagenized *V. fischeri* ES114 by Tn*5* mutagenesis with the erythromycin resistance-encoding transposon carried on pMJM10, and arrayed the mutants into 96-well trays for individual analysis. Because a subset of transposon insertions additionally retain the transposon/transposase donor plasmid (Lyell *et al.*, 2008), we screened for strains that contained a transposon insertion (*i.e.,* erythromycin-resistant), but that did not retain the donor plasmid (*i.e.,* kanamycin sensitive). The resulting 23,904 strains, named the MB mutant collection, were rearrayed, frozen as glycerol stocks, and used for further analysis (Figure2-1, and Materials and Methods).

V. fischeri mutants that were defective in swimming motility were identified by performing a multiplex soft-agar motility assay in agar trays. Briefly, each tray of mutant strains was replicated to fresh medium and grown overnight. The cultures were then pin-replicated into trays containing SWT medium containing 0.3% agar in which the cells from all 96-wells swam out from their center-point in synchrony (Figure 2-2A). Using this assay, 205 mutants characterized as candidate amotile strains were selected; almost all (97%) of these transposon insertion sites were located on Chromosome 1 (Figure 2-2B). One representative mutant was selected per gene (Table 2-1) and analyzed in a controlled soft-agar motility assay in which culture densities were normalized by optical density. Mutants with less than 30% of a wild-type migration distance were designated as severely affected in flagellar motility

A

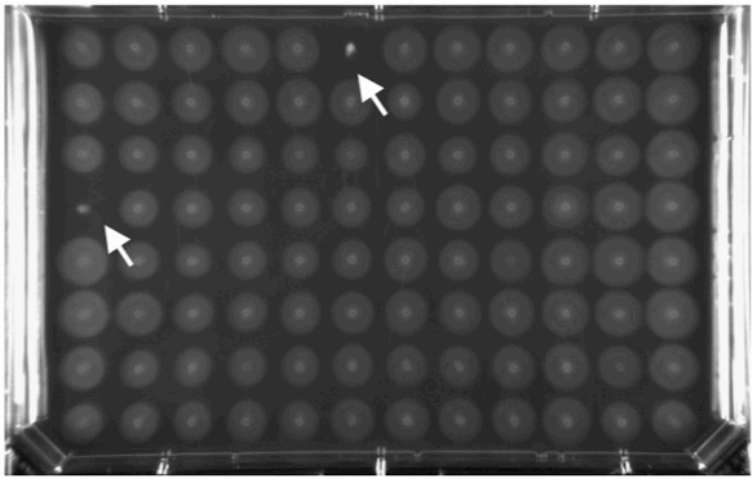

B

Library size	23904
Candidate non-motile mutants	205
Insertion sites identified	193[a]
Independent insertion mutants[b]	133
Chromosome 1 mutants	129
Insertion directionality (+/-)	75/54
Insertion location (coding sequence/intergenic)	126/3
Chromosome 2 mutants	4
Insertion directionality (+/-)	2/2
Insertion location (coding sequence/intergenic)	4/0
Plasmid mutants	0

[a] Value excludes 12 mutants whose insertion site could not be identified after >5 arb reactions (3), mutants that maintained the vector (3), and mutants in 1 of the 12 *rrn* loci (6).
[b] Minimum number of distinct mutants

Figure 2-2. Soft-agar motility screening of a *V. fischeri* transposon mutant library. (A) A representative soft-agar motility plate. White arrows indicate strains considered as candidate amotile mutants. (B) Summary of the characteristics of the transposon mutant library and the results of the soft-agar motility screen. Directionality refers to the direction of the transposon's *erm* cassette relative to chromosome nucleotide orientation as deposited in GenBank.

(Table 2-3). Of the 66 representative mutants, 21 had motility that were not as severely affected as the 30% threshold, yet still exhibited reproducible motility less than wild type in the individual assays (Table 2-4). These reduced-motility mutants largely mapped to the lipopolysaccharide biosynthesis locus, defects in which have been tied to altered motility in several organisms (Cullen and Trent, 2010, Girgis *et al.*, 2007). However, three mutants in this category had insertions in homologs of flagellar genes. These genes include *flgL*, encoding a hook-associated protein, as well as *flaA* and *flaD*, two of the six flagellin-encoding genes in the *V. fischeri* genome. The phenotype of the *flaA* mutant is consistent with a previous report (Millikan and Ruby, 2004), but the requirement for *flaD* in normal soft-agar motility represents a novel finding. Other mutants within this category were disrupted in genes whose mutation is likely to cause growth defects, or in genes encoding hypothetical proteins. As these 21 moderately defective mutants exhibited a weaker phenotype upon secondary screening, they were not pursued in this study.

Of the 45 representative mutants with severe defects in flagellar motility, the proteins encoded by the disrupted genes were categorized into 5 functional groups (Table 2-3): (i) predicted and known flagellar regulatory proteins, such as the flagellar master activator FlrA; (ii) proteins with homologs that are involved in the flagellar secretory/export apparatus or the flagellum structure itself; (iii) motor proteins; (iv) chemotaxis-related proteins; and, (v) a final collection of 9 mutants that were disrupted in, or upstream of, genes we did not *a priori* predict to be involved in flagellar motility. Mutants in this fifth group map to two subsets: genes related to cell division and DNA repair, and genes encoding proteins that were of unknown function. There is also one insertion in an intergenic region, whose effect is not

Table 2-3. Characterization of transposon mutants with greatly reduced (<30%) soft-agar motility

Function	ORF	Gene	Description	% wild-type motility[a]	FlrA-activation[b]	# independent mutants	Predicted operon structure[c]
Regulation	VF_0387	*rpoN*	RNA polymerase sigma-54 factor	0	NS[d]	7	*kdsDC-0390-lptAB-**rpoN**-lpfptsN-yhbJ-0383*[e]
	VF_1856	*flrA*	Sigma-54-dependent regulator	0	ND[f]	2	***flrA***
	VF_1854	*flrC*	Two-component response regulator	0	8.1	4	***flrBC***
	VF_1855	*flrB*	Two-component sensor kinase	17	16	1	***flrB**C*
	VF_1834	*fliA*	RNA polymerase sigma-28 factor	0	NS	2	*flhAFG-**fliA**-cheYZAB-1829-1828-cheW-1825*
	VF_1835	*flhG*	Flagellar synthesis regulator	0	NS	1	***flhA**FG-fliA-cheYZAB-1829-1828-cheW-1825*
	VF_1836	*flhF*	Flagellar regulator	23	2.6	4	***flhAF**G-fliA-cheYZAB-1829-1828-cheW-1825*
Structure/	VF_1837	*flhA*	Flagellar biosynthesis protein	0	NS	5	***flhA**FG-fliA-cheYZAB-1829-1828-cheW-1825*
Secretion	VF_1840	*fliR*	Flagellar biosynthesis protein	0	2.9	1	***fliL1**MNOPQ**R***
	VF_1844	*fliN*	Flagellar motor switch component	0	6.4	1	***fliL1**MNOPQR*
	VF_1845	*fliM*	Flagellar motor switch protein	0	6.8	1	***fliL1M**NOPQR*
	VF_1846	*fliL1*	Flagellar basal body-associated protein	0	8.1	1	***fliL1**MNOPQR*
	VF_1847	*fliK*	Flagellar hook length control protein	0	9.2	2	***fliK***
	VF_1849	*fliI*	Flagellum-specific ATP synthase	0	NS	2	***fliHI**J*
	VF_1850	*fliH*	Flagellar assembly protein	0	NS	3	***fliH**IJ*
	VF_1851	*fliG*	Flagellar motor switch protein	0	6.8	5	***fliEF**G*
	VF_1852	*fliF*	Flagellar M ring protein	0	6.6	2	***fliE**FG*
	VF_1860	*fliD*	Flagellar hook-associated protein 2	19	7.4	3	*flaG-**fliD** -flaI-fliS*
	VF_1868	*flgK*	Flagellar hook-associated protein 1	0	41	4	***flgK**L*
	VF_1870	*flgI*	Flagellar P ring protein	0	3.5	5	***flgFGHI***
	VF_1871	*flgH*	Flagellar L ring protein	0	6.3	1	***flgFGH**I*
	VF_1872	*flgG*	Flagellar distal rod protein	0	12	2	***flgF**GHI*
	VF_1873	*flgF*	Flagellar proximal rod protein	0	9.6	2	***flgF**GHI*
	VF_1874	*flgE*	Flagellar hook protein	0	5.7	1	***flgE***
	igVF_1874		(intergenic region)	0	ND	1	
	VF_1875	*flgD*	Flagellar hook capping protein	0	7.5	2	***flgBC**D*
	VF_1882	*flgN*	Flagellar chaperone	0	2.5	1	***flgMN***
Motor	VF_0714	*motA1*	Flagellar motor protein	0	6.3	1	***motA1**B1*
	VF_0715	*motB1*	Flagellar motor protein	0	3.4	1	***motA1B1***
	VF_0926	*motY*	Flagellar motor protein	0	2.6	2	***motY***
	VF_2317	*motX*	Flagellar motor protein	0	11	2	***motX***
Chemotaxis	VF_1826	*cheW*	Chemotaxis coupling protein	10	2.6	1	*flhAFG-fliA-cheYZAB-1829-1828-**cheW**-1825*
	VF_1830	*cheB*	Chemotaxis methyl esterase	24	2.1	2	*flhAFG-fliA-**cheY**ZA**B**-1829-1828-cheW-1825*
	VF_1831	*cheA*	Chemotaxis histidine autokinase	7	2.0	6	*flhAFG-fliA-**cheY**ZA**B**-1829-1828-cheW-1825*
	VF_1832	*cheZ*	CheY phosphatase	8	2.2	1	*flhAFG-fliA-**cheYZ**AB-1829-1828-cheW-1825*
	VF_1833	*cheY*	Chemotaxis response regulator	6	2.2	1	*flhAFG-fliA-**cheY**ZAB-1829-1828-cheW-1825*
Unexpected	igVF_0135		(intergenic region)	21	ND	1	
	VF_0534	*mutS*[g]	Methyl-directed mismatch repair protein	0	NS	1	***mutS***
	VF_1491		Hypothetical protein	9	NS	3	***1491***
	VF_1883	*flgP*	Flagellar motility-associated protein	0	8.7	4	***flgOP***
	VF_1884	*flgO*	Flagellar motility-associated protein	0	10	2	***flgO**P*
	VF_1885	*flgT*	Flagellar motility-associated protein	0	NS	1	***flgT***
	VF_2326	*amiB*	N-acetylmuramoyl-l-alanine amidase II	0	NS	1	*yjeE-**amiB**-mutL-miaA*
	VF_A0430	*mukF*	Calcium-binding protein involved in chromosome partioning	23	NS	1	*smtA-**mukF**EB*
	VF_A0432	*mukB*	Fused chromosome partitioning protein	22	NS	2	*smtA-**mukFEB***

[a] As scored by the normalized soft-agar motility assay described in Materials and Methods

[b] FlrA-activation is defined as the fold-change of gene expression in wild type as compared to Δ*flrA*, as determined by microarray analysis

[c] Predicted operon structure based on DOOR (Database of prOkaryotic OpeRons) analysis of the *V. fischeri* genome

[d] NS, not significant at $p \leq 0.01$ and fold-change ≥ 2

[e] Four-digit numbers indicate locus tags and should be read as preceded by "*VF_*"

[f] ND, not determined

[g] When *mutS* is expressed *in trans*, the complemented strain does not regain the ability to swim through soft agar (data not shown), indicating that *mutS* expression does not directly mediate flagellar motility in this strain. MutS is a protein involved in DNA mismatch repair, and the loss of this function results in strains with higher mutation rates. We hypothesize that the mutagenic nature of the *mutS* strain enabled a secondary mutation that is responsible for the amotile phenotype, and we will not follow up on this mutant in this study.

Table 2-4. Description of mutants with moderately reduced (30-90%) soft-agar motility

ORF	Gene	Description	% wild-type motility[a]	FlrA-activation[b]	# independent insertions	Predicted operon structure[c]	Potential reason for defect
VF_0077		2-polyprenyl-3-methyl-5-hydroxy-6-metoxy-1,4-benzoquinol methylase	74	NS[d]	1	***0077***-*ihl0079*[e]	Altered LPS/surface structure
VF_0167	*rffH*	Glucose-1-phosphate thymidylyltransferase	44	NS	1	***rffGH***-*rfbC-rmlB-rfbX-0171-0172-0173-2581-0174-0175-0176-0177-0178-kpsF*	Altered LPS/surface structure
VF_0169	*rmlB*	dTDP-glucose-4,6-dehydratase	56	NS	1	*rffGH-rfbC-**rmlB**-rfbX-0171-0172-0173-2581-0174-0175-0176-0177-0178-kpsF*	Altered LPS/surface structure
VF_0170	*rfbX*	Polisoprenol-linked O-antigen transporter	49	NS	3	*rffGH-rfbC-rmlB-**rfbX**-0171-0172-0173-2581-0174-0175-0176-0177-0178-kpsF*	Altered LPS/surface structure
VF_0171		Hypothetical protein	40	NS	1	*rffGH-rfbC-rmlB-rfbX-**0171**-0172-0173-2581-0174-0175-0176-0177-0178-kpsF*	Altered LPS/surface structure
VF_0172		O-acetyltransferase	39	NS	1	*rffGH-rfbC-rmlB-rfbX-0171-**0172**-0173-2581-0174-0175-0176-0177-0178-kpsF*	Altered LPS/surface structure
VF_0173		Hypothetical protein	43	NS	1	*rffGH-rfbC-rmlB-rfbX-0171-0172-**0173**-2581-0174-0175-0176-0177-0178-kpsF*	Altered LPS/surface structure
VF_2581		Hypothetical membrane protein	55	NS	2	*rffGH-rfbC-rmlB-rfbX-0171-0172-0173-**2581**-0174-0175-0176-0177-0178-kpsF*	Altered LPS/surface structure
VF_0174		beta-D-GlcNAc beta-1,3-galactosyltransferase	49	NS	3	*rffGH-rfbC-rmlB-rfbX-0171-0172-0173-2581-**0174**-0175-0176-0177-0178-kpsF*	Altered LPS/surface structure
VF_0189		Hypothetical membrane protein	73	NS	1	*0187-0188-**0189**-0190*	Altered LPS/surface structure
VF_0192	*fnlB*	UDP-2-acetamido-2,6-dideoxy-beta-L-talose 4-dehydrogenase	69	NS	2	***fnlAB***-*rffE-wbjE-0195*-0196-*0197*	Altered LPS/surface structure
VF_0365	*mshB*	Mannose-sensitive hemagglutinin pilin protein	87	NS	1	***mshB***	Unknown
VF_1697		Hypothetical protein	32	NS	4	***1697***	Unknown
igVF_1837		(intergenic region)	30	ND[f]	1		Incomplete flagellar structures
VF_1863	*flaD*	Flagellin	60	52	2	***flaD***	Incomplete flagellar structures
VF_1866	*flaA*	Flagellin	38	32	2	***flaA***	Incomplete flagellar structures
VF_1867	*flgL*	Flagellar hook-associated protein 3	56	8.7	5	***flgKL***	Incomplete flagellar structures
VF_2174	*can*	Carbonic anhydrase	80	NS	1	***can***	Growth defect
VF_A0058		Hypothetical protein	51	NS	1	*A0059-**A0058**-A0057*	Unknown
		16S rRNA	56	ND	3		Growth defect
		23S rRNA	56	ND	3		Growth defect

[a] As scored by the normalized soft-agar motility assay described in Materials and Methods

[b] FlrA-activation is defined as the fold-change of gene expression in wild type as compared to Δ*flrA*, as determined by microarray analysis

[c] Predicted operon structure based on DOOR analysis of the *V. fischeri* genome

[d] NS, not significant at $p \leq 0.01$ and fold-change ≥ 2

[e] Four-digit numbers indicate locus tags and should be read as preceded by "*VF_*"

[f] ND, not determined

clear. In short, this study has identified mutants disrupted in 38 homologs of previously identified motility genes (33 of which are new for *V. fischeri*), and seven additional genes that are non-canonically "motility" genes, but that have severe motility defects when disrupted by a transposon. We next utilized this array of mutants to examine the role of motility in symbiotic initiation.

Flagellar motility, but not chemotaxis, is required for entrance into a productive symbiosis with juvenile *E. scolopes*

To elucidate the roles of flagellar motility and chemotaxis in the initiation of the vibrio-squid symbiosis, strains representing the four primary functional groups of motility mutants isolated from the screen (Table 2-3) were exposed to juvenile *E. scolopes* to assay their ability to enter into a productive (*i.e.*, detectably luminescent) symbiosis (Figure 2-3). Regardless of their grouping, mutants that were unable to migrate through soft agar did not colonize juvenile squid to the level at which luminescence is detectable (*i.e.*, ~1% wild type, (Graf and Ruby, 1998)), even though all strains were able to produce wild-type levels of light in culture.

Transposon mutants in *fliD*, *flaD*, *cheA*, and *cheZ*, which were all able to migrate through soft agar to some level and also exhibited swimming motility in liquid, were able to colonize at least a portion of squid to luminous levels. The percentage of animals colonized by the *fliD*::Tn*erm* mutant, which has 19% of the soft-agar motility of wild type (Figure 2-3), is similarly reduced relative to squid exposed to wild-type *V. fischeri*, suggesting that motility rate contributes to efficiency even under these permissive conditions, in which the squid are

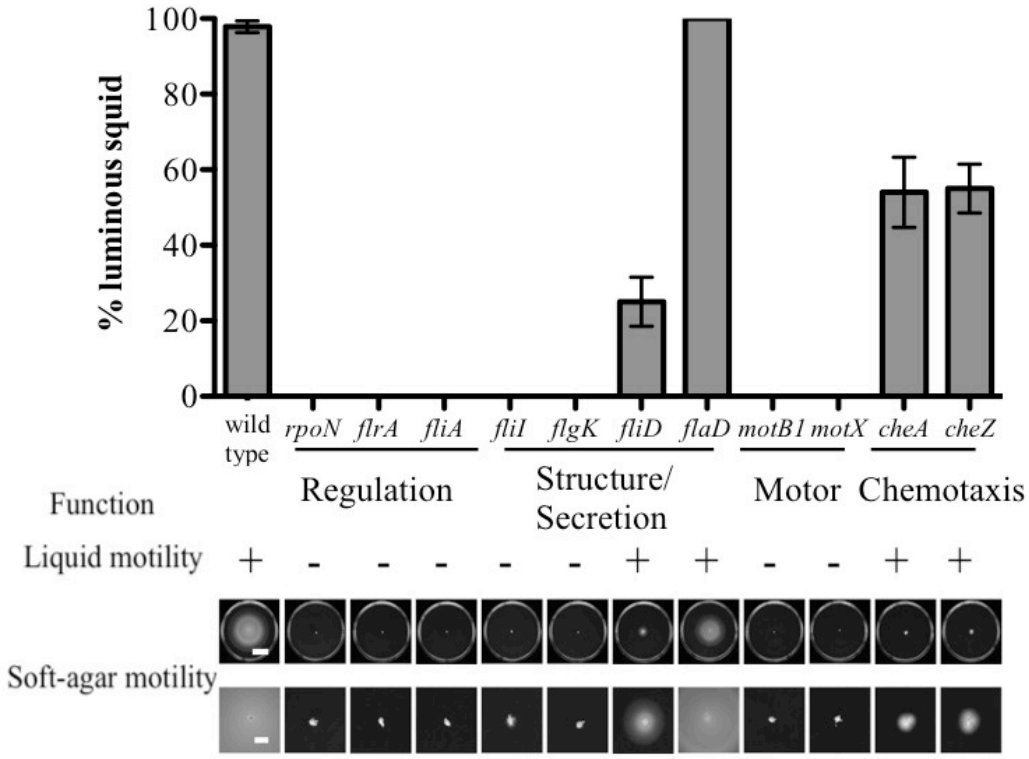

Figure 2-3. Entrance into a productive symbiosis with juvenile *E. scolopes* by selected swimming-motility mutants. Squid were exposed to ~8000 CFU per mL for 24 h, transferred to FSIO, and the percentage that produced detectable luminescence at 48 h post-colonization was determined. Functional groups indicated beneath the strains correspond to those in Table 2-3. Liquid motility and soft-agar motility assays were performed as described in Materials and Methods. White scale bars in wild-type soft-agar motility plates represent a distance of 20 mm in whole-plate views (top), and 5 mm in the higher-magnification images (bottom).

exposed to the inoculating bacteria for 24 h. The *cheA* and *cheZ* mutants colonized only about 50% of the squid to luminous levels, suggesting that, while chemotaxis is not essential for initiation, it is still required for wild-type colonization efficiency.

FlrA regulates both flagellar and non-flagellar genes

To more fully examine the relationship between genes required for normal motility and those activated by FlrA, we coupled our functional studies with a complete transcriptional profile of the flagellar regulon in *V. fischeri*. Prokaryotic flagellar systems have been models for hierarchical regulation, and flagellar-gene discovery based on transcriptional profiling has proven successful in other bacteria(Frye *et al.*, 2006, Morris *et al.*, 2008). To identify the flagellar regulon of *V. fischeri*, we used a whole-genome microarray analysis that compared the transcriptomes of the wild-type strain and an isogenic Δ*flrA*::*kan* strain. In the absence of FlrA, the expression of 131 genes was significantly reduced, including 39 predicted flagellar and chemotaxis genes (Table 2-5).

Control of flagellar promoters by FlrA was confirmed using β-galactosidase transcriptional reporter fusions (Figure 2-4). Of the nine flagellar promoters tested, eight constructs exhibited significantly reduced β-galactosidase activity in the *flrA*::Tn*erm* mutant relative to wild type. The *flgA'-lacZ*$^{+}$ construct yielded similar levels of β-galactosidase activity regardless of strain background, consistent with both the microarray data (Table 2-5) and previous work performed with its ortholog in *V. cholerae* (Prouty *et al.*, 2001). Of the novel genes required for normal flagellar elaboration, only the *flgO'-lacZ*$^{+}$ reporter responded to the absence of FlrA, suggesting that the promoter serving *flgO* and *flgP* (discussed later).

Table 2-5. All genes differentially regulated in the absence of FlrA

Locus Tag	Fold change	Gene	Description
VF_0094	5.7		Diguanylate cyclase
VF_0714	6.3	*motA1*	Flagellar motor protein
VF_0715	3.4	*motB1*	Flagellar motor protein
VF_0777	10.2		Methyl-accepting chemotaxis protein
VF_0915	4.5		Hypothetical protein
VF_0920	49.5		Hypothetical protein
VF_0926	2.6	*motY*	Flagellar motor protein
VF_1125	2.5		Hypothetical protein
VF_1330	2.5		Carbohydrate binding domain-containing protein
VF_1422	2.2		von Willebrand factor type A domain protein
VF_1427	2.2	*aslA*	Acrylsulfatase like protein
VF_1493	2.6		Hypothetical protein
VF_1556	3.4	*pldA*	Outer membrane phospholipase A
VF_1559	2.4		Hypothetical protein
VF_1771	2.2	*prkA*	Serine kinase
VF_1774	2.3	*ycgB*	SpoVR family protein
VF_1789	17.4		Methyl-accepting chemotaxis protein
VF_1827	2.6	*cheW*	Chemotaxis coupling protein
VF_1829	2.3	*parA2*	Chromosome partioning protein
VF_1830	2.1	*cheB*	Chemotaxis methyl esterase
VF_1831	2.0	*cheA*	Chemotaxis histidine kinase
VF_1832	2.2	*cheZ*	Chemotaxis phosphatase
VF_1833	2.2	*cheY*	Chemotaxis response regulator
VF_1836	2.6	*flhF*	Flagellar regulator
VF_1839	2.3	*flhB*	Flagellar biosynthesis protein
VF_1840	2.9	*fliR*	Flagellar biosynthesis protein
VF_1841	3.9	*fliQ*	Flagellar biosynthesis protein
VF_1842	3.2	*fliP*	Flagellar biosynthesis protein
VF_1843	7.1	*fliO*	Flagellar biosynthesis protein
VF_1844	6.4	*fliN*	Flagellar motor switch component
VF_1845	6.8	*fliM*	Flagellar motor switch protein
VF_1846	8.1	*fliL1*	Flagellar basal body-associated protein
VF_1847	9.2	*fliK*	Flagellar hook length control protein
VF_1851	6.7	*fliG*	Flagellar motor switch protein
VF_1852	6.6	*fliF*	Flagellar M-ring protein
VF_1853	16.1	*fliE*	Flagellar hook-basal body protein
VF_1854	8.1	*flrC*	Flagellar two-component response regulator
VF_1855	16.1	*flrB*	Flagellar two-component sensor kinase
VF_1856	17.5	*flrA*	Flagellar sigma-54-dependent transcriptional activator
VF_1858	8.8	*fliS*	Flagellin chaperone
VF_1859	8.4	*flaI*	Flagellar protein
VF_1860	7.4	*fliD*	Flagellar hook-associated protein 2
VF_1861	22.7	*flaG*	Flagellar protein
VF_1862	43.3	*flaE*	Flagellin
VF_1863	51.5	*flaD*	Flagellin
VF_1864	19.7	*flaC*	Flagellin
VF_1865	5.1	*flaB*	Flagellin

VF_1866	32.0	*flaA*	Flagellin
VF_1867	8.7	*flgL*	Flagellar hook-associated protein 3
VF_1868	41.3	*flgK*	Flagellar hook-associated protein 1
VF_1869	12.7	*flgJ*	Flagellum-specific peptidoglycan hydrolase
VF_1870	3.5	*flgI*	Flagellar P-ring protein
VF_1871	6.3	*flgH*	Flagellar L ring protein
VF_1872	12.3	*flgG*	Flagellar distal rod protein
VF_1873	9.6	*flgF*	Flagellar proximal rod protein
VF_1874	5.7	*flgE*	Flagellar hook protein
VF_1875	7.5	*flgD*	Flagellar hook capping protein
VF_1876	8.5	*flgC*	Flagellar proximal rod protein
VF_1877	8.2	*flgB*	Flagellar proximal rod protein
VF_1882	2.5	*flgN*	Chaperone
VF_1883	8.7	*flgP*	Flagellar motility-associate protein
VF_1884	10.1	*flgO*	Flagellar motility-associate protein
VF_2009	3.3		Hypothetical protein
VF_2010	2.4		Hypothetical protein
VF_2011	2.2		Hypothetical protein
VF_2012	2.3		Major capsid protein
VF_2013	3.3		Probable capsid scaffolding protein
VF_2015	2.9		Capsid scaffolding protein
VF_2016	2.5		Hypothetical protein
VF_2017	2.9		L-alanyl-D-glutamate peptidase
VF_2025	2.9		Phade baseplate assembly protein
VF_2026	2.6		Phage tail protein
VF_2027	3.1		Hypothetical protein
VF_2029	2.0		Hypothetical protein
VF_2031	2.4		Conserved hypothetical protein
VF_2033	3.2		Hypothetical bacteriophage protein
VF_2034	3.2		Hypothetical protein
VF_2035	2.5		Hypothetical protein
VF_2036	3.4		Phage regulatory protein (CII)
VF_2079	12.1	*flaF*	Flagellin
VF_2317	11.1	*motX*	Flagellar motor protein
VF_2446	2.2	*fliL2*	Flagellar basal body-associated protein
VF_A0071	2.3	*hnoX*	Heme nitric oxide binding protein
VF_A0287	16.1		Hypothetical protein
VF_A0325	5.9		Methyl-accepting chemotaxis protein
VF_A0502	6.3		Hypothetical protein
VF_A0564	11.2	*traF*	TraF protein
VF_A0677	10.3		Methyl-accepting chemotaxis protein
VF_A0715	7.5		Chitodextrinase precursor
VF_A0788	2.7		Hypothetical protein
VF_A0802	2.7	*cheV2*	CheW/CheY hybrid
VF_A0834	9.7		NirV precursor
VF_A0856	6.7		Hypothetical protein
VF_A1014	4.2		Diguanylate phosphodiesterase
VF_A1015	4.3	*rpoQ*	Quorum-sensing regulated RpoS-like sigma factor
VF_A1016	2.4		Two-component sensory histidine kinase
VF_A1017	2.7		Two-component response regulator
VF_B20	3.5		Hypothetical protein
VF_B21	4.8		Hypothetical protein

VF_B22	3.0		Hypothetical protein
VF_B23	3.6		Hypothetical protein
VF_B24	3.8		Hypothetical protein
VF_B25	3.4		Hypothetical protein
VF_B26	3.1		Hypothetical protein
VF_B27	3.9		Hypothetical protein
VF_B28	3.6		Hypothetical protein
VF_B29	3.4	*sbcC*	Exonuclease
VF_B30	3.1		Hypothetical protein
VF_B31	3.4		Hypothetical protein
VF_B32	3.3		Transporter
VF_B33	3.0		Hypothetical protein
VF_B34	2.9		Hypothetical protein
VF_B37	2.9		Hypothetical protein
VF_B38	3.4		Attachment mediating VirB2-like protein
VF_B39	2.7		VirB4 ATPase
VF_B40	4.0		Channel protein VirB8
VF_B41	3.0		Channel protein VirB9
VF_B42	3.2		Channel protein VirB10
VF_B43	2.6		VirB11 ATPase
VF_B44	2.8		Protein VirD4
VF_B45	3.1		Single-strand DNA binding protein
VF_B46	4.3		DNA topoisomerase III
VF_B47	3.6		Outer membrane protein
VF_B48	4.1		Hypothetical protein
VF_B49	3.2		Hypothetical protein
VF_B50	2.7		Relaxase
VF_B51	2.8		Hypothetical protein
VF_B52	2.8		Hypothetical protein
VF_B53	3.0		Hypothetical protein
VF_B54	3.3		Attachment mediating VirB5-like protein
VF_B55	2.5		Channel protein VirB6
VF_0349	-2.2		Chain length regulator, EPS biosynthesis protein
VF_0350	-2.2		Polysaccharise export periplasmic protein
VF_0352	-3.0		UDP-glucose lipid carrier transferase
VF_0510	-3.7		Fimbrial protein
VF_A0191	-2.4		FhuE receptor precursor
VF_A0193	-2.0		TolQ protein
VF_A0199	-2.1	*oppD*	Chitooligosaccharide transport ATP-binding protein
VF_A0328	-2.1	*yiaD*	Outer membrane lipoprotein
VF_A0329	-3.4		Hypothetical protein
VF_A0330	-3.0		Hypothetical protein
VF_A0331	-2.6		Hypothetical protein
VF_A0332	-2.7		TonB system receptor
VF_A0333	-2.5	*ptrB*	Oligopeptidase B
VF_A0610	-2.5		Hypothetical protein
VF_A0848	-2.4		Hypothetical protein
VF_A0885	-2.3		Hypothetical protein
VF_A1038	-2.1		Diguanylate phosphodiesterase

[a] Fold change of wild-type expression relative to Δ*flrA* condition, (*i.e.*, positive values indicate putative activation by FlrA)

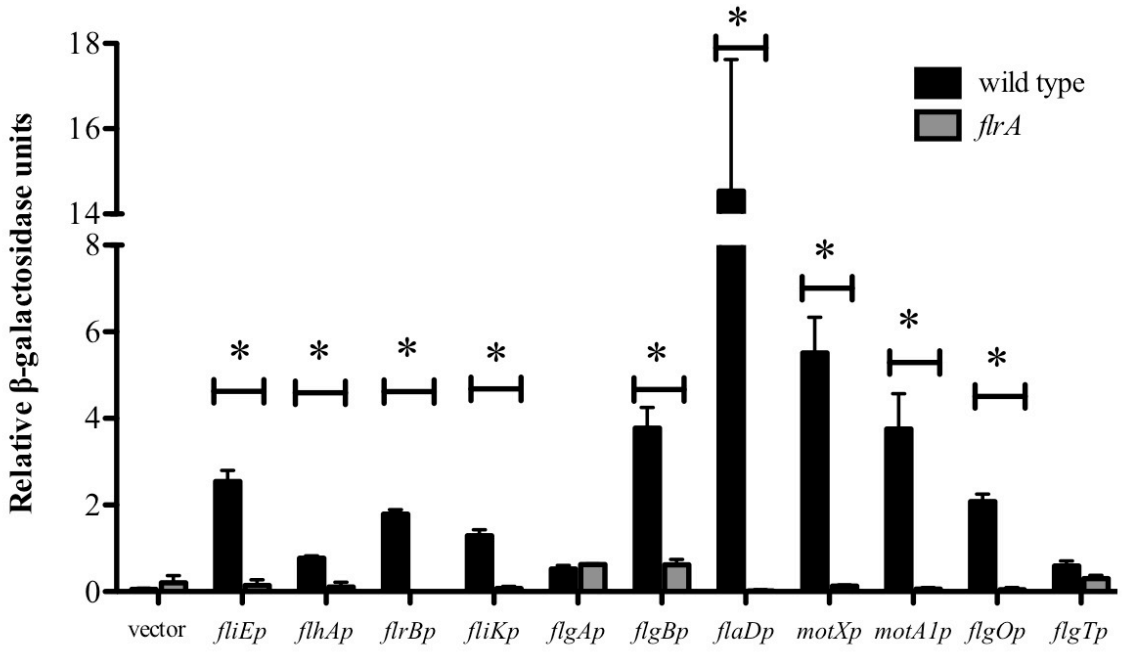

Figure 2-4. Flagellar-gene promoter activities in wild-type and *flrA*-mutant strains. Promoters for 11 genes were transcriptionally fused to *lacZ* as described in Materials and Methods, and β-galactosidase activity was measured in wild-type and *flrA*-mutant strains after growth in SWT to an OD_{600} of ~ 0.3. Asterisks indicate both a significance difference at $p \leq 0.05$ using a Student's t-test, and a fold-change ≥ 2.

Confirming the microarray data, the activity of the *flgT'-lacZ*$^{+}$ reporter, while slightly reduced, was not significantly changed in the absence of FlrA.

We compared (i) the genes in the microarray analysis that were activated by FlrA (*i.e.* down-regulated in Δ*flrA*::*kan* relative to wild type) with (ii) the genes that the genetic screen suggested were required for motility. The overlap between these two groups was considered to constitute the 'core flagellar genes' (Figure 2-5). This core includes predicted flagellar and chemotaxis genes, as well as *flgO* and *flgP*. Some predicted flagellar genes, which we had anticipated finding in this core, were found in only one of the two data sets. For instance, *flaC*, which encodes one of the six flagellin proteins, is FlrA-controlled but not required for flagellar motility (Millikan and Ruby, 2004). Interestingly, a paralog of one flagellar gene, *fliL2*, (VF_2446), which can be found in many *Vibrio* species and whose role in motility is unknown, was reduced in the absence of FlrA. Conversely, the flagellum-specific ATP synthase-encoding gene *fliI* was required for soft-agar motility (Table 2-3), but was not significantly regulated in the FlrA transcriptomic study (Table 2-5). A small subset of predicted flagellar genes, including *flgA*, is absent from both data sets (data not shown), suggesting that either, (i) even in combination, these techniques are not fully comprehensive, or (ii) these genes are disassociated from the flagellar regulatory process in *V. fischeri*.

The FlrA-regulon also include a large number of genes predicted to be found among mobile elements, specifically the cryptic phages encoded on Chromosome 1 of *V. fischeri* ES114, as well as genes located on this strain's large conjugative plasmid. In addition, 17 genes were upregulated in the Δ*flrA*::*kan* strain between 2- and 4-fold, suggesting negative regulation by FlrA; however, these targets were annotated to have functions unrelated to

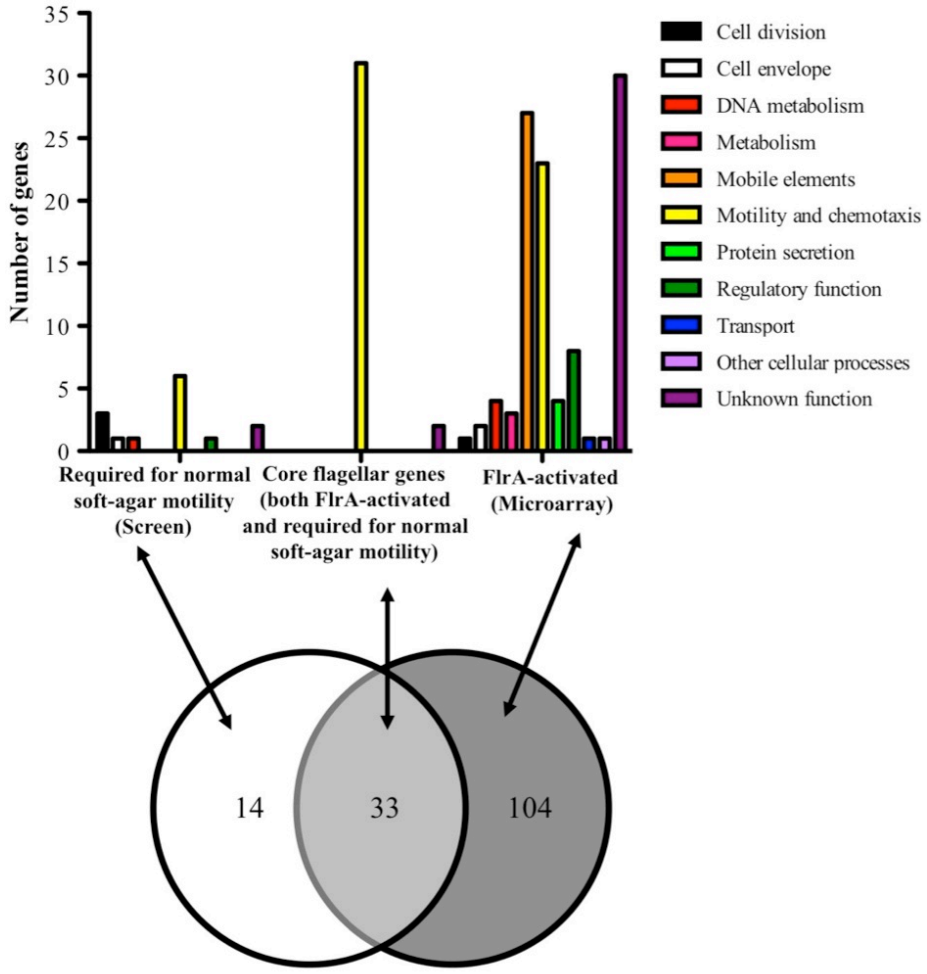

Figure 2-5. Comparison of soft-agar motility screening and microarray analyses. The set of genes required for normal soft-agar motility (genes disrupted in those mutants with severe defects; Table 2-3) were compared to the flagellar regulon (FlrA-activated genes; Table 2-5). The 33 genes present in both data sets are considered 'core flagellar genes', and include 31 predicted flagellar motility and chemotaxis genes, together with *flgO* and *flgP* ('unknown function').

flagellar motility (Table 2-5). As FlrA is not known to act directly to repress transcription, we postulate that regulation of these genes is indirect.

Genes encoding proteins of unknown function are required for soft-agar motility and normal flagellar structure

We further examined the unexpected mutants identified in the motility screen, beginning with four mutants disrupted in genes encoding hypothetical proteins. Three of these genes, *VF_1883* (*flgP*), *VF_1884* (*flgO*), and *VF_1885* (*flgT*), were described as associated with flagellar motility in *V. cholerae* concurrently with our study (Cameron *et al.*, 2008, Martinez *et al.*, 2009, Morris *et al.*, 2008), and we have adopted their nomenclature. The genomic organization of *flgO*, *flgP*, and *flgT* suggests two transcriptional units: *flgOP* and *flgT*, which are located at one end of the flagellar locus on Chromosome 1 (Figure 2-6A). In *V. fischeri*, all three mutants are completely amotile in soft agar (Figure 2-6B). Further, while the *flgP*::Tn*erm* and *flgT*::Tn*erm* mutants can be complemented by expression on a plasmid, the *flgO*::Tn*erm* mutant requires expression of both $flgO^+$ and $flgP^+$ to restore wild-type motility, indicating at least part (but not all) of the defect in this mutant is due to polar effects on *flgP*. When examined by phase-contrast microscopy, these three mutants have normal cell morphology, but only the *flgP*::Tn*erm* mutant showed even an occasional motile cell (data not shown).

Because of the large defects in flagellar motility of these mutants, we used negative-staining TEM to determine whether the cells possessed flagella. Unlike wild-type *V. fischeri* cells, which present a tuft of sheathed, polar flagella, the vast majority of cells of the

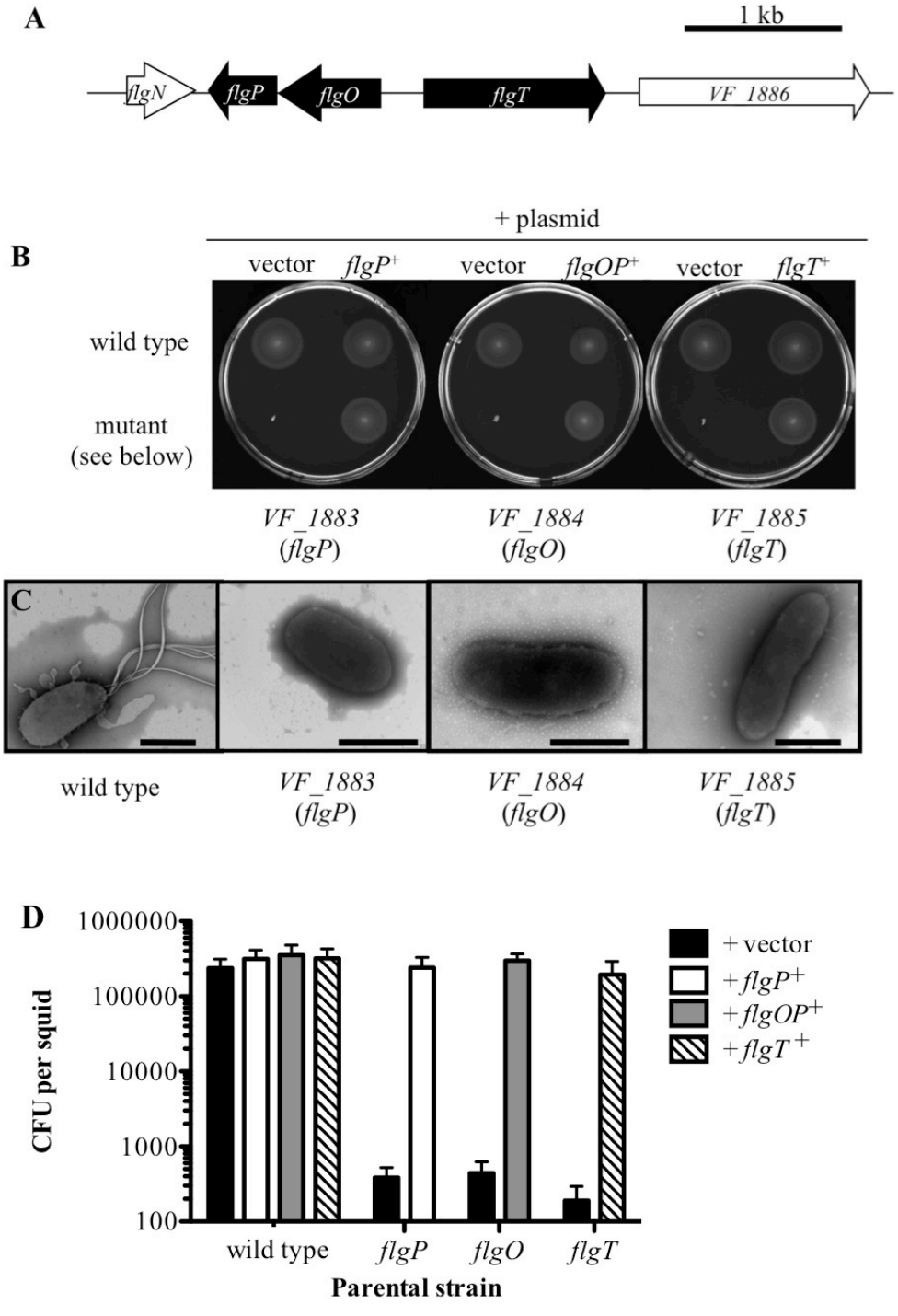
A
1 kb
flgN
flgP
flgO
flgT
VF_1886
B
+ plasmid
vector
flgP+
vector
flgOP+
vector
flgT+
wild type
mutant
(see below)
VF_1883
(flgP)
VF_1884
(flgO)
VF_1885
(flgT)
C
wild type
VF_1883
(flgP)
VF_1884
(flgO)
VF_1885
(flgT)
D
CFU per squid
1000000
100000
10000
1000
100
wild type
flgP
flgO
flgT
Parental strain
+ vector
+ flgP+
+ flgOP+
+ flgT+

Figure 2-6. Mutants in the *V. fischeri flgOP* and *flgT* loci. (A) Genomic organization of the *flgOP* and *flgT* loci. (B) Motility of indicated strains in SWT containing 0.3% agar. (C) Negative-stained transmission electron micrographs of strains grown in SWT broth. Scale bars indicate 1 μm. (D) CFU levels of symbiotic colonization by mutant and genetically complemented strains. Squid were exposed to ~8000 CFU per mL for 24 hours, transferred to FSIO, and sacrificed for homogenization at 48 h.

flgO::Tn*erm*, *flgP*::Tn*erm*, and *flgT*::Tn*erm* mutants were aflagellate (Figure 2-6C). However, flagellar-like structures could be observed in the media from all preparations and, at very low frequency, we observed what appeared to be a single, unsheathed flagellum on *flgP*::Tn*erm* and *flgO*::Tn*erm* cells (data not shown). Therefore, *V. fischeri flgO*, *flgP*, and *flgT* play an essential role in soft-agar motility, as well as in the normal presentation of flagella on the cell surface.

We also analyzed the ability of the mutants disrupted in *flgP*, *flgO*, and *flgT* to enter into a symbiotic relationship with juvenile squid, and observed colonization defects of approximately 1,000-fold relative to both wild type and the respective complemented strains (Figure 2-6D). Whereas squid exposed to the mutant strains harbored fewer than 500 bacterial cells on average; the complemented strains were present at over 100,000 cells per squid. The *flgP* mutant, which exhibited rare motile cells under phase-contrast microscopy, was similarly unable to enter into productive symbioses, even at 1,000-fold higher inoculum levels (~10^7 CFU/mL, data not shown). These data suggest that the *flgO*::Tn*erm*, *flgP*::Tn*erm*, and *flgT*::Tn*erm* mutant strains are severely attenuated in colonization of juvenile squid, similar to previous observations with mutants disrupted in *flrA* and *rpoN* (Millikan and Ruby, 2003, Wolfe et al., 2004).

The remaining mutant disrupted a gene of unknown function, *VF_1491*, predicted to be monocistronic (Figure 2-7A) and found throughout the sequenced *Vibrio* species. The *VF_1491*::Tn*erm* mutant exhibited motility through soft agar at a rate that is only 9% that of wild type (Figure 2-7B). The *VF_1491*::Tn*erm* cells are motile in liquid medium and present a tuft of polar flagella that is indistinguishable from that of wild-type cells (Figure 2-7C).

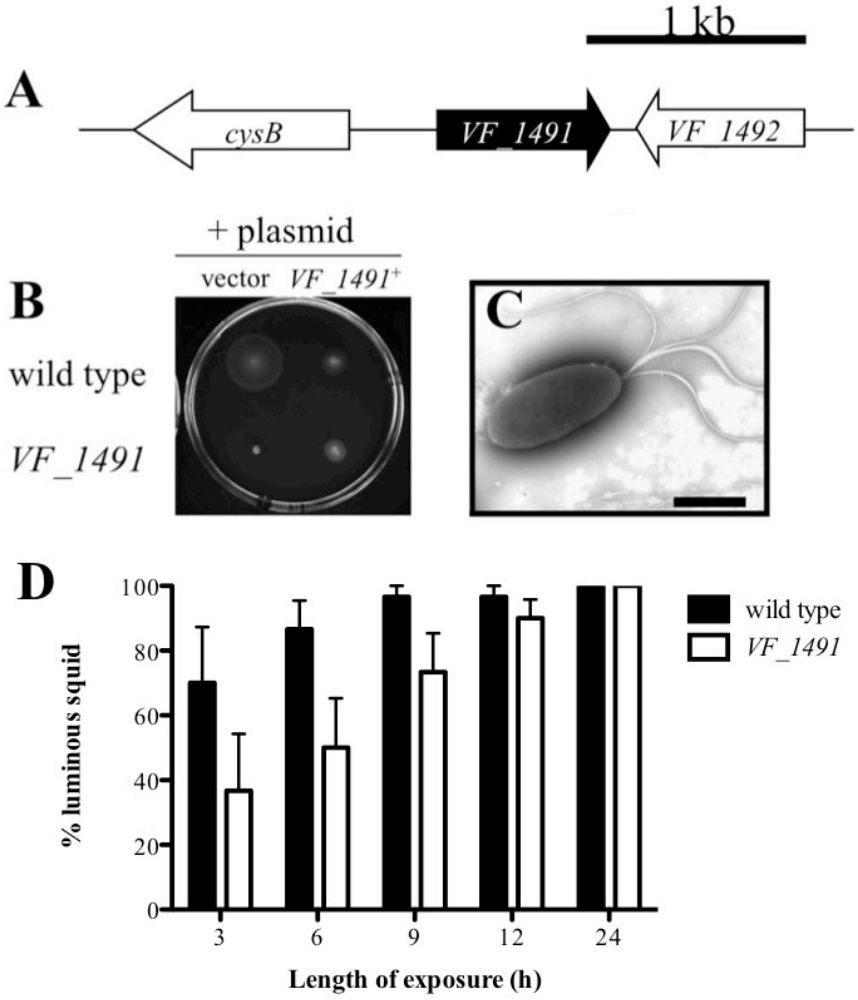

Figure 2-7. Motility and symbiotic-competence analysis of a *VF_1491* mutant.

(A) Genomic organization of the *VF_1491* locus. (B) Motility of indicated strains in SWT containing 0.3% agar. (C) Negative-stained transmission electron micrographs of the *VF_1491* mutant grown in SWT broth. Scale bars indicate 1 μm. (D) Relative effectiveness of *VF_1491* in colonizing juvenile squid. Squid were exposed to ~8000 CFU per mL for indicated period, transferred to FSIO, and a successful colonization was indicated by the presence of luminescence at 24 h post-colonization.

When *VF_1491*$^{+}$ is expressed *in trans* to complement the *VF_1491*::Tn*erm* strain, the soft-agar motility observed is greater than that of the *VF_1491*::Tn*erm* strain alone, but less than wild type carrying a vector control (Figure 2-7B). Furthermore, expression of *VF_1491*$^{+}$ *in trans* in the wild-type background leads to a reduction in soft-agar motility relative to wild type carrying the vector control. However, both mutant and wild type carrying plasmid-borne *VF_1491*$^{+}$ swim at approximately the same level in the soft-agar motility assay (Figure 2-7A). Because expression of *VF_1491* on a multi-copy plasmid alters the motility of wild type, the stoichiometry of this protein may be important. Therefore, perhaps it is not surprising that the complementing construct does not fully restore wild-type motility to the *VF_1491*::Tn*erm* mutant. This phenotype is similar to what is seen with the chemotaxis protein CheW, in which both overexpression and disruption affect the chemotactic ability of *E. coli* (Sanders *et al.*, 1989). The basis for the *VF_1491*::Tn*erm* defect in soft-agar motility is less clear, but VF_1491 may also play a role in chemotaxis or, indirectly, in flagellar rotation in agar.

We examined the competence of the *VF_1491*::Tn*erm* mutant to enter into symbiosis with juvenile squid under permissive conditions (Figure 2-7D). After 24 h of exposure to squid, both the *VF_1491*::Tn*erm* mutant and wild type colonized 100% of squid to luminous levels. However, at shorter exposure times, the *VF_1491*::Tn*erm* mutant colonized fewer squid to luminous levels than wild type, suggesting a reduced efficiency of symbiosis initiation in *VF_1491*::Tn*erm*-exposed squid.

Mutations in predicted cell division genes lead to reduced soft-agar motility

Three mutations s in genes predicted to play important roles during cell division- *amiB*, *mukF*, and *mukB*- were found to exhibit profound motility defects (Table 2-3). AmiB encodes an amidase involved in septal cleavage during cell division (Uehara *et al.*, 2010). MukF and MukB, along with MukE, form a complex that mediates chromosome partitioning (Yamazoe *et al.*, 1999). The *amiB*::Tn*erm* mutant is unable to swim through soft agar, while the *mukF*::Tn*erm* and *mukB*::Tn*erm* mutants are each reduced to 22-23% of the wild-type motility level (Figure 2-8A and Table 2-3). Because MukFBE form a complex, we chose one, MukB, to pursue. To complement the *amiB*::Tn*erm* and *mukB*::Tn*erm* mutant phenotypes, we expressed the wild-type copy of each gene *in trans*, resulting in a restoration of normal motility (Figure 2-8A). When the *amiB*::Tn*erm* and *mukB*::Tn*erm* mutants were examined by phase-contrast microscopy, abnormal cell morphologies were observed (Figure 2-8B). Specifically, the *amiB*::Tn*erm* mutant forms long chains of cells, whereas the *mukB*::Tn*erm* mutant has increased numbers of doublets and triplets of cells. In both mutants, only the rare single cells and, even less frequently, doublets exhibit effective motility in liquid media, suggesting that the morphological defect is the primary reason for the mutants' reduced soft-agar motility. Because of these pleiotropic defects, we did not examine the ability of these strains to colonize juvenile squid.

Paralogs have distinct phenotypes in soft-agar motility

The *V. fischeri* ES114 genome contains pairs of paralogs of the flagellar and chemotaxis genes *fliL*, *motA*, and *motB* (Figure 2-9A), as well as three *cheV* paralogs (Hussa *et al.*, 2007). As our screen coverage was likely not saturating, we may have not obtained

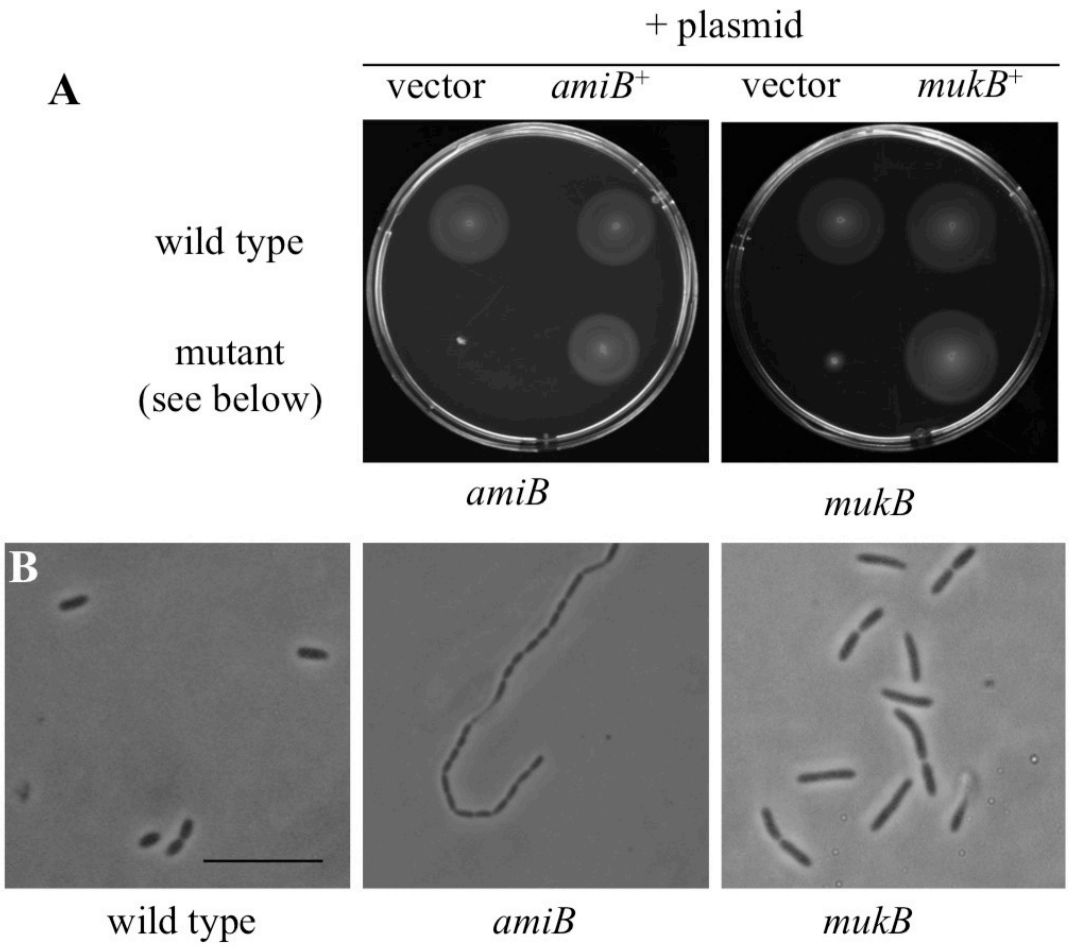

Figure 2-8. Soft-agar motility and phase-contrast microscopy of cell-division mutants. (A) Motility of indicated strains in SWT containing 0.3% agar. (B) Phase-contrast micrographs of SWT broth cultures of indicated strains. Scale bar indicate 5 μm.

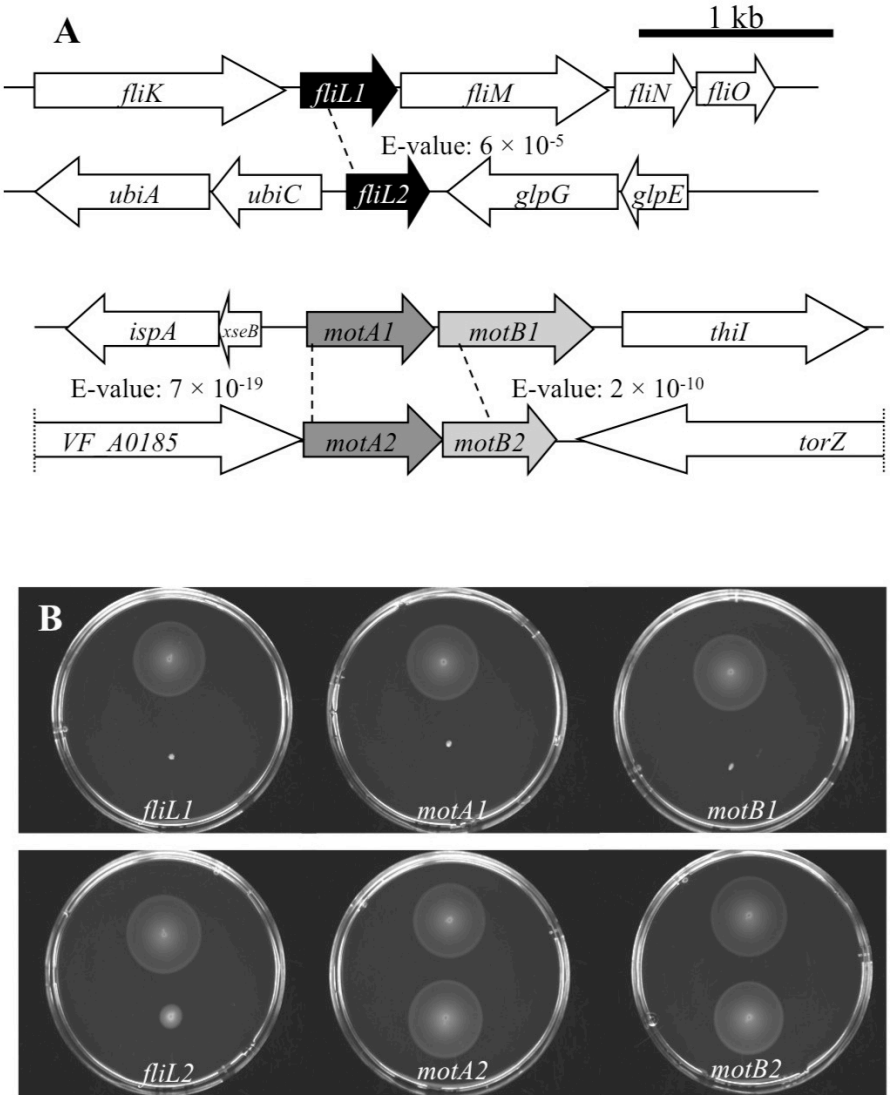

Figure 2-9. Genomic organization and soft-agar motility analysis of mutants in predicted paralogs of three flagellar genes (*fliL*, *motA* and *motB*). (A) Genomic organization of loci surrounding *fliL1*, *fliL2*, *motA1B1* and *motA2B2*. E-values listed were determined by BLASTP analysis. (B) Motility of indicated strains in SWT containing 0.3% agar. On all plates, the upper strain is wild-type *V. fischeri*, and the lower strain carries a mutation in the gene/locus indicated at the bottom of the plate.

insertions in all of the paralogous loci. Therefore, when we observed transposon hits in only one paralog (*e.g.*, *motA1*), we did not know whether the other paralog (*motA2*) was not identified in the screen, or whether mutation of the other paralog did not affect the cell's motility phenotype; thus, we chose to investigate these pairs directly. The presence of *motA2B2* in *V. fischeri* is unique among the completely sequenced *Vibrio* species currently in NCBI.

Transcription of *motA1B1*, but not *motA2B2* is activated in the presence of FlrA (Table 2-5). In addition, MotA1 and MotB1 are more similar to the motor proteins of *V. cholerae*, PomA and PomB, than are *V. fischeri* MotA2 and MotB2. To investigate the contributions of these four genes to normal flagellar motility, individual insertion mutations were constructed in *motA1*, *motB1*, *motA2*, and *motB2,* and their behaviors were observed. The mutants disrupted in either *motA1* or *motB1* were entirely defective in soft-agar motility, confirming the results we noted with the *motA1* and *motB1* transposon mutants (Figure 2-9B and Table 2-3). In contrast, insertion mutations in *motA2* or *motB2* had no effect on soft-agar motility. Taken together, these data suggest that *motA1B1* encode the canonical flagellar motor proteins, and *motA2B2* are not required for flagellar motility, at least under the conditions assayed.

The presence of two paralogs encoding the predicted flagellar basal-body associated protein FliL is a conserved trait among the sequenced *Vibrio* spp (McCarter, 2006). In *V. fischeri*, only *fliL1* is located in the flagellar locus and was found to be required for motility in our screen (Figure 2-9A and Table 2-3). Unlike *motA1B1* and *motA2B2*, both *fliL1* and *fliL2* are activated by FlrA, and therefore, belong to the flagellar regulon of *V. fischeri* (Table 2-5).

Specifically constructed insertion mutations in either *fliL1* or *fliL2* result in distinct defects in soft-agar motility (Figure 2-9B). The *fliL1* mutant is amotile; however, because it is predicted to be part of a downstream operon, the insertion is likely to be polar on *fliMNOPQR* (Figure 2-9A). In contrast, the motility of the monocistronic *fliL2* mutant is reduced relative to wild type, and can be complemented by *fliL2* expression *in trans* (data not shown). Thus, while the individual roles of *fliL1* and *fliL2* cannot be clearly determined, both genes are associated with flagellar motility in *V. fischeri*.

DISCUSSION:

In this study, we (i) generated a 23,904 member transposon insertion library, a useful new tool for the study of *V. fischeri*, (ii) identified new genetic determinants of flagellar motility, (iii) utilized a *flrA* microarray as a discovery tool, and (iv) expanded on the importance of this behavior in the initiation of the squid-vibrio symbiosis.

V. fischeri arrayed mutant library

We describe the construction and validation of the *V. fischeri* ES114 MB mutant collection. By coupling the construction of this library with a phenotypic screen of a well-characterized behavior, rather than performing the screen after completion of the collection, we were able to assay quality throughout the library construction process, immediately address any problems, and verify that the strains in the collection are in good condition. For example, we observed highly variable soft-agar motility in a batch of ten 96-well trays prepared on the same day, and discarded them after determining they were likely damaged due to an unintended exposure to high temperature. This process also allowed us to obtain estimates of sibling membership in the library. These quality-assurance measures establish the MB collection as a useful and immediately available tool for use by the squid-vibrio community. In fact, the collection has already been used to quickly locate mutants of interest by PCR screening of strain lysate pools (Studer *et al.*, 2008), and to isolate mutants with additional chemotactic and motility phenotypes (Post *et al.*, 2012).

Genetic determinants of soft-agar motility

Through genetic analysis, we identified mutants in 38 homologs of flagellar motility-associated genes required for normal soft-agar motility in *V. fischeri*. These data are largely consistent with studies into the genetic basis of motility, a behavior whose core machinery is well-characterized, in other *Vibrio* spp (Cameron *et al.*, 2008, McCarter, 1995), and serve as confirmation of the depth of our screen. Surprisingly, we also isolated a mutant in *flaD*, one of the six flagellin-encoding genes in *V. fischeri*, which has been shown to be dispensable for normal motility in both *V. cholerae* (Klose and Mekalanos, 1998) and *V. anguillarum* (Milton *et al.*, 1996). Our data, along with previous work (Millikan and Ruby, 2004), indicate that the contributions of individual flagellin homologs vary between the multiple polar flagella of *V. fischeri* and the single polar flagellum of the other *Vibrio* spp. These observations provide clues to the long-standing question of the function(s) underlying the presence of multiple flagellins in the *Vibrionaceae*.

Our work has also identified novel genetic determinants of motility in *V. fischeri* that have not been previously reported. First, we observed a strong association between normal cell morphology and soft-agar motility in *V. fischeri*. The *amiB* mutant formed chained cells that were amotile even in liquid; a homologous transposon mutant in *V. cholerae* exhibited reduced, but not entirely deficient, soft-agar motility (Rashid *et al.*, 2003). Similarly, while mutants in the *muk* locus of *V. fischeri* were severely attenuated in soft-agar motility, this locus has not been shown to be associated with soft-agar motility in *V. cholerae*. While the basis for these differences between *V. fischeri* and *V. cholerae* are unknown, it is possible that a tighter regulation between flagellar motility and cellular division is important during the

symbiotic lifestyle of *V. fischeri*. Other determinants of motility thus far unique to *V. fischeri* include VF_1491, a protein of unknown function, and FliL2, a paralog of the basal-body protein FliL1. Neither of these genes has been identified in soft-agar motility screens of other *Vibrio* spp, despite the presence of homologs in many vibrio species and other gamma-proteobacteria.

Finally, whereas previous investigations of mutations in any one of the three paralogs of the chemotaxis protein CheV in *V. fischeri* identified no discernable reductions in soft-agar motility (Hussa *et al.*, 2007), suggesting functional redundancy, we have shown that differences in soft-agar motility can be observed between mutants in the *fliL1* and *fliL2* genes, as well as the in the *motA1B1* and *motA2B2* loci. In contrast to the dominant role of the *motA1B1* motor proteins in *V. fischeri* under the conditions of our assay, work in *Aeromonas hydrophila* has shown that the two pairs of *pomAB*-like genes identified in the genome have largely redundant functions (Wilhelms *et al.*, 2009). Taken together, these results reinforce the idea that the roles of motility-gene paralogs cannot be predicted *a priori* and that, in some cases, they have likely diverged from an ancestral involvement in motility.

Transcriptional profiling of the flagellar regulon

In the absence of the flagellar master activator, FlrA, expression levels of most flagellar and chemotaxis genes are reduced relative to wild-type in both *V. fischeri*, as was seen with *V. cholerae* (Syed *et al.*, 2009). One exception is the methyl-accepting chemotaxis proteins (MCPs), which serve as receptors and recognize environmental signals. Whereas, in *E. coli* K12, all 5 of the MCPs are regulated by this species' master regulator, FlhDC (Zhao *et*

al., 2007), only four of the 43 predicted MCPs were significantly regulated by FlrA in our transcriptional analysis. Similarly, only seven of the 44 MCPs in *V. cholerae* O395 were identified as part of its flagellar regulon (Syed *et al.*, 2009). This difference may indicate a fundamental divergence in the way chemotaxis is regulated between the *Vibrionaceae* and *Enterobacteriaceae*. Beyond motility-gene expression, flagellar master regulators of a number of bacterial species both positively and negatively modulate genes that are not involved in flagellar motility. In *E. coli* K12, a predominant example is in the regulation of anaerobic metabolism (Pruss *et al.*, 2003), while in *V. cholerae*, the flagellar regulon controls virulence gene expression, including the toxin coregulated pilin (Tcp) genes (Syed *et al.*, 2009). Our data suggest that, while non-flagellar genes may be regulated by FlrA in *V. fischeri,* FlrA does not control either anaerobic metabolism or the *Vibrio*-specific Tcp genes, intimating that the flagellar regulation machinery has been co-opted for differing functions even between closely-related species of bacteria.

Flagellar motility and chemotaxis in symbiosis

Flagellar motility and chemotaxis have been implicated, to different degrees, in many host-microbe interactions. In *V. cholerae*, for example, the impact of these behaviors on colonization varies both by bacterial strain and by the infection model used (Richardson, 1991). Similarly, flagellar and chemotaxis mutants of uropathogenic *E. coli* exhibit a range of phenotypes depending on the organ of interest (*i.e.*, kidney or bladder) and on whether the strains are assessed in single- or dual-strain (competitive) analyses (Lane *et al.*, 2005, Wright

et al., 2005). Even with these ambiguities, chemotaxis and flagellar motility have been proposed to play important roles in these, and many other, host-microbe associations.

In our screen, we identified *V. fischeri* mutants in 43 genes required for normal soft-agar motility, and assayed 14 of these strains for colonization of the juvenile squid light organ. In this more exhaustive study, we confirmed previous data (Graf *et al.*, 1994, Hussa *et al.*, 2007, Millikan and Ruby, 2003, Wolfe *et al.*, 2004) and showed that flagellar motility is required for entrance into a productive symbiosis. Interestingly, mutants disrupted in core chemotaxis genes were able to colonize juvenile squid, albeit with reduced success. These data, and those showing that mutants in *cheY* and *cheR* are significantly out-competed by wild type (DeLoney-Marino and Visick, 2012, Hussa *et al.*, 2007), suggest that chemotaxis is an important symbiotic behavior, especially under natural, competitive conditions. To explain the different phenotypes for motility and chemotaxis mutants, we propose that either (i) non-chemotactic mutants are able to "blindly" locate the light organ, which would suggest that chemotaxis is required only over a short distance, and/or (ii) both non-chemotactic and chemotactic motility play a role in initiating colonization.

The specific stages at which chemotaxis and flagellar motility mediate colonization are not yet well-characterized in any bacterium-animal interaction. The squid-vibrio system is posed as an excellent model to address both how and when these bacterial behaviors underlie symbiotic initiation, as colonization occurs naturally from the surrounding seawater and can be easily manipulated and observed. While they have been examined in plant symbioses (Gage *et al.*, 1996), mechanisms of natural initiation are under-represented in studies of animal-microbe interactions. As such, the complexity observed during initiation of the squid-

vibrio symbiosis continues to illuminate general mechanisms that underlie host-microbe interactions and serves as a natural, yet experimentally tractable, model of mutualism.

ACKNOWLEDGMENTS:

We thank Amy Schaefer for experimental support, and all the members of Ruby and McFall-Ngai laboratories for valuable advice and discussion. This work was supported by NIH Grant RR12294 to EGR and MJM-N from NCRR and the Office of Research Infrastructural Programs, and by NSF Grant IOS-0817232 to MM-N and EGR. CAB was funded by NIH Molecular Biosciences, and by NIH Microbes in Health and Disease training grants to the University of Wisconsin-Madison. MJM was supported by an NIGMS NRSA Postdoctoral Fellowship.

REFERENCES:

Adler, J. (1966) Chemotaxis in bacteria. *Science* **153**(3737): p. 708-16.

Allen, R.D. and Baumann, P. (1971) Structure and arrangement of flagella in species of the genus *Beneckea* and *Photobacterium fischeri*. *J Bacteriol* **107**(1): p. 295-302.

Arnosti, D.N. and Chamberlin, M.J. (1989) Secondary σ factor controls transcription of flagellar and chemotaxis genes in *Escherichia coli*. *Proc Natl Acad Sci U S A* **86**(3): p. 830-4.

Baldi, P. and Long, A.D. (2001) A Bayesian framework for the analysis of microarray expression data: regularized t -test and statistical inferences of gene changes. *Bioinformatics* **17**(6): p. 509-19.

Boettcher, K.J. and Ruby, E.G. (1990) Depressed light emission by symbiotic *Vibrio fischeri* of the sepiolid squid Euprymna scolopes. *J Bacteriol* **172**(7): p. 3701-6.

Butler, S.M. and Camilli, A. (2004) Both chemotaxis and net motility greatly influence the infectivity of *Vibrio cholerae*. *Proc Natl Acad Sci U S A* **101**(14): p. 5018-23.

Caetano-Anolles, G. (1993) Amplifying DNA with arbitrary oligonucleotide primers. *PCR Methods Appl* **3**(2): p. 85-94.

Cameron, D.E., Urbach, J.M., and Mekalanos, J.J. (2008) A defined transposon mutant library and its use in identifying motility genes in *Vibrio cholerae*. *Proc Natl Acad Sci U S A* **105**(25): p. 8736-41.

Correa, N.E., Peng, F., and Klose, K.E. (2005) Roles of the regulatory proteins FlhF and FlhG in the *Vibrio cholerae* flagellar transcription hierarchy. *J Bacteriol* **187**(18): p. 6324-32.

Cullen, T.W. and Trent, M.S. (2010) A link between the assembly of flagella and lipooligosaccharide of the Gram-negative bacterium *Campylobacter jejuni*. *Proc Natl Acad Sci U S A* **107**(11): p. 5160-5.

Dam, P., Olman, V., Harris, K., Su, Z., and Xu, Y. (2007) Operon prediction using both genome-specific and general genomic information. *Nucleic Acids Res* **35**(1): p. 288-98.

DeLoney-Marino, C.R. and Visick, K.L. (2012) Role for *cheR* of *Vibrio fischeri* in the *Vibrio*-squid symbiosis. *Can J Microbiol* **58**(1): p. 29-38.

DeLoney-Marino, C.R., Wolfe, A.J., and Visick, K.L. (2003) Chemoattraction of *Vibrio fischeri* to serine, nucleosides, and N-acetylneuraminic acid, a component of squid light-organ mucus. *Appl Environ Microbiol* **69**(12): p. 7527-30.

Dunn, A.K., Martin, M.O., and Stabb, E.V. (2005) Characterization of pES213, a small mobilizable plasmid from *Vibrio fischeri*. *Plasmid* **54**(2): p. 114-34.

Dunn, A.K., Millikan, D.S., Adin, D.M., Bose, J.L., and Stabb, E.V. (2006) New rfp- and pES213-derived tools for analyzing symbiotic *Vibrio fischeri* reveal patterns of infection and *lux* expression in situ. *Appl Environ Microbiol* **72**(1): p. 802-10.

Dunn, A.K. and Stabb, E.V. (2008) Genetic analysis of trimethylamine N-oxide reductases in the light organ symbiont *Vibrio fischeri* ES114. *J Bacteriol* **190**(17): p. 5814-23.

Freter, R., Allweiss, B., O'Brien, P.C., Halstead, S.A., and Macsai, M.S. (1981) Role of chemotaxis in the association of motile bacteria with intestinal mucosa: in vitro studies. *Infect Immun* **34**(1): p. 241-9.

Gage, D.J., Bobo, T., and Long, S.R. (1996) Use of green fluorescent protein to visualize the early events of symbiosis between *Rhizobium meliloti* and alfalfa (*Medicago sativa*). *J Bacteriol* **178**(24): p. 7159-66.

Girgis, H.S., Liu, Y., Ryu, W.S., and Tavazoie, S. (2007) A comprehensive genetic characterization of bacterial motility. *PLoS Genet* **3**(9): p. 1644-60.

Graf, J., Dunlap, P.V., and Ruby, E.G. (1994) Effect of transposon-induced motility mutations on colonization of the host light organ by *Vibrio fischeri*. *J Bacteriol* **176**(22): p. 6986-91.

Graf, J. and Ruby, E.G. (1998) Host-derived amino acids support the proliferation of symbiotic bacteria. *Proc Natl Acad Sci U S A* **95**(4): p. 1818-22.

Hayashi, F., Smith, K.D., Ozinsky, A., Hawn, T.R., Yi, E.C., Goodlett, D.R., Eng, J.K., Akira, S., Underhill, D.M., and Aderem, A. (2001) The innate immune response to bacterial flagellin is mediated by Toll-like receptor 5. *Nature* **410**(6832): p. 1099-103.

Henrichsen, J. (1972) Bacterial surface translocation: a survey and a classification. *Bacteriol Rev* **36**(4): p. 478-503.

Hussa, E.A., O'Shea, T.M., Darnell, C.L., Ruby, E.G., and Visick, K.L. (2007) Two-component response regulators of *Vibrio fischeri*: identification, mutagenesis, and characterization. *J Bacteriol* **189**(16): p. 5825-38.

Iino, T., Komeda, Y., Kutsukake, K., Macnab, R.M., Matsumura, P., Parkinson, J.S., Simon, M.I., and Yamaguchi, S. (1988) New unified nomenclature for the flagellar genes of *Escherichia coli* and *Salmonella typhimurium*. *Microbiol Rev* **52**(4): p. 533-5.

Kapatral, V., Campbell, J.W., Minnich, S.A., Thomson, N.R., Matsumura, P., and Pruss, B.M. (2004) Gene array analysis of *Yersinia enterocolitica* FlhD and FlhC: regulation of enzymes affecting synthesis and degradation of carbamoylphosphate. *Microbiology* **150**(Pt 7): p. 2289-300.

Kim, Y.K. and McCarter, L.L. (2000) Analysis of the polar flagellar gene system of *Vibrio parahaemolyticus*. *J Bacteriol* **182**(13): p. 3693-704.

Klose, K.E. and Mekalanos, J.J. (1998) Differential regulation of multiple flagellins in *Vibrio cholerae*. *J Bacteriol* **180**(2): p. 303-16.

Klose, K.E. and Mekalanos, J.J. (1998) Distinct roles of an alternative sigma factor during both free-swimming and colonizing phases of the *Vibrio cholerae* pathogenic cycle. *Mol Microbiol* **28**(3): p. 501-20.

Lane, M.C., Lockatell, V., Monterosso, G., Lamphier, D., Weinert, J., Hebel, J.R., Johnson, D.E., and Mobley, H.L. (2005) Role of motility in the colonization of uropathogenic *Escherichia coli* in the urinary tract. *Infect Immun* **73**(11): p. 7644-56.

Lemon, K.P., Higgins, D.E., and Kolter, R. (2007) Flagellar motility is critical for *Listeria monocytogenes* biofilm formation. *J Bacteriol* **189**(12): p. 4418-24.

Liu, Z., Miyashiro, T., Tsou, A., Hsiao, A., Goulian, M., and Zhu, J. (2008) Mucosal penetration primes *Vibrio cholerae* for host colonization by repressing quorum sensing. *Proc Natl Acad Sci U S A* **105**(28): p. 9769-74.

Lyell, N.L., Dunn, A.K., Bose, J.L., Vescovi, S.L., and Stabb, E.V. (2008) Effective mutagenesis of *Vibrio fischeri* by using hyperactive mini-Tn*5* derivatives. *Appl Environ Microbiol* **74**(22): p. 7059-63.

Macnab, R.M. (2003) How bacteria assemble flagella. *Annu Rev Microbiol* **57**: p. 77-100.

Mandel, M.J., Schaefer, A.L., Brennan, C.A., Heath-Heckman, E.A., Deloney-Marino, C.R., McFall-Ngai, M.J., and Ruby, E.G. (2012) Squid-derived chitin oligosaccharides are a chemotactic signal during colonization by *Vibrio fischeri*. *Appl Environ Microbiol* **78**(13): p. 4620-6.

Mandel, M.J., Stabb, E.V., and Ruby, E.G. (2008) Comparative genomics-based investigation of resequencing targets in *Vibrio fischeri*: focus on point miscalls and artefactual expansions. *BMC Genomics* **9**: p. 138.

McCarter, L., *Motility and Chemotaxis* in *The Biology of Vibrios*, F.L. Thompson, B. Austin, and J. Swings, Editors. 2006, ASM Press: Washington, D.C. p. 115-132.

McCarter, L. and Silverman, M. (1990) Surface-induced swarmer cell differentiation of *Vibrio parahaemolyticus*. *Mol Microbiol* **4**(7): p. 1057-62.

McCarter, L.L. (1995) Genetic and molecular characterization of the polar flagellum of *Vibrio parahaemolyticus*. *J Bacteriol* **177**(6): p. 1595-609.

Miller, L.D., Russell, M.H., and Alexandre, G. (2009) Diversity in bacterial chemotactic responses and niche adaptation. *Adv Appl Microbiol* **66**: p. 53-75.

Millikan, D.S. and Ruby, E.G. (2002) Alterations in *Vibrio fischeri* motility correlate with a delay in symbiosis initiation and are associated with additional symbiotic colonization defects. *Appl Environ Microbiol* **68**(5): p. 2519-28.

Millikan, D.S. and Ruby, E.G. (2003) FlrA, a σ^{54}-dependent transcriptional activator in *Vibrio fischeri*, is required for motility and symbiotic light-organ colonization. *J Bacteriol* **185**(12): p. 3547-57.

Millikan, D.S. and Ruby, E.G. (2004) *Vibrio fischeri* flagellin A is essential for normal motility and for symbiotic competence during initial squid light organ colonization. *J Bacteriol* **186**(13): p. 4315-25.

Milton, D.L., O'Toole, R., Horstedt, P., and Wolf-Watz, H. (1996) Flagellin A is essential for the virulence of *Vibrio anguillarum*. *J Bacteriol* **178**(5): p. 1310-9.

Moisi, M., Jenul, C., Butler, S.M., New, A., Tutz, S., Reidl, J., Klose, K.E., Camilli, A., and Schild, S. (2009) A novel regulatory protein involved in motility of *Vibrio cholerae*. *J Bacteriol* **191**(22): p. 7027-38.

Morris, D.C., Peng, F., Barker, J.R., and Klose, K.E. (2008) Lipidation of an FlrC-dependent protein is required for enhanced intestinal colonization by *Vibrio cholerae*. *J Bacteriol* **190**(1): p. 231-9.

Naughton, L.M. and Mandel, M.J. (2012) Colonization of *Euprymna scolopes* squid by *Vibrio fischeri*. *J Vis Exp* (61).

Nyholm, S.V. and McFall-Ngai, M.J. (2004) The winnowing: establishing the squid-vibrio symbiosis. *Nat Rev Microbiol* **2**(8): p. 632-42.

Nyholm, S.V., Stabb, E.V., Ruby, E.G., and McFall-Ngai, M.J. (2000) Establishment of an animal-bacterial association: recruiting symbiotic vibrios from the environment. *Proc Natl Acad Sci U S A* **97**(18): p. 10231-5.

O'Toole, G.A., Pratt, L.A., Watnick, P.I., Newman, D.K., Weaver, V.B., and Kolter, R. (1999) Genetic approaches to study of biofilms. *Methods Enzymol* **310**: p. 91-109.

Overhage, J., Lewenza, S., Marr, A.K., and Hancock, R.E. (2007) Identification of genes involved in swarming motility using a *Pseudomonas aeruginosa* PAO1 mini-Tn*5*-*lux* mutant library. *J Bacteriol* **189**(5): p. 2164-9.

Peterson, J.D., Umayam, L.A., Dickinson, T., Hickey, E.K., and White, O. (2001) The Comprehensive Microbial Resource. *Nucleic Acids Res* **29**(1): p. 123-5.

Post, D.M., Yu, L., Krasity, B.C., Choudhury, B., Mandel, M.J., Brennan, C.A., Ruby, E.G., McFall-Ngai, M.J., Gibson, B.W., and Apicella, M.A. (2012) O-antigen and core carbohydrate of *Vibrio fischeri* lipopolysaccharide: composition and analysis of their role in *Euprymna scolopes* light organ colonization. *J Biol Chem* **287**(11): p. 8515-30.

Prouty, M.G., Correa, N.E., and Klose, K.E. (2001) The novel σ^{54}- and σ^{28}-dependent flagellar gene transcription hierarchy of *Vibrio cholerae*. *Mol Microbiol* **39**(6): p. 1595-609.

Pruss, B.M., Campbell, J.W., Van Dyk, T.K., Zhu, C., Kogan, Y., and Matsumura, P. (2003) FlhD/FlhC is a regulator of anaerobic respiration and the Entner-Doudoroff pathway through induction of the methyl-accepting chemotaxis protein Aer. *J Bacteriol* **185**(2): p. 534-43.

Rashid, M.H., Rajanna, C., Ali, A., and Karaolis, D.K. (2003) Identification of genes involved in the switch between the smooth and rugose phenotypes of *Vibrio cholerae*. *FEMS Microbiol Lett* **227**(1): p. 113-9.

Richardson, K. (1991) Roles of motility and flagellar structure in pathogenicity of *Vibrio cholerae*: analysis of motility mutants in three animal models. *Infect Immun* **59**(8): p. 2727-36.

Ruby, E.G., Urbanowski, M., Campbell, J., Dunn, A., Faini, M., Gunsalus, R., Lostroh, P., Lupp, C., McCann, J., Millikan, D., Schaefer, A., Stabb, E., Stevens, A., Visick, K., Whistler, C., and Greenberg, E.P. (2005) Complete genome sequence of *Vibrio fischeri*: a symbiotic bacterium with pathogenic congeners. *Proc Natl Acad Sci U S A* **102**(8): p. 3004-9.

Sanders, D.A., Mendez, B., and Koshland, D.E., Jr. (1989) Role of the CheW protein in bacterial chemotaxis: overexpression is equivalent to absence. *J Bacteriol* **171**(11): p. 6271-8.

Shinoda, S. and Okamoto, K. (1977) Formation and function of *Vibrio parahaemolyticus* lateral flagella. *J Bacteriol* **129**(3): p. 1266-71.

Stabb, E.V., Reich, K.A., and Ruby, E.G. (2001) *Vibrio fischeri* genes hvnA and hvnB encode secreted NAD(+)-glycohydrolases. *J Bacteriol* **183**(1): p. 309-17.

Studer, S.V., Mandel, M.J., and Ruby, E.G. (2008) AinS quorum sensing regulates the V*ibrio fischeri* acetate switch. *J Bacteriol* **190**(17): p. 5915-23.

Syed, K.A., Beyhan, S., Correa, N., Queen, J., Liu, J., Peng, F., Satchell, K.J., Yildiz, F., and Klose, K.E. (2009) The *Vibrio cholerae* flagellar regulatory hierarchy controls expression of virulence factors. *J Bacteriol* **191**(21): p. 6555-70.

Uehara, T., Parzych, K.R., Dinh, T., and Bernhardt, T.G. (2010) Daughter cell separation is controlled by cytokinetic ring-activated cell wall hydrolysis. *EMBO J* **29**(8): p. 1412-22.

Visick, K.L. and Ruby, E.G. (2006) *Vibrio fischeri* and its host: it takes two to tango. *Curr Opin Microbiol* **9**(6): p. 632-8.

Wang, Y., Dufour, Y.S., Carlson, H.K., Donohue, T.J., Marletta, M.A., and Ruby, E.G. (2010) H-NOX-mediated nitric oxide sensing modulates symbiotic colonization by *Vibrio fischeri*. *Proc Natl Acad Sci U S A* **107**(18): p. 8375-80.

Wier, A.M., Nyholm, S.V., Mandel, M.J., Massengo-Tiasse, R.P., Schaefer, A.L., Koroleva, I., Splinter-Bondurant, S., Brown, B., Manzella, L., Snir, E., Almabrazi, H., Scheetz, T.E., Bonaldo Mde, F., Casavant, T.L., Soares, M.B., Cronan, J.E., Reed, J.L., Ruby, E.G., and McFall-Ngai, M.J. (2010) Transcriptional patterns in both host and bacterium underlie a daily rhythm of anatomical and metabolic change in a beneficial symbiosis. *Proc Natl Acad Sci U S A* **107**(5): p. 2259-64.

Wilhelms, M., Vilches, S., Molero, R., Shaw, J.G., Tomas, J.M., and Merino, S. (2009) Two redundant sodium-driven stator motor proteins are involved in *Aeromonas hydrophila* polar flagellum rotation. *J Bacteriol* **191**(7): p. 2206-17.

Wolfe, A.J., Millikan, D.S., Campbell, J.M., and Visick, K.L. (2004) *Vibrio fischeri* σ^{54} controls motility, biofilm formation, luminescence, and colonization. *Appl Environ Microbiol* **70**(4): p. 2520-4.

Wright, K.J., Seed, P.C., and Hultgren, S.J. (2005) Uropathogenic *Escherichia coli* flagella aid in efficient urinary tract colonization. *Infect Immun* **73**(11): p. 7657-68.

Yamazoe, M., Onogi, T., Sunako, Y., Niki, H., Yamanaka, K., Ichimura, T., and Hiraga, S. (1999) Complex formation of MukB, MukE and MukF proteins involved in chromosome partitioning in *Escherichia coli*. *EMBO J* **18**(21): p. 5873-84.

Young, G.M., Schmiel, D.H., and Miller, V.L. (1999) A new pathway for the secretion of virulence factors by bacteria: the flagellar export apparatus functions as a protein-secretion system. *Proc Natl Acad Sci U S A* **96**(11): p. 6456-61.

Zhao, K., Liu, M., and Burgess, R.R. (2007) Adaptation in bacterial flagellar and motility systems: from regulon members to 'foraging'-like behavior in *E. coli*. *Nucleic Acids Res* **35**(13): p. 4441-52.

Chapter 3

The Chemoreceptor VfcA Mediates Amino Acid Chemotaxis in *Vibrio fischeri*

PREFACE:

Accepted for publication in Applied and Environmental Microbiology in January 2013 as: Brennan CA, DeLoney-Marino CR, Mandel MJ. "The chemoreceptor VfcA mediates amino acid chemotaxis in *Vibrio fischeri*."

CAB and MJM planned experiments. CAB, CRD-M (University of Southern Indiana), and MJM performed experiments. CAB and MJM wrote and edited the chapter. EGR provided additional intellectual contributions.

ABSTRACT:

Flagellar motility and chemotaxis by *Vibrio fischeri* are important behaviors mediating colonization of its mutualistic host, the Hawaiian bobtail squid. However, none of the 43 putative methyl-accepting chemotaxis proteins (MCPs) in the *V. fischeri* genome has been previously characterized. Using both an available transposon mutant collection and directed mutagenesis, we isolated mutants in 19 of these genes, and screened these mutants for altered chemotaxis to six previously identified chemoattractants. Only one mutant, disrupted in a gene we name *vfcA* (*Vibrio fischeri* chemoreceptor A; locus tag VF_0777), was defective in responding to any of the tested compounds. In soft-agar plates, mutants disrupted in *vfcA* did not exhibit the serine-sensing chemotactic ring, and the pattern of migration in the mutant was unaffected by the addition of exogenous serine. Using a capillary chemotaxis assay, we showed that, unlike wild-type *V. fischeri*, the *vfcA* mutant did not undergo chemotaxis towards serine, and that expression of *vfcA* on a plasmid in the mutant was sufficient to restore the behavior. In addition to serine, we demonstrated that alanine, cysteine, and threonine are strong attractants for wild-type *V. fischeri* and that the attraction is also mediated by VfcA. This study thus provides the first insights into how *V. fischeri* integrates information from one of its 43 MCPs to respond to environmental stimuli.

INTRODUCTION:

Flagellar motility is one of several behaviors used by bacteria to migrate through their surroundings (Henrichsen, 1972). Migration to preferred environmental conditions is mediated by chemotaxis (Adler, 1966), which allows the bacterium to sense gradients of attractants and respond by controlling the directionality of the flagellar motor (Larsen *et al.*, 1974). Methyl-accepting chemotaxis proteins (MCPs) function as receptors that bind attractants or repellants, usually in the periplasm, and transduce a signal through the histidine kinase CheA. The consequence of CheA phosphorylation or dephosphorylation is signaling via phosphorelay that ends at FliM, a protein in the flagellar switch apparatus (Stock, 1996, Eisenbach, 1996). By altering the tumbling frequency, MCPs direct an average change in the direction of travel for the bacteria. In *Escherichia coli* K12, a total of five MCPs enable sensing of numerous attractants, including amino acids, peptides, galactose, ribose, and oxygen (Bibikov *et al.*, 1997, Hazelbauer *et al.*, 1969, Springer *et al.*, 1977, Manson *et al.*, 1986, Kondoh *et al.*, 1979). However, as more diverse bacterial species have been studied, we have learned that bacterial chemotaxis is frequently more complex than the *E. coli* paradigm (Porter *et al.*, 2008, Zusman *et al.*, 2007). Bioinformatics and increased genome sequence availability have revealed that both the number and domain structure of predicted MCPs vary greatly between species (Lacal *et al.*, 2010, Krell *et al.*, 2011, Miller *et al.*, 2009). Work in *Pseudomonas aeruginosa*, a species that encodes 26 MCPs in strain PAO1, has characterized 9 MCPs that mediate chemotaxis toward ligands such as amino acids, trichloroethylene and malate (Alvarez-Ortega & Harwood, 2007, Kato *et al.*, 2008, Taguchi *et*

al., 1997, Kim *et al.*, 2006). However, even in this relatively well-studied organism, high-throughput attempts to identify MCP ligands have been largely inconclusive and in one case, only successful when energy taxis, mediated by Aer, is also disrupted (Alvarez-Ortega & Harwood, 2007).

Within the *Vibrionaceae*, the genetic basis of chemotaxis has not been well characterized. Even in the human pathogen *Vibrio cholerae*, only three of up to 45 putative MCPs, contributing to aerotaxis, amino acid chemotaxis, and chemotaxis towards the chitin-derived sugars *N*-acetyl-glucosamine, (GlcNAc), and *N*-*N'*-diacetylchitobiose, $(GlcNAc)_2$, have been described (Boin & Hase, 2007, Meibom *et al.*, 2004, Nishiyama *et al.*, 2012). The genome of the squid symbiont *Vibrio fischeri* (strain ES114) encodes 43 predicted MCPs (Ruby *et al.*, 2005, Mandel *et al.*, 2008), none of which have been studied, despite the importance of chemotaxis and flagellar motility in the symbiotic lifestyle of this organism (DeLoney-Marino & Visick, 2012, Hussa *et al.*, 2007, Graf *et al.*, 1994, Millikan & Ruby, 2003, Mandel *et al.*, 2012). Because some of the nutrients provided by its squid host have been shown to be chemoattractants for *V. fischeri* (Mandel *et al*., 2012, DeLoney-Marino *et al.*, 2003), we hypothesized that it would be possible to delimit the chemotactic signaling pathways in the bacterium—and during host colonization—by assigning ligands to the MCPs encoded by the bacterium. Therefore, the goal of this study was to begin to determine how some of the 43 MCPs in *V. fischeri* sense specific macromolecules.

MATERIALS AND METHODS:

Bacterial strains and growth conditions

Strains and plasmids used in this work are listed in Table 3-1. *V. fischeri* strains are derived from strain ES114 (Boettcher & Ruby, 1990) (isolate MJM1100) and were grown at 28°C in either Luria-Bertani salt (LBS) medium (per liter, 10 g Bacto-tryptone, 5 g yeast extract and 20 g NaCl, 50 mL 1 M Tris buffer, pH 7.5, in distilled water) or seawater-based tryptone (SWT) medium (per liter, 5 g Bacto-tryptone, 3 g yeast extract, 3 mL glycerol, 700 mL Instant Ocean [Aquarium Systems, Inc, Mentor, OH] at a salinity of 33-35 ppt, and 300 ml distilled water). *E. coli* strains, as used for cloning, were grown at 37°C in Luria-Bertani medium or brain heart infusion medium (BD, Sparks, MD). When appropriate, antibiotics were added to media at the following concentrations: erythromycin, 5 μg/ml for *V. fischeri* and 150 μg/ml for *E. coli*; and chloramphenicol, 2.5 μg/ml for *V. fischeri* and 25 μg/ml for *E. coli*. Growth media were solidified with 1.5% agar as needed.

Construction and isolation of MCP mutants

To isolate mutants disrupted in one of the *V. fischeri* MCP genes, we utilized the MB transposon mutant collection (Chapter 2) and modified an approach we have successfully used previously to identify mutants carrying a transposon insertion in a specific gene (Studer *et al.*, 2008). Briefly, pooled templates were amplified by PCR with one primer anchored in the transposon (MJM-127; approximately 100 bp from either end) and a second primer or primer mixture that anneals to a conserved region within MCP genes (either MJM-179, or a

Table 3-1. Strains and plasmids used in this study

Strain or plasmid	Description	Reference or source
Strains		
V. fischeri		
MJM1100	ES114, sequenced wild-type *E. scolopes* light organ isolate	(Boettcher & Ruby, 1990)
CAB1500	*vfcA*::pCAB15 Campbell mutant	This work
CAB1501	*VF_1133*::pCAB16 Campbell mutant	This work
CAB1502	*VF_1789*::pCAB17 Campbell mutant	This work
CAB1503	*VF_2161*::pCAB18 Campbell mutant	This work
CAB1504	*VF_A0325*::pCAB19 Campbell mutant	This work
CAB1505	*VF_A0448*::pCAB20 Campbell mutant	This work
CAB1506	*VF_A0677*::pCAB21 Campbell mutant	This work
MB06594	*VF_1503*::Tn*erm*	This work
MB08238	*VF_A0528*::Tn*erm*	This work
MB08251	*VF_A0481*::Tn*erm*	This work
MB08831	*VF_A0527*::Tn*erm*	This work
MB20125	*VF_1138*::Tn*erm*	This work
MB20164	*VF_A0170*::Tn*erm*	This work
MB21095	*VF_1652*::Tn*erm*	This work
MB20465	*VF_A1072*::Tn*erm*	This work
MB20467	*VF_1117*::Tn*erm*	This work
MB09616	*VF_A1084*::Tn*erm*	This work
MB09969	*VF_0987*::Tn*erm*	This work
MB21134	*VF_1618*::Tn*erm*	This work
MB09076	*vfcA*::Tn*erm*	This work
MB08701	*cheA*::Tn*erm*	Chapter 2
CAB1516	MJM1100 harboring pVSV105	This work
CAB1517	MJM1100 harboring pCAB26	This work
CAB1523	MB09076 harboring pVSV105	This work
CAB1524	MB09076 harboring pCAB26	This work
E. coli		
DH5*α*-*λ*pir	Cloning vector	(Hanahan, 1983)
Plasmids		
pEVS122	*oriR6K*-based suicide vector, Erm^R	(Dunn *et al*., 2005)
pEVS104	conjugative helper plasmid, Kan^R	(Stabb & Ruby, 2002)
pCAB15	pEVS122::'*vfcA'*	This work
pCAB16	pEVS122::'*VF_1133'*	This work
pCAB17	pEVS122::'*VF_1789*'	This work
pCAB18	pEVS122::'*VF_2161'*	This work
pCAB19	pEVS122::'*VF_A0325*'	This work
pCAB20	pEVS122::'*VF_A0448*'	This work
pCAB21	pEVS122::'*VF_A0677*'	This work
pVSV105	pES213-based plasmid used for complementation, Cm^R	(Dunn *et al*., 2006)
pCAB26	pVSV105 containing *vfcA* ORF and 350 bp upstream	This work

mixture of 13 primers: MJM-173, MJM-175, MJM-176, MJM-181, MJM-184, MJM-186, MJM-187, MJM-192, MJM-193, MJM-195, MJM-201, MJM-205, and MJM-206; Table 3-2). We predicted that a band of approximately 500-1500 bp would appear only if there were a transposon insertion in or near an MCP. As MCPs are often encoded in tandem in the genome, it was also possible to identify an insertion in the 3' end of an MCP encoded upstream of the one in which the MCP-specific primer bound. Bands identified in this manner were purified and sequenced with primer 170Int2. The strain containing the mutation of interest was subsequently isolated. Using this approach, we screened 3,168 members of the MB collection and identified mutants separately disrupted in 12 of the 43 MCP-encoding genes.

Campbell-type mutagenesis using the suicide vector pEVS122 (Dunn *et al.*, 2005) was performed to generate disruptions in an additional seven MCP genes: *vfcA* (*VF_0777*), *VF_1133*, *VF_1789*, *VF_A0325*, *VF_A0448*, *VF_A0677*, and *VF_2161*. Using the following primer pairs, 500 bp of homology near the 5' end of each ORF was amplified for each gene by PCR: *VF_0777*, MJM-313F and MJM-314R; *VF_1133*, MJM-315F and MJM-316R; *VF_1789*, MJM-317F and MJM-318R; *VF_2161*, MJM-319F and MJM-320R; *VF_A0325*, MJM-321F and MJM-322R; *VF_A0448*, MJM-323F and MJM-324R; and *VF_A0677*, MJM-325F and MJM-326R. The primer pairs also added XmaI and SphI restriction enzyme sites, which were used to clone the amplified products into the XmaI/SphI-digested pEVS122 using standard techniques. The resulting constructs were conjugated into *V. fischeri* ES114 (MJM1100 isolate) as previously described (Stabb & Ruby, 2002).

Table 3-2. Primers used in this study

Primer	Sequence (5'-3')
MJM-313F	GCCCCGGGGCTCTTACTTGGTTGGCTTCTAAC
MJM-314R	GCGCATGCATCGTAATGGTATCTTTACCTGCAT
MJM-315F	GCCCCGGGATCCATGCCTTTAGTGAGCTTATC
MJM-316R	GCGCATGCTTTGATTAACGGCTTTATTAACCA
MJM-317F	GCCCCGGGTCAACTTGCTGCAAATATTGACTA
MJM-318R	GCGCATGCAAAGTAATGGTAAGCTGATGGTTG
MJM-319F	GCCCCGGGCGAGTTGCAAGTACAATAGACAACA
MJM-320R	GCGCATGCGCAATGATAAAAGCTAACCCGAAT
MJM-321F	GCCCCGGGACACAAATGATGGAGATGAAACG
MJM-322R	GCGCATGCGCCACAATAACTAATGTGAACAACA
MJM-323F	GCCCCGGGGCCTCTACACTTGAGGAAGAACA
MJM-324R	GCGCATGCGCTAAAATAGTTAGACCTGCTGTGG
MJM-325F	GCCCCGGGCACGCTTGAGCTTCCTACTATTCT
MJM-326R	GCGCATGCTGATATTACCGTCACCATCCATTA
MJM-127	ACAAGCATAAAGCTTGCTCAATCAATCACC
MJM-179	GCCACGGCCTTGTTCGCCGGC
MJM-173	ACCACGGCCACTTTCACCGGC
MJM-175	ACCACGCCCCATTTCACCAGC
MJM-176	GCCTCGACCATATTCACCAGC
MJM-181	TCCTCGACCTTGTTCGCCAGC
MJM-184	ACCTCGCCCTTGTTCACCCGC
MJM-186	TCCTCTTCCTTGTTCACCAGC
MJM-187	ACCACGACCATATTCACCTGC
MJM-192	ACCTCGGCCTTGCTCTCCAGC
MJM-193	ACCACGACCTTGTTCGCCAGC
MJM-195	CCCTCGCCCACTCTCACCAGC
MJM-201	ACCTCGACCAGATTCACCAGC
MJM-205	ACCACGACCATGATCACCAGC
MJM-206	ACCTCTTCCCGCTTCACCGGC
170Int2	AGCTTGCTCAATCAATCACC
ARB1	GGCCACGCGTCGACTAGTACNNNNNNNNNNGATAT
170Ext3	GCAGTTCAACCTGTTGATAGTACG
ARB2	GGCCACGCGTCGACTAGTAC
170Int3	CAAAGCAATTTTGAGTGACACAGG
170Seq1	AACACTTAACGGCTGACA
0777compF	GCGCATGCCCAAGTTTAAAAGAATTACG
0777compR	GCGGTACCTTACAGTTTAAATCGGTCGA

Plate-based chemotaxis assays

For assessment of chemotaxis in soft agar strains were grown overnight and then spotted onto SWT supplemented with 1.5 mM serine and 0.35% agar as previously described (DeLoney-Marino *et al*., 2003). Plates were incubated at 28°C for 4-6 hours, at which point 10 μL of each chemoattractant was spotted outside of the migrating rings. The chemoattractants were spotted at the following concentrations: 2 M serine, 1.1 M GlcNAc, 0.24 M $(GlcNAc)_2$, 0.17 M *N*-acetylneuraminic acid (NANA), 4.8 M thymidine, and 1 M glucose.

Screening for inner-ring migration defects and transposon insertion site identification

We selected five 96-well plates from the MB collection of *V. fischeri* transposon mutants (Chapter 2). These strains were inoculated into 100 μL SWT buffered with 50 mM HEPES, pH 7.5, directly from frozen stocks, and grown overnight. Omnitrays (Nunc, Rochester, NY) containing SWT 0.3% agar supplemented with 1.5 mM serine were inoculated, in duplicate, with 1 μL of each overnight culture using a 96-pin replicator (V&P Scientific, San Diego, CA). Soft-agar plates were then incubated at 28°C for 4-6 h and examined for altered inner-ring migration. Candidate strains were further examined by inoculation into individual SWT-serine soft-agar plates, which were subsequently incubated at room temperature (23-24°C) for ~12 h.

The insertion site of the validated candidate *vfcA*::Tn*erm* mutant, MB09076, was identified using arbitrarily-primed PCR as previously described (Chapter 2, Caetano-Anolles, 1993, O'Toole *et al.*, 1999). Briefly, the transposon junction site was amplified from a diluted

overnight culture in two successive rounds of PCR using primer sets ARB1/170Ext3, followed by ARB2/170Int3 (Table 3-2). The sample was submitted for sequencing to the DNA Sequencing Center at the University of Wisconsin Biotechnology Center (Madison, WI) with primer 170Seq1. Analysis of the sequencing results was performed with DNASTAR (Madison, WI) Lasergene Seqman software.

Capillary chemotaxis assay

Strains were grown in SWT liquid medium to an optical density of OD_{600} ~0.3, pelleted gently for 5 min at 800 x *g*, and resuspended in buffered artificial seawater (H-ASW: 100 mM $MgSO_4$, 20 mM $CaCl_2$, 20 mM KCl, 400 mM NaCl, and 50 mM HEPES, pH 7.5) (Ruby & Nealson, 1976). One microliter capillary tubes (Drummond Scientific, Broomall, PA) were sealed at one end, filled with either H-ASW alone or H-ASW containing the indicated attractant, and inserted into microcentrifuge tubes containing the cell suspension. The tubes were incubated on their side for 5 min at room temperature (23-24°C), after which the capillary tubes were removed from the cell suspension and washed. The contents were expelled into 150 µL buffer (either H-ASW or 70% Instant Ocean), and dilutions were plated for colony counts on LBS plates.

Construction of *vfcA* complementation plasmid

The *vfcA* open reading frame and 350 base pairs upstream were amplified by PCR using primer pair 0777compF and 0777compR (Table 3-2), and cloned into the SphI/KpnI-digested fragment of pVSV105 (Dunn *et al.*, 2006), using standard molecular techniques.

Both the complementation construct and vector control were conjugated into wild-type *V. fischeri* and into the *vfcA*::Tn*erm* mutant using standard technique (Stabb & Ruby, 2002).

Squid colonization assay

Newly hatched squid were colonized by exposure to approximately 3,000 CFU/mL of the indicated strain(s) in 100 mL filter-sterilized Instant Ocean (FSIO) for 3 hours. Squid were then transferred to vials containing 4 mL uninoculated FSIO for an additional 18-21 hours, at which point they were euthanized and surface-sterilized by storage at -80°C. Individual squid were then homogenized, and each homogenate was diluted and plated for colony counts on LBS agar using standard methods (Naughton & Mandel, 2012). In competitive colonization experiments, 100 colonies were then patched onto LBS plates supplemented with erythromycin to determine the ratio of the *vfcA*::Tn*erm* mutant to wild type. The competitive index (CI) for each individual squid is calculated as: (homogenate mutant CFU/wild-type CFU)/(inoculum mutant CFU/wild-type CFU).

RESULTS:

Generation and initial characterization of MCP mutants

The *V. fischeri* ES114 genome (Mandel *et al*., 2008, Ruby *et al*., 2005) encodes 43 predicted MCPs. Our preliminary analyses included BLAST (Johnson *et al.*, 2008) queries with full-length proteins and with the N-terminal sensing domains against characterized chemoreceptors in other organisms; however, this approach did not yield ligand-specific signatures. Categorization by domain structure (Figure 3-1) revealed four domain architectures that were common to at least 5 *V. fischeri* MCPs, and an additional eleven architectures represented in the genome. Because it appeared that many of the MCPs could be functional for chemotaxis signal transduction, we took an empirical approach to identifying whether mutants in MCP genes exhibited chemotaxis defects during an initial screen in a rich-medium soft-agar assay. We identified twelve mutants disrupted in MCP-encoding genes by PCR analysis of a transposon mutant collection as described in Materials and Methods (Table 3-1, Figure 3-1). We also constructed plasmid-integration (Campbell-type) mutants in seven other MCP genes that were not identified by this method (Table 3-1, Figure 3-1). Six of these seven specific target genes (*VF_0777* [*vfcA*], *VF_1133*, *VF_1789*, *VF_A0325*, *VF_A0448*, and *VF_A0677*) were selected as candidates because of evidence they might be regulated under conditions relevant to symbiosis: *vfcA*, *VF_1789*, *VF_A0325*, and *VF_A0677* were regulated by the flagellar master regulator FlrA in a transcriptomic study (Chapter 2); *vfcA* is regulated by the AinS C8-homoserine lactone autoinduction pathway that exhibits squid initiation and maintenance phenotypes (Lupp & Ruby, 2005); and *VF_A0448* and

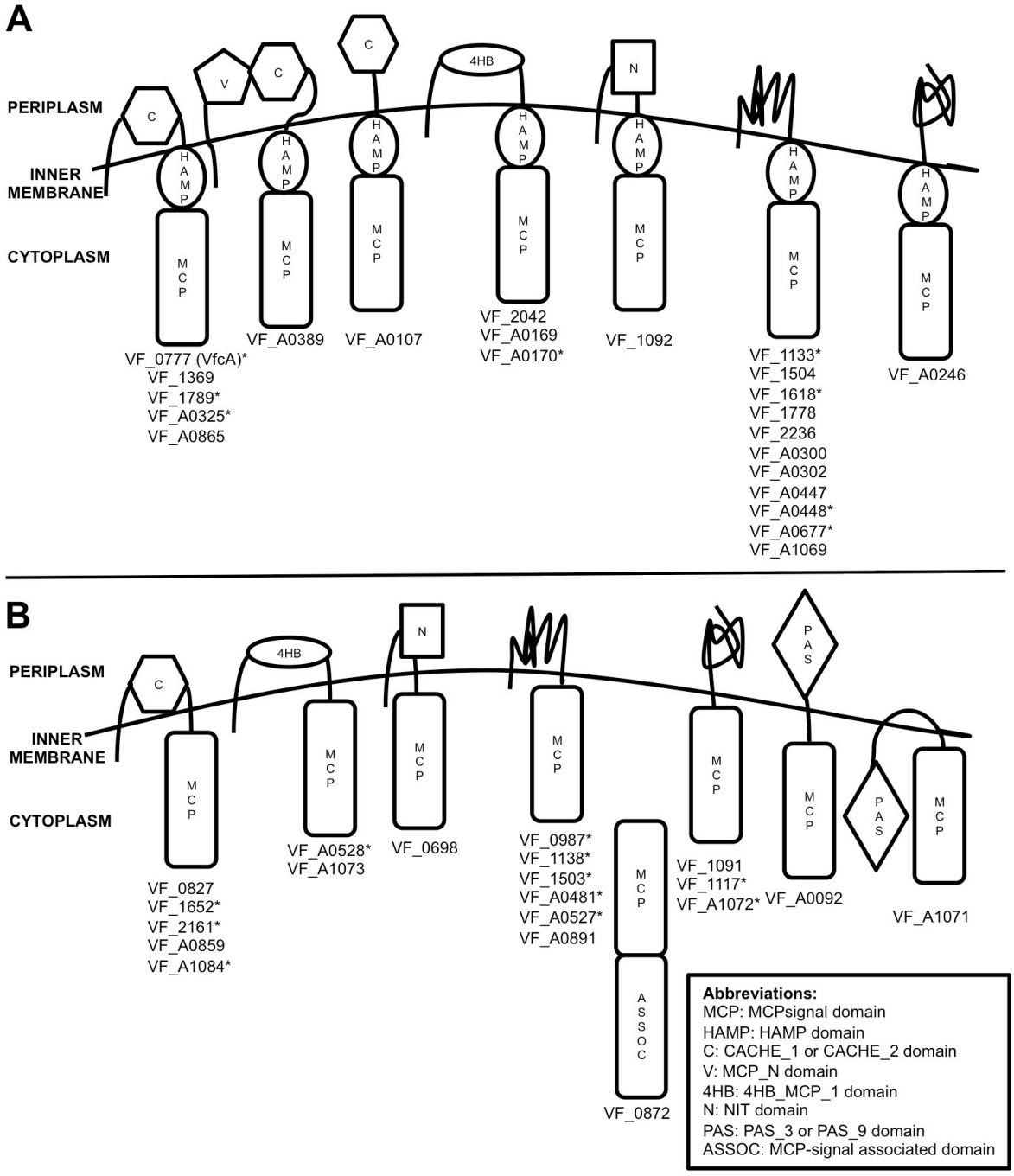
A
PERIPLASM
INNER MEMBRANE
CYTOPLASM
C
V
C
C
4HB
N
HAMP
MCP
VF_0777 (VfcA)*
VF_1369
VF_1789*
VF_A0325*
VF_A0865
VF_A0389
VF_A0107
VF_2042
VF_A0169
VF_A0170*
VF_1092
VF_1133*
VF_1504
VF_1618*
VF_1778
VF_2236
VF_A0300
VF_A0302
VF_A0447
VF_A0448*
VF_A0677*
VF_A1069
VF_A0246
B
PERIPLASM
INNER MEMBRANE
CYTOPLASM
C
4HB
N
PAS
MCP
ASSOC
VF_0827
VF_1652*
VF_2161*
VF_A0859
VF_A1084*
VF_A0528*
VF_A1073
VF_0698
VF_0987*
VF_1138*
VF_1503*
VF_A0481*
VF_A0527*
VF_A0891
VF_0872
VF_1091
VF_1117*
VF_A1072*
VF_A0092
VF_A1071
Abbreviations:
MCP: MCPsignal domain
HAMP: HAMP domain
C: CACHE_1 or CACHE_2 domain
V: MCP_N domain
4HB: 4HB_MCP_1 domain
N: NIT domain
PAS: PAS_3 or PAS_9 domain
ASSOC: MCP-signal associated domain

Figure 3-1. Representation of MCP domain-containing proteins in *V. fischeri* with (A) and without (B) predicted HAMP domains. Predicted domain structures of the 43 MCP domain-containing proteins as determined by Pfam and TmHMM analyses (Sonnhammer *et al.*, 1997, Krogh *et al.*, 2001). In each model, the N-terminus is orientated to the upper-left, and the C-terminus is marked by the MCP domain, except in the case of VF_0872 in which the ASSOC domain is C-terminal. Asterisks indicate loci in which a mutant in the corresponding gene has been identified and analyzed in this study. Abbreviations: MCP, MCPsignal domain; HAMP, HAMP domain; C, CACHE_1 or CACHE_2 domain; V, MCP_N domain; 4HB, 4HB_MCP_1 domain; N, NIT domain; PAS, PAS_3 or PAS_9 domain; ASSOC, MCP-signal associated domain (Hanlon *et al.*, 1992, Aravind & Ponting, 1999, Anantharaman & Aravind, 2000, Ulrich & Zhulin, 2005, Shu *et al.*, 2003, Zhulin *et al.*, 1997).

VF_1133 were activated when grown in either GlcNAc or $(GlcNAC)_2$, respectively (Amy Schaefer and Edward Ruby, personal communication). The final directed mutant we analyzed, *VF_2161*::pCAB18, was constructed with an insertion in a gene whose N-terminal sensing domain was highly similar to the *V. cholerae* gene encoded by *VC_0449*, which, when mutated, has been reported to reduce chemotaxis towards GlcNAc and $(GlcNAc)_2$ (Meibom et al., 2004).

All 19 of these mutants strains, as well as wild-type *V. fischeri,* were assayed for responses to glucose, serine, GlcNAc, $(GlcNAc)_2$, NANA, and thymidine in plate-based assays, as previously described (DeLoney-Marino *et al*., 2003, Mandel *et al*., 2012). Only one strain exhibited an altered chemotactic response to any of the assayed chemoattractants. The mutant disrupted in *VF_0777* (henceforth referred to as *vfcA* for *V. fischeri* chemoreceptor A) did not respond to exogenous serine, but exhibited wild-type responses to the other chemoattractants (Figure 3-2, and data not shown). It has been shown previously that, on SWT soft-agar plates, the outer ring of motile *V. fischeri* cells swim toward thymidine and the inner ring of cells swim toward serine (DeLoney-Marino *et al*., 2003). As shown in Figure 3-2B, the *vfcA*::pCAB15 mutant's inner ring did not exhibit a robust response to the addition of serine that is observed in wild-type cells (Figure 3-2A). Together, the mutant's lack of response to exogenous serine and its lack of a robust serine ring suggested that VfcA plays a role in mediating serine chemotaxis in *V. fischeri*.

We sought to identify an independent transposon-insertion mutant disrupted in *vfcA*. We took advantage of our observation that *vfcA* mutants lacked the inner motility ring and screened directly for random transposon insertion mutants that lacked the ring. We reasoned

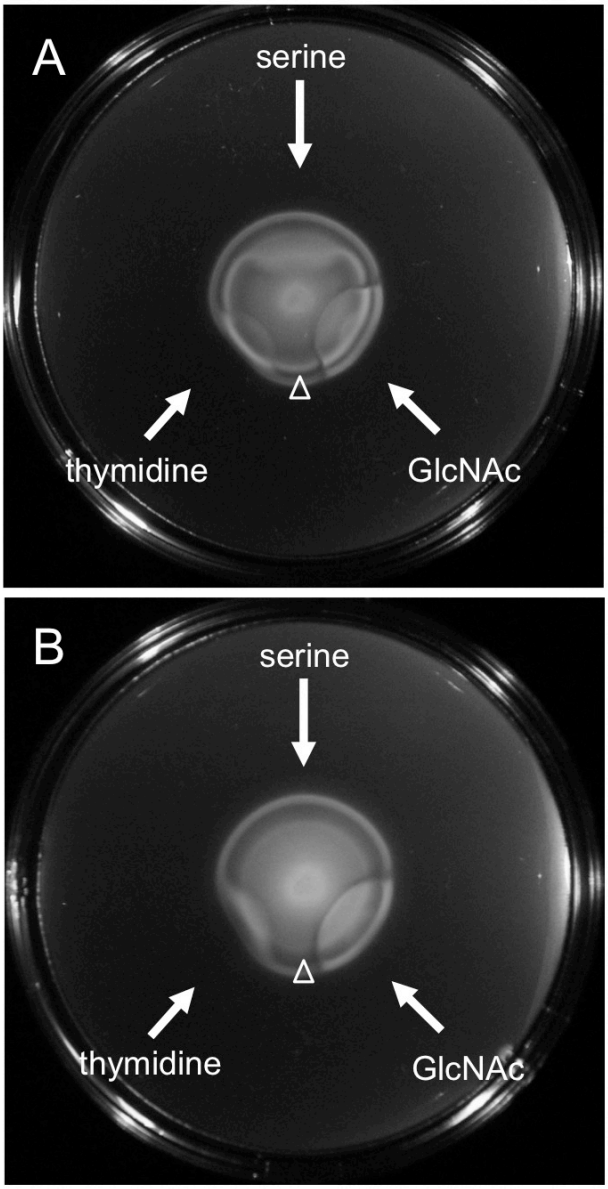

Figure 3-2. Responses of wild type and the *vfcA*::pCAB15 mutant to exogenous chemoattractants. (A) Wild-type (MJM1100) and (B) *vfcA::*pCAB15 mutant (CAB1500) cells were inoculated into SWT-serine soft-agar plates and incubated at 28°C for 5 h, at which time chemoattractants (serine, thymidine, or GlcNAc) were spotted (as indicated by arrows) and allowed to incubate an additional 2 h. Open arrowheads mark migration of the inner ring.

that such a screen would yield insertions in *vfcA* or in genes that modulated other aspects of serine chemotaxis. We screened 480 transposon mutants in serine-supplemented SWT soft agar and isolated a single candidate, MB09076, that did not have an obvious inner ring (Figure 3-3). The transposon insertion site was identified by arbitrarily-primed PCR and determined to be within the *vfcA* open-reading frame. Because the transposon mutation was less likely to revert than the plasmid- integration mutation, subsequent experiments were performed with the *vfcA*::Tn*erm* mutant.

Examination of chemotaxis behavior by capillary assay

Plate-based chemotaxis assays are indirect and require not only chemotaxis but also utilization of putative attractants to generate a gradient (Parales & Harwood, 2002). Therefore, to directly test whether VfcA plays a role in serine chemotaxis we performed a capillary chemotaxis assay, which has not previously been reported in *V. fischeri*, to directly test whether the *vfcA*::Tn*erm* mutant is chemotactic toward serine. In this assay, wild-type *V. fischeri* responded strongly to and migrated toward serine at concentrations of 100 μM, 1 mM, and 10 mM, as toward 1 mM GlcNAc, a structurally distinct chemoattractant used as a positive control (Figure 3-4). The *vfcA*::Tn*erm* mutant responded only to 1 mM GlcNAc, and did not respond to any of the tested serine concentrations. As expected, a non-chemotactic *cheA*::Tn*erm* mutant, isolated from another study (Chapter 2) also did not migrate toward any of the chemoattractants.

We then examined whether the phenotype of the *vfcA*::Tn*erm* mutant could be complemented by expression of a wild-type copy of *vfcA in trans*. As shown in Figure 3-5,

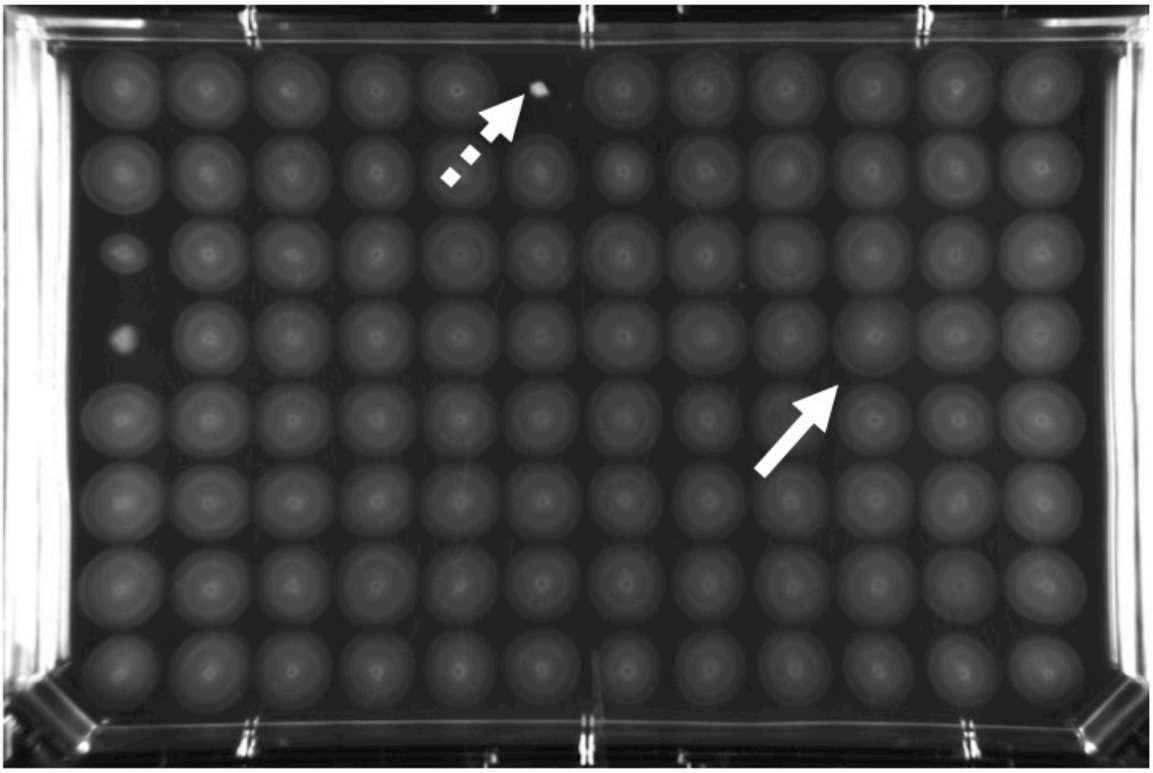

Figure 3-3. Screening for altered inner-ring migration in soft-agar motility plates. A representative SWT-serine soft-agar plate inoculated with 96 transposon mutants from the MB collection, as described in the Materials and Methods, and incubated for 4-6 h at 28°C. The white arrow indicates the identified *vfcA*::Tn*erm* mutant (MB09076), and the dashed arrow indicates a non-motile strain.

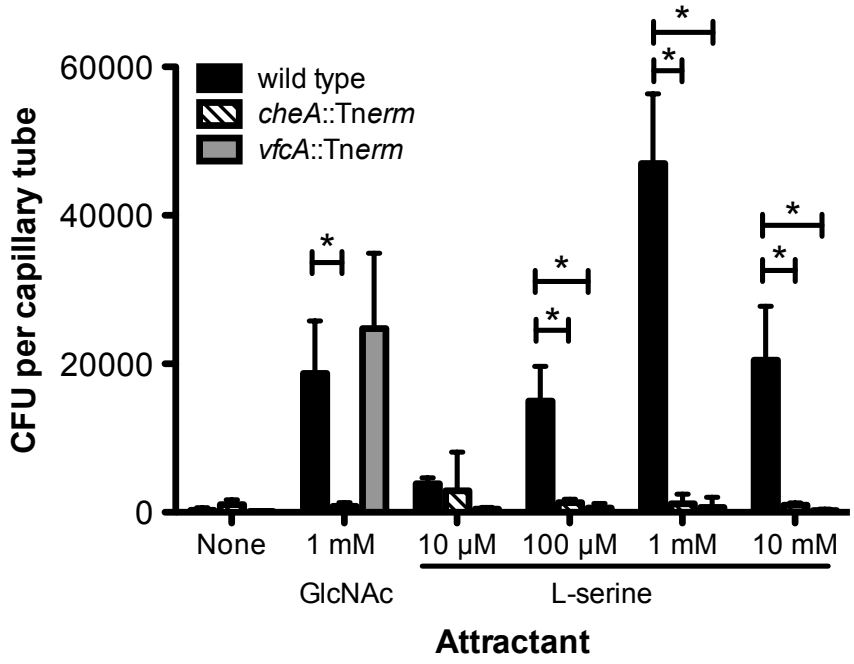

Figure 3-4. Responses to serine and GlcNAc in a capillary chemotaxis assay. Chemotactic responses of wild type, the *cheA*::Tn*erm* mutant (MB08701), and the *vfcA*::Tn*erm* (MB09076) mutant to varying concentrations of serine and 1 mM GlcNAc were measured by capillary chemotaxis assay. Data represent the mean and SEM of three independent assays performed in duplicate. Asterisks indicate significance at a p-value <0.01, as determined by two-way ANalysis Of VAriance (ANOVA) with a Bonferroni correction.

the chemotaxis response towards serine in the *vfcA*::Tn*erm* strain was restored upon heterologous expression of *vfcA*, supporting that it is the VfcA gene product that mediates the serine attraction. The complementation vector also enhanced the ability of wild-type *V. fischeri* to exhibit chemoattraction toward serine, but not GlcNAc (Figure 3-5), further supporting a role for VfcA is mediating chemotaxis toward serine and not toward GlcNAc (Figure 3-2, Figure 3-4). Together, these data suggested that *vfcA* encodes the serine chemoreceptor in *V. fischeri*, which is functionally analogous to *tsr* in *E. coli*.

Because MCPs can sense multiple chemoattractants, we then investigated whether VfcA mediates chemotaxis towards other amino acids in *V. fischeri*. Previous work using plate-based assays showed that wild-type *V. fischeri* responded most strongly to serine and, to a lesser extent, alanine, arginine, asparagine, histidine, and threonine (DeLoney-Marino *et al*., 2003). Again, soft-agar assays report on a combination of growth and chemotaxis phenotypes. We therefore applied our capillary assay to quantify the wild-type chemotaxis repertoire across all 20 amino acids (Table 3-3). We observed strong (>$5x10^3$ CFU/capillary) to 1 mM concentrations of serine, cysteine, threonine, and alanine (Table 3-3). These responses were abrogated in the *vfcA* mutant, suggesting that VfcA mediates chemotaxis towards each of these four amino acids. We also noticed that the *vfcA* mutant showed increased chemotaxis towards the aromatic hydrophobic amino acids (phenylalanine, tyrosine, and tryptophan) compared to wild-type *V. fischeri*.

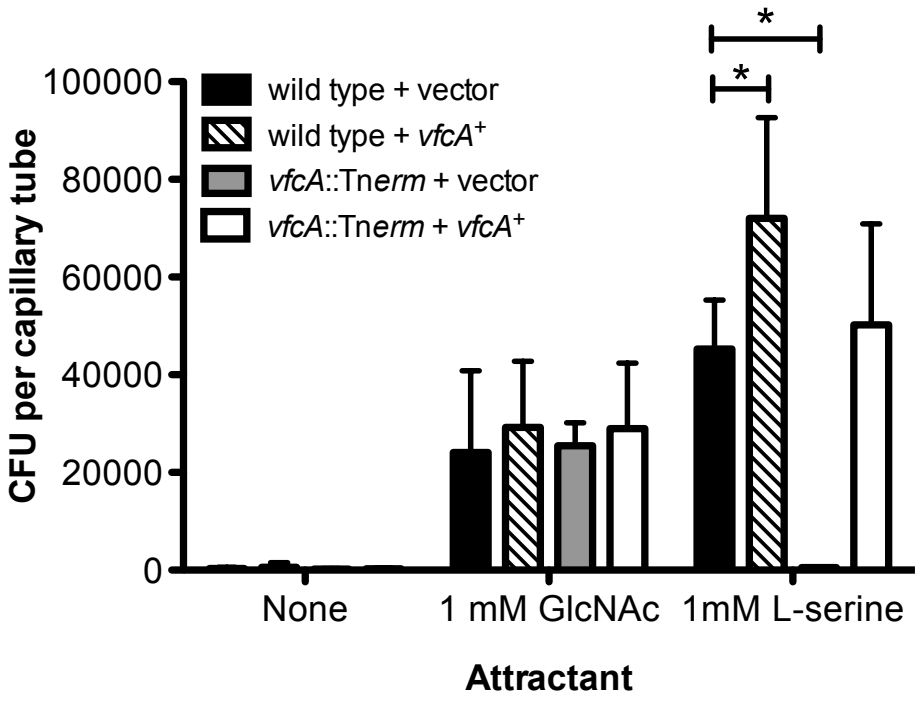

Figure 3-5. VfcA complementation as assayed by the capillary chemotaxis assay. Chemotactic responses of wild type harboring the vector control (CAB1516), wild type harboring the *vfcA* complementation construct (CAB1517), the *vfcA*::Tn*erm* mutant harboring the vector control (CAB1523), and the *vfcA*::Tn*erm* mutant harboring the *vfcA* complementation construct (CAB1524) to 1 mM GlcNAc or 1 mM L-serine, as measured by capillary chemotaxis assay. Data represent the mean and SEM of three independent assays performed in duplicate. Single asterisk indicates $p < 0.01$ by two-way ANOVA with a Bonferroni correction.

Table 3-3. Normalized chemotactic responses of wild-type and *vfcA*::Tn*erm* mutant strains to 1 mM L-amino acids.

Amino acid classification	Attractant	$\times 10^3$ CFU per capillary tube[a]	
		wild type	*vfcA*::Tn*erm*
Polar- basic	Arginine	BD[b]	0.8 ± 0.5
	Histidine	BD	BD
	Lysine	BD	BD
Polar- acidic	Aspartic Acid	0.3 ± 0.2	0.5 ± 0.8
	Glutamic Acid	**0.6 ± 0.2**[c]	0.2 ± 0.2
Polar- neutral	Serine	**55.6 ± 2.8**	BD
	Cysteine	**78.3 ± 12.3**	BD
	Threonine	**22.0 ± 6.2**	0.1 ± 0.2
	Asparagine	BD	3.0 ± 3.2
	Glutamine	0.2 ± 0.2	BD
	Methionine	0.4 ± 0.2	BD
Hydrophobic- aliphatic	Alanine	**8.0 ± 2.1**	BD
	Valine	BD	1.4 ± 0.8
	Isoleucine	BD	BD
	Leucine	BD	BD
Hydrophobic- aromatic	Phenylalanine	**0.3 ± 0.1**	**1.6 ± 0.6**
	Tyrosine	**0.6 ± 0.2**	**11.5 ± 5.1**
	Tryptophan	**1.6 ± 0.5**	**9.3 ± 2.3**
Unique	Glycine	**0.3 ± 0.1**	BD
	Proline	0.4 ± 0.3	BD

[a] Values represent the mean ± SEM of four independent assays performed in duplicate, and normalized by subtraction of no attractant controls.

[b] BD indicates below detection (0.1×10^3 adjusted CFU per capillary tube).

[c] **Bold font** indicates significance as compared to no attractant (0 adjusted CFU per capillary tube) at $p < 0.05$, as determined by one-tailed Student's t-test.

Squid colonization

Chemotaxis is important during squid colonization (Hussa *et al*., 2007, DeLoney-Marino & Visick, 2012) and host amino acids are critical to successful colonization by *V. fischeri* (Graf & Ruby, 1998). Because VfcA mediates essentially all of the significant amino acid chemotaxis in *V. fischeri* (Table 3-3), the *vfcA* mutant permitted us to test whether host-derived amino acids served as a signal for colonizing *V. fischeri* to locate their symbiotic niche. Our prediction was that, if amino acid chemoattraction is developmentally relevant, then the *vfcA* strain would exhibit a squid colonization defect. We colonized juvenile *E. scolopes* with culture-grown wild-type and *vfcA*::Tn*erm* strains, either individually (single-strain colonization) or in a competitive colonization assay. In the single-strain assays, wild-type and mutant strains each colonized to comparable levels (Figure 3-6A). Similarly, in competition, we observed a neutral competition phenotype, so this result did not find any competitive advantage or disadvantage for the mutant (Figure 3-6B).

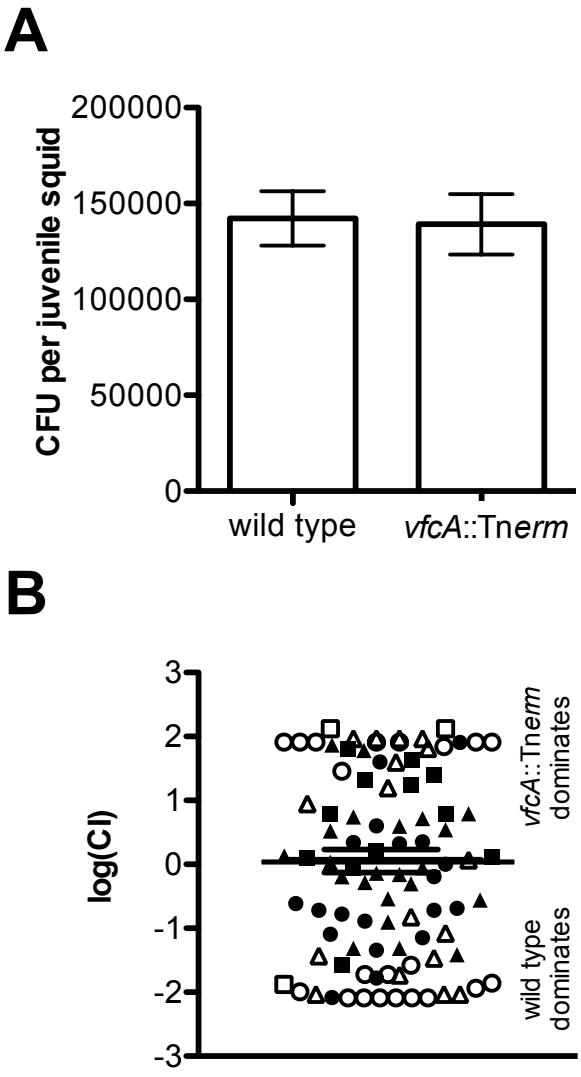
A
200000
150000
100000
50000
0
CFU per juvenile squid
wild type
vfcA::Tnerm
B
3
2
1
0
-1
-2
-3
log(CI)
vfcA::Tnerm dominates
wild type dominates

Figure 3-6. Single-strain and competitive colonization of juvenile squid. (A) Bacterial levels after 24 hours in squid exposed to either wild type (MJM1100) or *vfcA:*:Tn*erm* (MB09076) from three independent experiments, representing a total of 80 squid per condition. Starting inoculum levels ranged from 2300 CFU/mL to 4200 CFU/mL. (B) Relative competitive index (RCI) values of squid exposed to both wild type (MJM1100) and *vfcA:*:Tn*erm* (MB09076). Circles represent individual squid from one experiment (inoculum: 3465 CFU/mL, with a ratio of 1.22 *vfcA*::Tn*erm* to wild type; n=15 squid); squares represent individual squid from a second experiment (inoculum: 2410 CFU/mL, with a ratio of 0.75 *vfcA*::Tn*erm* to wild type; n=40 squid); triangles represent individual squid from a third experiment (inoculum: 4370 CFU/mL, with a ratio of 1.08 *vfcA*::Tn*erm* to wild type; n=39 squid). Open markers indicate squid in which only one strain was detected. Bars indicate mean ± SEM, as determined for all squid in which both strains were observed.

DISCUSSION:

The main contributiond from this work are as follows. (i) Using a capillary assay for the quantification of chemoattraction for the first time in *V. fischeri*, we probed the amino acid chemotaxis response of wild-type *V. fischeri* and revealed the strongest attraction to cysteine, serine, threonine, and alanine. (ii) Analyzing 19 mutants disrupted in individual predicted MCP-encoding genes, we identified one MCP, VfcA, that mediates chemotaxis toward a wide range of amino acids. (iii) The *vfcA* mutant colonizes squid as effectively as wild-type *V. fischeri*, both alone and in competition. These conclusions are addressed in turn below.

A number of studies have examined flagellar motility and chemotaxis in *V. fischeri* (Mandel *et al*., 2012, DeLoney-Marino *et al*., 2003, DeLoney-Marino & Visick, 2012, Graf *et al*., 1994, Hussa *et al*., 2007). Chemotaxis experiments in these works have relied on soft-agar motility assays. Our work has affirmed conclusions in those studies (*e.g.*, chemotaxis toward serine), and the capillary chemotaxis assay provides the ability to assay chemotaxis in liquid medium without confounding factors such as growth (Parales & Harwood, 2002). This technique permitted us to examine chemotaxis toward all twenty standard amino acids. In wild type, we measured significant chemotaxis toward nine of these amino acids, and this technique can now be applied to other relevant macromolecules in *V. fischeri*.

We mutated 19 of the 43 putative *V. fischeri* MCPs and found that only the *vfcA* mutant exhibited detectable chemotactic defects to any of the six *V. fischeri* chemoattractants tested. Using the capillary chemotaxis assay, we showed that the *vfcA* mutant does not exhibit strong chemotaxis toward serine, cysteine, threonine, and alanine. As we observed no

alteration in the *vfcA* mutant's ability to respond toward the structurally distinct chemoattractant GlcNAc, we attribute the amino acid phenotypes to specific signal transduction through VfcA, rather than to pleiotropic effects on chemotaxis overall. Furthermore, the mutant displays 5-10 fold enhanced attraction toward aromatic amino acids phenylalanine, tyrosine, and tryptophan. These data may indicate either that such aromatic amino acids act directly as VfcA-mediated chemorepellents, or that the loss of VfcA enhances recognition of this class of amino acids, perhaps by biasing the highly-organized structure of MCP arrays (Levit *et al.*, 2002).

Amino acids, including alanine and serine, are found in the squid light organ environment at micromolar concentrations (Graf & Ruby, 1998), and we hypothesized that these amino acids could serve as a chemotactic signal during symbiotic initiation. However, the *vfcA* mutant did not exhibit a colonization defect. As *vfcA* mutants are defective in essentially all of the major amino acid chemotaxis responses observed in wild type, we conclude that amino acid chemotaxis is not relevant for the colonizing symbiont to be directed into the its symbiotic niche. An alternate interpretation of the colonization data is that the mutant's enhanced chemoattraction toward aromatic amino acids mediates symbiotic colonization through a distinct pathway from wild-type *V. fischeri*; however, it is more parsimonious that amino acid chemotaxis does not play a significant role in bacterial migration into the light organ.

This work characterizes the first identification of MCP-chemoattractant pairing in *V. fischeri*. This could not have been predicted by sequence alone, as BLASTP comparison of the ligand-binding domain from the *E. coli* serine-sensing chemoreceptor, Tsr, to the ES114

proteome does not yield a single MCP within the significant hits. Additionally, recent work identified a distinct MCP in *V. cholerae*, named Mlp24/McpX, that mediates chemotaxis towards multiple amino acids (Nishiyama *et al*., 2012). It is not yet known whether amino acid chemotaxis appears elsewhere among the other 42 MCP-domain encoding proteins of *V. fischeri* such as the McpX ortholog.

Although we identified an amino-acid chemoreceptor in *V. fischeri*, the genetic basis for chemotaxis by the bacterium toward the other tested chemoattractants remains elusive. As we identified mutants in only 44% of the MCPs, it is possible that these behaviors are mediated by the remaining chemoreceptors and could be clarified by continuing to construct single MCP mutants. However, functional redundancy or masking by other behaviors (*i.e.* energy taxis) could similarly prevent chemoreceptor-ligand identification (Alvarez-Ortega & Harwood, 2007). Alternative approaches may be needed to uncover these relationships. Interestingly, *vfcA* is one of only four MCP genes that are regulated by the flagellar master activator FlrA in *V. fischeri* (Chapter 2). As such, it resembles the five *E. coli* MCPs that are all part of the flagellar regulon (Zhao *et al.*, 2007). Identifying such characteristics that show similarity to the canonical MCPs in *E. coli* may suggest an initial filter for chemoreceptors that mediate general (*e.g*., amino-acid) chemoattraction, rather than lifestyle-specific chemotactic responses that might require specific induction (Parales *et al.*, 2000).

This study and other recent works (Chapter 2, DeLoney-Marino & Visick, 2012, Mandel *et al*., 2012) have expanded the tools available for studying chemotaxis and motility in *V. fischeri*, including large-scale mutant availability and chemoattractant disruption in the host. As there is evidence that chemoattraction to the carbohydrate *N-N'*-diacetylchitobiose is

relevant during squid colonization (Mandel *et al*., 2012), it will be of interest to apply these methods to examine the genetic basis for *V. fischeri* to swim toward additional molecules. While the chemoattractant-chemoreceptor networks in bacterial species that encode high numbers of MCPs remain poorly understood, our work suggests that *V. fischeri* may serve as a strong model for characterizing the relevant roles of MCPs in mediating both planktonic and symbiotic chemotactic signals.

ACKNOWLEDGMENTS:

We thank Edward Ruby, Erica Raterman, and Ashleigh Janiga for helpful discussions and experimental assistance. This work was supported by NSF grant IOS-0843633 (MJM), NSF grant IOS-0843370 (CDM), and NSF grant IOS-0841507 and NIH grant RR12294 (to Margaret McFall-Ngai and E. Ruby). CAB was supported by an NIH Molecular Biosciences Training Grant and an NIH Microbes in Health and Disease Training Grant to the University of Wisconsin-Madison; CDM was also supported by a Pott Foundation Summer Research Fellowship and a Faculty Research and Creative Works Award through the University of Southern Indiana.

REFERENCES:

Adler, J. (1966) Chemotaxis in bacteria. *Science* **153**(3737): p. 708-16.

Alvarez-Ortega, C. and Harwood, C.S. (2007) Identification of a malate chemoreceptor in *Pseudomonas aeruginosa* by screening for chemotaxis defects in an energy taxis-deficient mutant. *Appl Environ Microbiol* **73**(23): p. 7793-5.

Anantharaman, V. and Aravind, L. (2000) Cache - a signaling domain common to animal Ca(2+)-channel subunits and a class of prokaryotic chemotaxis receptors. *Trends Biochem Sci* **25**(11): p. 535-7.

Aravind, L. and Ponting, C.P. (1999) The cytoplasmic helical linker domain of receptor histidine kinase and methyl-accepting proteins is common to many prokaryotic signalling proteins. *FEMS Microbiol Lett* **176**(1): p. 111-6.

Bibikov, S.I., Biran, R., Rudd, K.E., and Parkinson, J.S. (1997) A signal transducer for aerotaxis in *Escherichia coli*. *J Bacteriol* **179**(12): p. 4075-9.

Boettcher, K.J. and Ruby, E.G. (1990) Depressed light emission by symbiotic *Vibrio fischeri* of the sepiolid squid *Euprymna scolopes*. *J Bacteriol* **172**(7): p. 3701-6.

Boin, M.A. and Hase, C.C. (2007) Characterization of *Vibrio cholerae* aerotaxis. *FEMS Microbiol Lett* **276**(2): p. 193-201.

Caetano-Anolles, G. (1993) Amplifying DNA with arbitrary oligonucleotide primers. *PCR Methods Appl* **3**(2): p. 85-94.

DeLoney-Marino, C.R. and Visick, K.L. (2012) Role for *cheR* of *Vibrio fischeri* in the *Vibrio*-squid symbiosis. *Can J Microbiol* **58**(1): p. 29-38.

DeLoney-Marino, C.R., Wolfe, A.J., and Visick, K.L. (2003) Chemoattraction of *Vibrio fischeri* to serine, nucleosides, and N-acetylneuraminic acid, a component of squid light-organ mucus. *Appl Environ Microbiol* **69**(12): p. 7527-30.

Dunn, A.K., Martin, M.O., and Stabb, E.V. (2005) Characterization of pES213, a small mobilizable plasmid from *Vibrio fischeri*. *Plasmid* **54**(2): p. 114-34.

Dunn, A.K., Millikan, D.S., Adin, D.M., Bose, J.L., and Stabb, E.V. (2006) New rfp- and pES213-derived tools for analyzing symbiotic *Vibrio fischeri* reveal patterns of infection and *lux* expression in situ. *Appl Environ Microbiol* **72**(1): p. 802-10.

Eisenbach, M. (1996) Control of bacterial chemotaxis. *Mol Microbiol* **20**(5): p. 903-10.

Graf, J., Dunlap, P.V., and Ruby, E.G. (1994) Effect of transposon-induced motility mutations on colonization of the host light organ by *Vibrio fischeri*. *J Bacteriol* **176**(22): p. 6986-91.

Graf, J. and Ruby, E.G. (1998) Host-derived amino acids support the proliferation of symbiotic bacteria. *Proc Natl Acad Sci U S A* **95**(4): p. 1818-22.

Hanahan, D. (1983) Studies on transformation of *Escherichia coli* with plasmids. *J Mol Biol* **166**(4): p. 557-80.

Hanlon, D.W., Marquez-Magana, L.M., Carpenter, P.B., Chamberlin, M.J., and Ordal, G.W. (1992) Sequence and characterization of *Bacillus subtilis* CheW. *J Biol Chem* **267**(17): p. 12055-60.

Hazelbauer, G.L., Mesibov, R.E., and Adler, J. (1969) *Escherichia coli* mutants defective in chemotaxis toward specific chemicals. *Proc Natl Acad Sci U S A* **64**(4): p. 1300-7.

Henrichsen, J. (1972) Bacterial surface translocation: a survey and a classification. *Bacteriol Rev* **36**(4): p. 478-503.

Hussa, E.A., O'Shea, T.M., Darnell, C.L., Ruby, E.G., and Visick, K.L. (2007) Two-component response regulators of *Vibrio fischeri*: identification, mutagenesis, and characterization. *J Bacteriol* **189**(16): p. 5825-38.

Johnson, M., Zaretskaya, I., Raytselis, Y., Merezhuk, Y., McGinnis, S., and Madden, T.L. (2008) NCBI BLAST: a better web interface. *Nucleic Acids Res* **36**(Web Server issue): p. W5-9.

Kato, J., Kim, H.E., Takiguchi, N., Kuroda, A., and Ohtake, H. (2008) *Pseudomonas aeruginosa* as a model microorganism for investigation of chemotactic behaviors in ecosystem. *J Biosci Bioeng* **106**(1): p. 1-7.

Kim, H.E., Shitashiro, M., Kuroda, A., Takiguchi, N., Ohtake, H., and Kato, J. (2006) Identification and characterization of the chemotactic transducer in *Pseudomonas aeruginosa* PAO1 for positive chemotaxis to trichloroethylene. *J Bacteriol* **188**(18): p. 6700-2.

Kondoh, H., Ball, C.B., and Adler, J. (1979) Identification of a methyl-accepting chemotaxis protein for the ribose and galactose chemoreceptors of *Escherichia coli*. *Proc Natl Acad Sci U S A* **76**(1): p. 260-4.

Krell, T., Lacal, J., Munoz-Martinez, F., Reyes-Darias, J.A., Cadirci, B.H., Garcia-Fontana, C., and Ramos, J.L. (2011) Diversity at its best: bacterial taxis. *Environ Microbiol* **13**(5): p. 1115-24.

Krogh, A., Larsson, B., von Heijne, G., and Sonnhammer, E.L. (2001) Predicting transmembrane protein topology with a hidden Markov model: application to complete genomes. *J Mol Biol* **305**(3): p. 567-80.

Lacal, J., Garcia-Fontana, C., Munoz-Martinez, F., Ramos, J.L., and Krell, T. (2010) Sensing of environmental signals: classification of chemoreceptors according to the size of their ligand binding regions. *Environ Microbiol* **12**(11): p. 2873-84.

Larsen, S.H., Reader, R.W., Kort, E.N., Tso, W.W., and Adler, J. (1974) Change in direction of flagellar rotation is the basis of the chemotactic response in *Escherichia coli*. *Nature* **249**(452): p. 74-7.

Levit, M.N., Grebe, T.W., and Stock, J.B. (2002) Organization of the receptor-kinase signaling array that regulates *Escherichia coli* chemotaxis. *J Biol Chem* **277**(39): p. 36748-54.

Lupp, C. and Ruby, E.G. (2005) *Vibrio fischeri* uses two quorum-sensing systems for the regulation of early and late colonization factors. *J Bacteriol* **187**(11): p. 3620-9.

Mandel, M.J., Schaefer, A.L., Brennan, C.A., Heath-Heckman, E.A., Deloney-Marino, C.R., McFall-Ngai, M.J., and Ruby, E.G. (2012) Squid-derived chitin oligosaccharides are a chemotactic signal during colonization by *Vibrio fischeri*. *Appl Environ Microbiol* **78**(13): p. 4620-6.

Mandel, M.J., Stabb, E.V., and Ruby, E.G. (2008) Comparative genomics-based investigation of resequencing targets in *Vibrio fischeri*: focus on point miscalls and artefactual expansions. *BMC Genomics* **9**: p. 138.

Manson, M.D., Blank, V., Brade, G., and Higgins, C.F. (1986) Peptide chemotaxis in *E. coli* involves the Tap signal transducer and the dipeptide permease. *Nature* **321**(6067): p. 253-6.

Meibom, K.L., Li, X.B., Nielsen, A.T., Wu, C.Y., Roseman, S., and Schoolnik, G.K. (2004) The *Vibrio cholerae* chitin utilization program. *Proc Natl Acad Sci U S A* **101**(8): p. 2524-9.

Miller, L.D., Russell, M.H., and Alexandre, G. (2009) Diversity in bacterial chemotactic responses and niche adaptation. *Adv Appl Microbiol* **66**: p. 53-75.

Millikan, D.S. and Ruby, E.G. (2003) FlrA, a σ^{54}-dependent transcriptional activator in *Vibrio fischeri*, is required for motility and symbiotic light-organ colonization. *J Bacteriol* **185**(12): p. 3547-57.

Naughton, L.M. and Mandel, M.J. (2012) Colonization of *Euprymna scolopes* squid by *Vibrio fischeri*. *J Vis Exp* (61).

Nishiyama, S., Suzuki, D., Itoh, Y., Suzuki, K., Tajima, H., Hyakutake, A.*, et al.* (2012) Mlp24 (McpX) of *Vibrio cholerae* implicated in pathogenicity functions as a chemoreceptor for multiple amino acids. *Infect Immun* **80**(9): p. 3170-8.

O'Toole, G.A., Pratt, L.A., Watnick, P.I., Newman, D.K., Weaver, V.B., and Kolter, R. (1999) Genetic approaches to study of biofilms. *Methods Enzymol* **310**: p. 91-109.

Parales, R.E., Ditty, J.L., and Harwood, C.S. (2000) Toluene-degrading bacteria are chemotactic towards the environmental pollutants benzene, toluene, and trichloroethylene. *Appl Environ Microbiol* **66**(9): p. 4098-104.

Parales, R.E. and Harwood, C.S. (2002) Bacterial chemotaxis to pollutants and plant-derived aromatic molecules. *Curr Opin Microbiol* **5**(3): p. 266-73.

Porter, S.L., Wadhams, G.H., and Armitage, J.P. (2008) *Rhodobacter sphaeroides*: complexity in chemotactic signalling. *Trends Microbiol* **16**(6): p. 251-60.

Ruby, E.G. and Nealson, K.H. (1976) Symbiotic association of *Photobacterium fischeri* with the marine luminous fish *Monocentris japonica*; a model of symbiosis based on bacterial studies. *Biol Bull* **151**(3): p. 574-86.

Ruby, E.G., Urbanowski, M., Campbell, J., Dunn, A., Faini, M., Gunsalus, R.*, et al.* (2005) Complete genome sequence of *Vibrio fischeri*: a symbiotic bacterium with pathogenic congeners. *Proc Natl Acad Sci U S A* **102**(8): p. 3004-9.

Shu, C.J., Ulrich, L.E., and Zhulin, I.B. (2003) The NIT domain: a predicted nitrate-responsive module in bacterial sensory receptors. *Trends Biochem Sci* **28**(3): p. 121-4.

Sonnhammer, E.L., Eddy, S.R., and Durbin, R. (1997) Pfam: a comprehensive database of protein domain families based on seed alignments. *Proteins* **28**(3): p. 405-20.

Springer, M.S., Goy, M.F., and Adler, J. (1977) Sensory transduction in *Escherichia coli*: two complementary pathways of information processing that involve methylated proteins. *Proc Natl Acad Sci U S A* **74**(8): p. 3312-6.

Stabb, E.V. and Ruby, E.G. (2002) RP4-based plasmids for conjugation between *Escherichia coli* and members of the *Vibrionaceae*. *Methods Enzymol* **358**: p. 413-26.

Stock, J.B., and M. G. Surette, *Chemotaxis, p. 1103-1129.* , in *Escherichia coli and Salmonella, 2nd ed.*, R.C.I. F. C. Neidhart, J. I. Ingraham, E. C. C. Lin, K. B. Low, B.

Magasanik, W. S. Reznikoff, M. Riley, M. Schaechter, and H. E. Umbarger, Editor 1996, ASM Press: Washington, DC.

Studer, S.V., Mandel, M.J., and Ruby, E.G. (2008) AinS quorum sensing regulates the *Vibrio fischeri* acetate switch. *J Bacteriol* **190**(17): p. 5915-23.

Taguchi, K., Fukutomi, H., Kuroda, A., Kato, J., and Ohtake, H. (1997) Genetic identification of chemotactic transducers for amino acids in *Pseudomonas aeruginosa*. *Microbiology* **143 (Pt 10)**: p. 3223-9.

Ulrich, L.E. and Zhulin, I.B. (2005) Four-helix bundle: a ubiquitous sensory module in prokaryotic signal transduction. *Bioinformatics* **21 Suppl 3**: p. iii45-8.

Zhao, K., Liu, M., and Burgess, R.R. (2007) Adaptation in bacterial flagellar and motility systems: from regulon members to 'foraging'-like behavior in *E. coli*. *Nucleic Acids Res* **35**(13): p. 4441-52.

Zhulin, I.B., Taylor, B.L., and Dixon, R. (1997) PAS domain S-boxes in Archaea, Bacteria and sensors for oxygen and redox. *Trends Biochem Sci* **22**(9): p. 331-3.

Zusman, D.R., Scott, A.E., Yang, Z., and Kirby, J.R. (2007) Chemosensory pathways, motility and development in *Myxococcus xanthus*. *Nat Rev Microbiol* **5**(11): p. 862-72.

Chapter 4

Ligand Identification Using FRET-Based Analysis of Chimeric Chemoreceptors

PREFACE:

CAB, EGR and John S. Parkinson (University of Utah) formulated ideas and planned the experiments within this chapter. CAB performed all experiments and wrote the chapter. Run-zhi Lai (University of Utah) provided technical assistance.

ABSTRACT:

The bioluminescent marine bacterium *Vibrio fischeri* uses chemotaxis during its migration from the seawater to its symbiotic niche within the squid light organ. However, the specific methyl-accepting chemotaxis proteins (MCPs) that mediate this process remain unclear: traditional genetic techniques have proved insufficient to easily identify MCP-ligand pairs in *V. fischeri*, whose genome encodes 43 putative MCPs. Therefore, we sought to study ligand-MCP interactions by examining the ability of individual *V. fischeri* MCP ligand-binding domains to confer chemoattractant sensing to an *Escherichia coli* strain lacking its native chemoreceptors. We generated chimeric proteins that fused the ligand-binding domain of a given *V. fischeri* MCP to the signaling domain of Tar, a well-characterized chemoreceptor from *Escherichia coli*. After initial screening for functionality, we selected four candidates for further analysis using a FRET (Förster resonance energy transfer) *in vivo* kinase assay in response to pools of putative ligands. We showed that the ligand-binding domain of VfcA, a chemoreceptor previously linked to amino acid chemotaxis, was sufficient for eliciting FRET signals consistent with chemoattraction to serine, alanine, threonine and cysteine. We also identified a chemoreceptor (VfcB, locus tag VF_A0448) that responds specifically to several sugars, including the chitin breakdown products *N*-acetyl-glucosamine and *N-N'*-diacetylchitobiose. This study continues to clarify the chemotactic repertoire of *V. fischeri*, as begun in Chapter 3, and describes a system by which to identify chemoattractant-ligand interactions in other bacteria with large numbers of predicted MCPs.

INTRODUCTION:

Chemotaxis is one of numerous mechanisms bacteria use to respond to changes in their environmental conditions. By sensing gradients of stimuli such as amino acids, sugars, and oxygen, cells are able to direct motility towards energetically preferable environments (Sourjik and Wingreen, 2012). In host-microbe associations, chemotaxis can both enable niche specificity and prevent localization in harsh or otherwise undesirable tissues (Burall *et al.*, 2004, Butler *et al.*, 2006, Foynes *et al.*, 2000, Jones *et al.*, 1992, Stecher *et al.*, 2004). One such association in which chemotaxis mediates symbiotic initiation is the mutualism between the bioluminescent marine bacterium *Vibrio fischeri* and the Hawaiian bobtail squid, *Euprymna scolopes* (DeLoney-Marino and Visick, 2012, Mandel *et al*., 2012). As a horizontally acquired symbiont, *V. fischeri* cells must be obtained from the surrounding seawater upon the hatching of each juvenile squid (Nyholm and McFall-Ngai, 2004). This process occurs by bacterial aggregation in host-derived mucus, after which the bacteria migrate to the epithelium-lined crypts, a distance of less than 100 μm (Nyholm *et al.*, 2000). Despite this relatively short distance, the initiation process is highly specific and limited to motile *V. fischeri* cells (Nyholm *et al.*, 2000).

Chemotaxis, while not essential, provides a substantial advantage in colonization, and host-derived chitin breakdown products serve as a specific chemotactic signal during initiation (DeLoney-Marino and Visick, 2012, Mandel *et al.*, 2012). The molecular basis of how *V. fischeri* recognizes specific chemoattractants, such as chitin breakdown products, remains unclear, as the methyl-accepting chemotaxis proteins (MCPs), which serve as the

receptors that recognize specific chemoeffectors, underlying this behavior have not yet been identified.

Additionally, specific chemoreceptors are transcriptionally regulated during colonization in several host-microbe models, including the squid-vibrio symbiosis (Camilli and Mekalanos, 1995, Osorio *et al.*, 2005, Wier *et al.*, 2010, Yang *et al.*, 2004); understanding the ligands sensed by these MCPs may provide new insights into host environment. MCP repertoires vary greatly among sequenced bacteria in both number and ligand-binding domain types (Krell *et al.*, 2011, Lacal *et al.*, 2010), and this complexity has limited the success of traditional genetic techniques and bioinformatics approaches in identifying MCP-ligand pairs. However, the importance of MCPs throughout host-microbe associations underscores the need for a novel approach to study these interactions

In a ligand-dependent manner, MCPs transduce a signal through the associated histidine kinase CheA, initiating a phosphorelay that eventually controls the run/tumble bias of the cell (Parkinson *et al.*, 2005). While there are some anomalies, MCPs typically consist of a periplasmic ligand-binding domain and two cytoplasmic domains: the regulatory HAMP domain and the MCP signaling domain (Lacal *et al.*, 2010). Forming complex arrays primarily at the cell poles (Briegel *et al.*, 2009), MCPs bind chemoeffectors either directly or indirectly via periplasmic binding proteins (Neumann *et al.*, 2010). In the absence of a ligand, the MCP exists in an active state that allows CheA autophosphorylation (Parkinson, 2003). This phosphoryl group is then transferred to the response regulator CheY. Phosphorylated CheY can then bind either the flagellar switch protein FliM or the phosphatase CheZ. In the presence of a ligand, the MCP enters an inactive state that limits the kinase activity of CheA,

and disrupts the association between CheY and CheZ. Sourjik and Berg (2002) exploited the dynamic association between CheY and CheZ by developing Förster resonance energy transfer (FRET) tools to study CheA kinase activity. This FRET *in vivo* kinase assay has since been used to probe broader chemotaxis topics, including chemoreceptor-ligand interactions within the model organism *Salmonella enterica* (Lazova et al., 2012).

We hypothesized that this approach could be modified to identify the ligands bound by foreign MCPs, such as those from *V. fischeri*, when expressed in a receptor-less *E. coli* strain. As a heterologous MCP from *Pseudomonas putida* has been shown to successfully modulate CheA activity in *E. coli*, but was unable to fully confer chemotaxis (Herrera Seitz *et al.*, 2012), we designed chimeras that fused *V. fischeri* ligand-binding domains to the HAMP and signaling domain of *E. coli* Tar, the chemoreceptor that mediates aspartate chemotaxis, in an effort to enhance interaction with the native chemotactic machinery. We then sought to identify the ligands sensed by these chimeras, using the FRET *in vivo* kinase activity in response to pools of stimuli.

MATERIALS AND METHODS:

Bacterial strains and growth conditions

Strains and plasmids used in this work are listed in Table 4-1. *E. coli* strains were grown at 37 °C, unless otherwise indicated, in either Luria-Bertani medium (LB; per liter, 10 g tryptone, 5 g yeast extract, 5 g NaCl) or tryptone broth (T-broth; per liter, 10 g tryptone, 5 g NaCl). When appropriate, antibiotics were added to media at the following concentrations: ampicillin (amp), 50 μg/ml (in T-broth) or 100 μg/ml (in LB); and chloramphenicol (cam), 12.5 μg/ml (in T-broth) or 25 μg/ml (in LB). Medium was supplemented with isopropyl β-D-1-thiogalactopyranoside (IPTG), at the concentration listed in individual experiments, and sodium salicylate (NaSal), at a concentration of 2 μM, when necessary. Growth media were solidified with 1.5% agar as needed.

Chimera construction

Briefly, the native *NdeI* site within the *tar* open reading frame (ORF) was modified and a *NotI* site was introduced within the transmembrane domain to generate pHP02 (JS Parkinson, personal communication). Primers were designed to amplify the LBD region of the MCPs of interest from the start codon to the splice point, as described in the Results section. The following primer pairs were used to construct the indicated chimeras: VfcA-1-Tar, 0777_US and 0777_DS3; VfcA-2-Tar, 0777_USNdeI and 0777_DS3; VF_1092-Tar, 1092_USNdeI and 1092_DS; VF_1133-Tar, 1133_USNdeI and 1133_DS; VF_1618-1-Tar, 1618_USNdeI and 1618_DS1; VF_1618-2-Tar, 1618_USNdeI and 1618_DS2; VF_2042-1-

Tar, 2042_USNdeI and 2042_DS1; VF_2042-2-Tar, 2042_USNdeI and 2042_DS2; VF_2236-1-Tar, 2236_USNdeI and 2236_DS1; VF_2236-2-Tar, 2236_USNdeI and 2236_DS2; VF_A0107-Tar, A0107_USNdeI and A0107_DS; VF_A0169-Tar, A0169_USNdeI and A0169_DS; VF_A0325-1-Tar, A0325_USNdeI and A0325_DS1; VF_A0325-2-Tar, A0325_USNdeI and A0325_DS2; VF_A0389-Tar, A0389_USNdeI and A0389_DS; VF_A0448-1-Tar, A0448_USNdeI and A0448_DS1; VF_A0448-2-Tar, A0448_USNdeI and A0448_DS2; VF_A0677-1-Tar, A0677_UsNdeI and A0677_DS1; and VF_A0677-2-Tar, A0677_USNdeI and A0677_DS2. Primer sequences are listed in Table 4-2. The primer pairs incorporate *NdeI* and *NotI* restriction enzyme sites, which were used to clone the amplified products into the NdeI/NotI-digested pHP02 using standard techniques. The final constructs were verified by sequencing and transformed into competent cells prepared by $CaCl_2$ treatment.

Chemotaxis assay and induction conditions

T-swim plates were prepared by supplementing T-broth with 0.25% agar before autoclaving, and adding 50 μg/ml ampicillin and IPTG, at the concentration indicated in specific experiments, after cooling. Individual colonies were inoculated into T-swim plates using toothpicks, and plates were incubated at 30°C for 8-10 h.

FRET *in vivo* kinase assay

Preparation of cells and subsequent FRET *in vivo* kinase assay were adapted from previous work (Sourjik and Berg, 2002). Briefly, overnight cultures of *E. coli* were

Table 4-1. Strains and plasmids used in this study.

Strain or plasmid	Description	Reference or source
Strains		
E. coli		
EC100	Cloning vector	Epicentre (Madison, WI)
UU2612	RP437 [Δ*aer-1* Δ(*tar-tap*) Δ*tsr* Δ*trg*]	(Zhou *et al.*, 2011)
UU2700	RP437 [Δ*aer-1* Δ(*tar-tap*) Δ*tsr* Δ*trg* Δ*cheYZ*]	JS Parkinson
Plasmids		
pRR48	Expression vector, *ampR*	(Studdert and Parkinson, 2005)
pHP02	IPTG-inducible *tar* expression construct, *ampR*	JS Parkinson
pHP08	IPTG-inducible attenuated *tar* expression construct, *ampR*	JS Parkinson
pRZ30	NaSal-inducible *cheY-yfp cheZ-cfp* construct, *camR*	JS Parkinson
pCAB69	IPTG-inducible *vfcA*-1-*tar* chimera construct	This work
pCAB72	IPTG-inducible *vfcA*-2-*tar* chimera construct	This work
pCAB74	IPTG-inducible *VF_1092-tar* chimera construct	This work
pCAB76	IPTG-inducible *VF_1133-tar* chimera construct	This work
pCAB78	IPTG-inducible *VF_1618-1-tar* chimera construct	This work
pCAB79	IPTG-inducible *VF_1618-2-tar* chimera construct	This work
pCAB80	IPTG-inducible *VF_2042-1-tar* chimera construct	This work
pCAB81	IPTG-inducible *VF_2042-2-tar* chimera construct	This work
pCAB82	IPTG-inducible *VF_2236-1-tar* chimera construct	This work
pCAB83	IPTG-inducible *VF_2236-2-tar* chimera construct	This work
pCAB84	IPTG-inducible *VF_A0107-tar* chimera construct	This work
pCAB85	IPTG-inducible *VF_A0169-tar* chimera construct	This work
pCAB86	IPTG-inducible *VF_A0325-1-tar* chimera construct	This work
pCAB87	IPTG-inducible *VF_A0325-2-tar* chimera construct	This work
pCAB88	IPTG-inducible *VF_A0389-tar* chimera construct	This work
pCAB89	IPTG-inducible *VF_A0448*-1-*tar* chimera construct	This work
pCAB90	IPTG-inducible *VF_A0448*-2-*tar* chimera construct	This work
pCAB93	IPTG-inducible *VF_A0667*-1-*tar* chimera construct	This work
pCAB94	IPTG-inducible *VF_A0667*-2-*tar* chimera construct	This work

Table 4-2. Primers used in this study.

Primer	Sequence (5'-3')
0777_US	GGGCCCCATATGATGAAATTAAAACATAAGTT
0777_USNdel	GGGCCCCATATGAAATTAAAACATAAGTT
1092_USNdel	GGGCCCCATATGAATTTCATAAAAAAACT
1133_USNdel	GGGCCCCATATGAAAGAGAGATACAACAT
1618_USNdel	GGGCCCCATATGAAGCTAATTGGACGTTT
2042_USNdel	GGGCCCCATATGAAGATAAAAGATTTAAG
2236_USNdel	GGGCCCCATATGTCAGTAATAACGTTTAA
A0107_USNdel	GGGCCCCATATGGCGTCAATTCAAACTTA
A0169_USNdel	GGGCCCCATATGAGTTACAAAAATTTAGC
A0325_USNdel	GGGCCCCATATGGAACTACCTGAGAGAAA
A0389_USNdel	GGGCCCCATATGAAGTTTCGACACAAAAT
A0448_USNdel	GGGCCCCATATGCAATTTTCATTAAAAAA
A0667_USNdel	GGGCCCCATATGATTAATCTAACAATAAA
0777_DS3	AAATTTTGCGGCCGCCGTTAACACAATGCTTAATA
1092_DS	AAATTTTGCGGCCGCTGATGAAACGATAGTAATAGATAA
1133_DS	AAATTTTGCGGCCGCACCCAGTGCAATCCCTTTATAAAG
1618_DS1	AAATTTTGCGGCCGCCATAGCAACAATAATCGCACT
1618_DS2	AAATTTTGCGGCCGCCGCACTAATCGCACTAACTTG
2042_DS1	AAATTTTGCGGCCGCGGTTGAAGCAATGAACAGTGCTCC
2042_DS2	AAATTTTGCGGCCGCAATGAACAGTGCTCCGATCC
2236_DS1	AAATTTTGCGGCCGCCATGAATGACACAATCATTGCCAA
2236_DS2	AAATTTTGCGGCCGCCATGAATGACACAATCATTGCCAA
A0107_DS	AAATTTTGCGGCCGCAAGCTGCAACATCACCATAAA
A0169_DS	AAATTTTGCGGCCGCTGCACTAAACGATACTTTTGTTG
A0325_DS1	AAATTTTGCGGCCGCTAATGTGAACAACACAATCGC
A0325_DS2	AAATTTTGCGGCCGCCACAATAACTAATGTGAACAA
A0389_DS	AAATTTTGCGGCCGCCGCAATAACTGAATATATTAATG
A0448_DS1	AAATTTTGCGGCCGCAATAGTTAGACCTGCTGTGGTTTT
A0448_DS2	AAATTTTGCGGCCGCAGCTAAAATAGTTAGACCTGCTGT
A0667_DS1	AAATTTTGCGGCCGCAATCCACATAATGATGTCTTG
A0667_DS2	AAATTTTGCGGCCGCAATAACCACAATCCACATAATG

diluted 1:100 into T-broth containing appropriate antibiotics. After ~1 h growth at 30 °C, inducers (IPTG and NaSal) were added and cultures were allowed to grow for an additional 5 h, to an OD600 of ~0.4-0.5. Cells were collected by centrifugation at 1000 RCF, then washed and resuspended in tethering buffer (10 mM potassium phosphate, 0.1 mM K-EDTA, 100 μM L-methionine, 10 mM sodium lactate, pH 7.0). Cultures were then placed at 4 °C for 1 h to arrest protein synthesis. The cell mixture was concentrated 30-fold by centrifugation and subsequent resuspension, then attached to a poly-L-lysine-coated coverslip and placed in a flow cell. Cells were kept under constant flow of tethering buffer, or indicated stimuli in tethering buffer, by a syringe pump at a rate 1 mL/min at a constant temperature of 30°C.

Using an inverted phase microscope, a xenon lamp and a CFP (donor) excitation filter, the samples were illuminated and the resulting FRET signal was determined by measuring the CheZ-CFP (donor) and CheY-YFP (recipient) emission signals using two photon-counting photomultipliers. Labview software (National Instruments, Austin, TX) was used to analyze the YFP/CFP ratio over the course of an experiment.

RESULTS:

Chimera construction and initial screening

Chimeric chemoreceptors were designed to fuse the N-terminal ligand-binding domain of a given *V. fischeri* MCP to the HAMP and MCP signaling domain of *E. coli* Tar within the second transmembrane domain (Figure 4-1A). We initially targeted VfcA, the only chemoreceptor in *V. fischeri* with a known function (Chapter 3), for chimera construction to serve as a control for which there are putative ligands. We next selected additional MCPs based on ease of splice site identification and other cloning concerns (*i.e.*, an absence of interfering *NdeI* or *NotI* restriction sites within the ligand binding domain). Previous work with chimeras of *E. coli* MCPs provided insight for locating the optimal splice site, as even slight changes to the length of the transmembrane region have been shown to have drastic effects on downstream signaling ability. We first used bioinformatics to identify the HAMP domain within each MCP (Ulrich and Zhulin, 2010), and then manually located the conserved residues downstream of the splice site (Figure 4-1B). However, this approach proved less than ideal, as this region is less conserved in *V. fischeri* than *E. coli*. For example, a proline residue that is invariable in *E. coli* chemoreceptors was present in fewer than half of the *V. fischeri* MCPs. Therefore, two distinct constructs were designed for some MCPs in which the ideal splice point was ambiguous. In total, we generated 19 chimeras representing the ligand binding domains of 12 *V. fischeri* MCPs (Table 4-1).

The chimera constructs were transformed in UU2612, an *E. coli* strain lacking all 5 native chemoreceptors. To test whether the chimeras were expressed and able to interact with

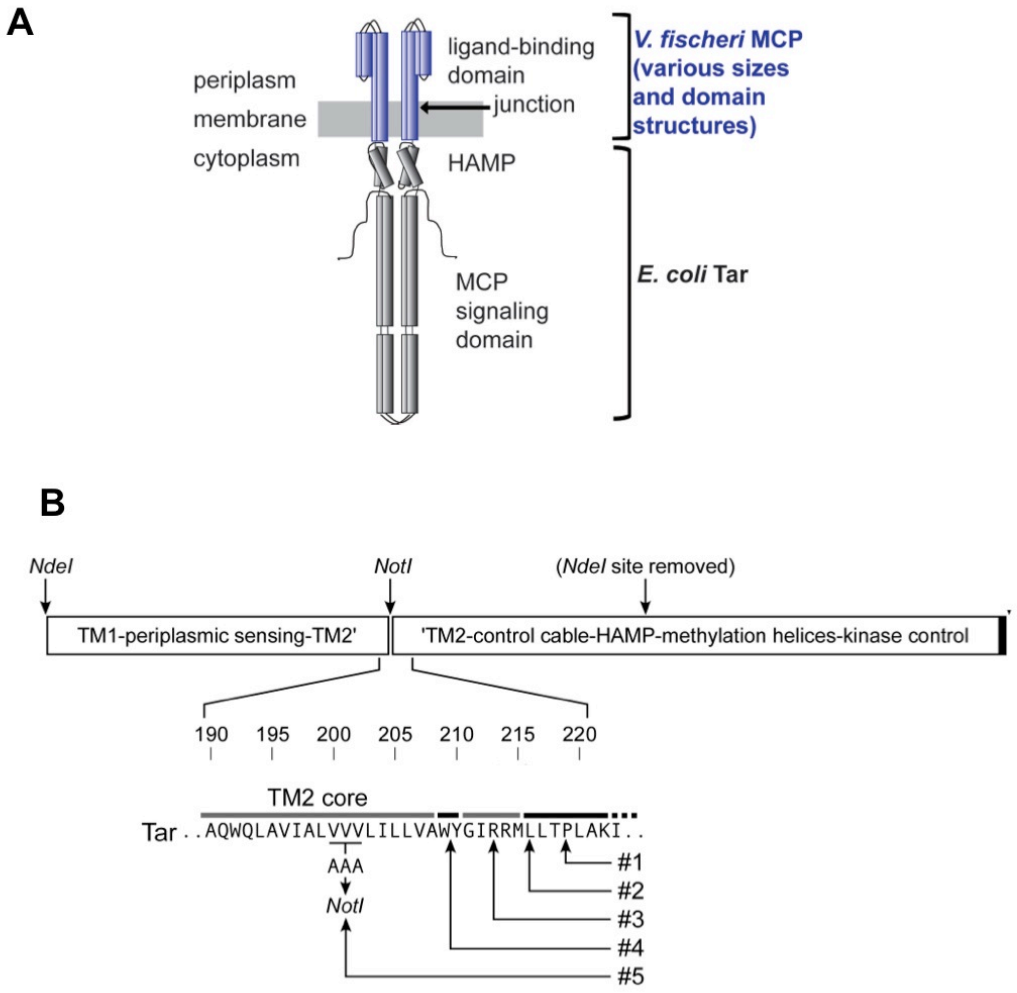

Figure 4-1. Chimera design and splice site identification. (A) Cartoon representation of a chimeric MCP homodimer. Blue represents regions from *V. fischeri* MCP; gray represents regions from *E. coli* Tar. (B) Chimera construct design and splice site recognition motif, as provided by JS Parkinson. #1-5 indicate conserved residues used for identifying junction.

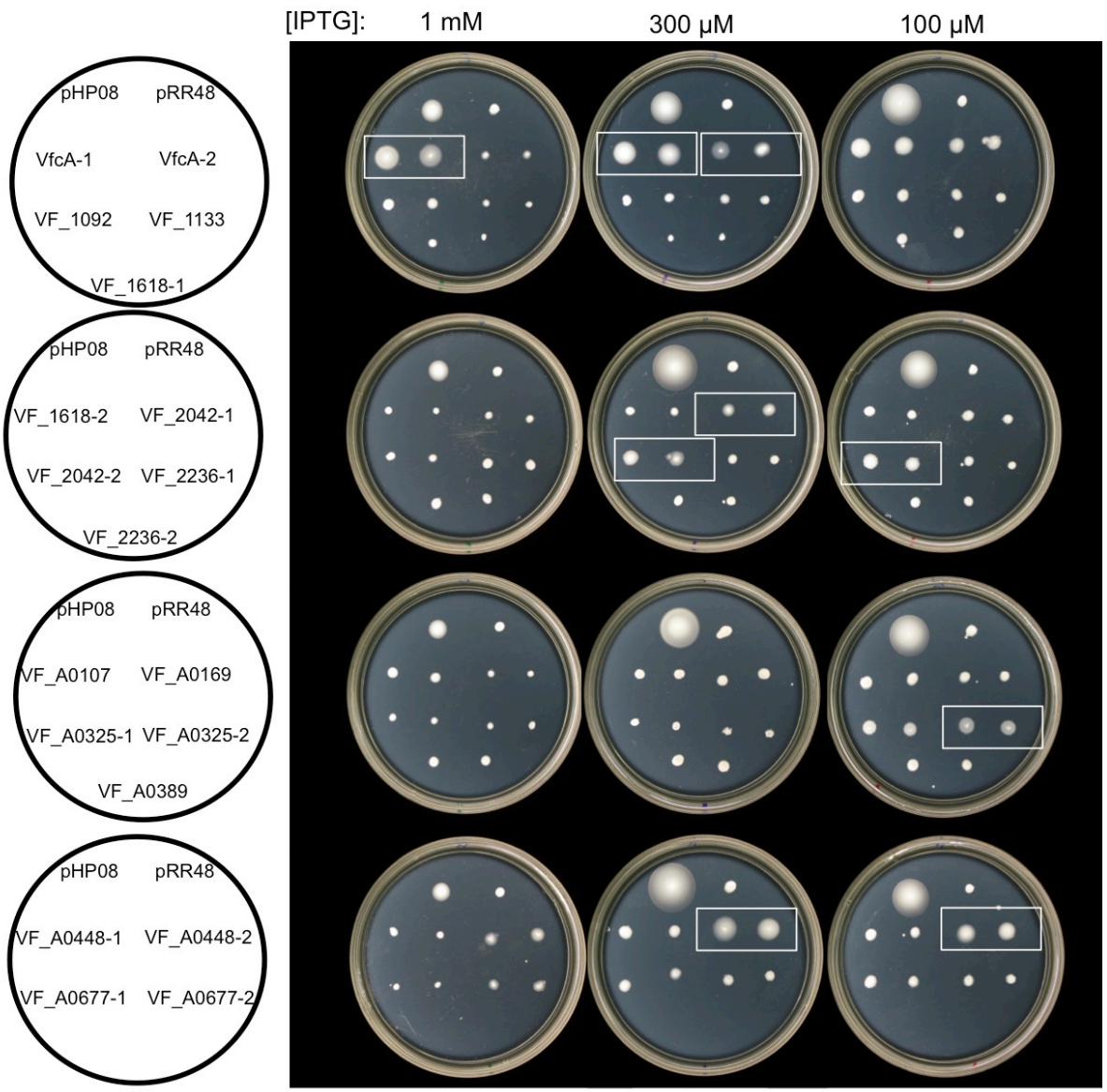
[IPTG]:
1 mM
300 µM
100 µM
pHP08
pRR48
VfcA-1
VfcA-2
VF_1092
VF_1133
VF_1618-1
pHP08
pRR48
VF_1618-2
VF_2042-1
VF_2042-2
VF_2236-1
VF_2236-2
pHP08
pRR48
VF_A0107
VF_A0169
VF_A0325-1
VF_A0325-2
VF_A0389
pHP08
pRR48
VF_A0448-1
VF_A0448-2
VF_A0677-1
VF_A0677-2

Figure 4-2. Characterization of chimera functionality in T-swim assay. Chimera constructs were transformed into the receptor-less UU2612 strain and resultant colonies were inoculated, in duplicate, into T-swim plates and inoculated as described in the Materials and Methods. IPTG was supplemented to induce chimera expression, at the concentration indicated above each column of plates. Plate layout is shown to the left of each row. pRR48, a vector control, and pHP08, which expresses a Tar variant under IPTG-inducible control, were used as negative and positive controls, respectively. White boxes mark constructs that exhibited altered colony morphology as compared to the negative control.

the native chemotaxis machinery, the strains were inoculated into T-swim plates containing various concentrations of IPTG (Figure 4-2). If a given chimera was both expressed and functional, we expected an alteration in swim colony morphology, as the MCP-dependent localization of CheA to the membrane affects kinase activity even in the absence of the appropriate ligand. Comparing the morphologies of the chimeras to the vector control (pRR48) and a positive control (pHP08), we observed 6 chimeras that had obvious effects on chemotaxis: VfcA-1-Tar and VfcA-2-Tar, VF_2042-1-Tar and VF_2042-2-Tar, VF_A0325-2-Tar, and VF_A0448-2-Tar (Figure 4-2). As both VfcA and VF_2042 had two chimeric constructs that exhibited functionality in this assay, we selected VfcA-1-Tar and VF_2042-2-Tar for further analysis.

As shown in Figure 3-1, VfcA and VF_A0325 both encode CACHE domains (Anantharaman and Aravind, 2000), whereas the ligand-binding domain of VF_2042 is apredicted four-helix bundle domain, the most similar class to *E. coli* chemoreceptors (Ulrich and Zhulin, 2005). The N-terminal region of VF_A0448 does not have any defined domains.

Confirmation of putative VfcA-Tar ligands by FRET *in vivo* kinase assay

The *E. coli* strain UU2700, designed for use in this assay, lacks all five MCPs, as well as CheY and CheZ. In preparation for the FRET *in vivo* kinase assay, CheY-YFP and CheZ-CFP are then expressed from a plasmid, pRZ30, under sodium salicylate-inducible control, and the chimeric MCP is expressed from a second plasmid under IPTG-inducible control. As described in the Materials and Methods, cells are grown under inducing conditions, attached to a coverslip, and placed in a flow cell, where they can be transiently treated with potential

ligands. Throughout the experiment, cells are exposed to a CFP-exciting wavelength, and both CFP (donor) and YFP (recipient) emissions are measured. When a chemoattractant is sensed by the chimeric MCP, activity of the kinase CheA will be reduced, resulting in both disassociation of the response regulator CheY-YFP (recipient) from the phosphatase CheZ-CFP (donor), and a lower FRET signal, as measured by the ratio of YFP/CFP (Figure 4-3). Conversely, the FRET signal is predicted to rise in the presence of a chemorepellent.

Because VfcA has been linked to amino acid chemotaxis (Chapter 3), we first characterized the VfcA-1-Tar chimera using the FRET *in vivo* kinase assay using the ligands predicted by the experiments performed in *V. fischeri*, including serine (Table 3-3). After exposing cells to a gradient of serine concentrations, we observed FRET responses consistent with chemoattraction at concentrations between 10 μM and 1 mM (Figure 4-4A). Higher concentrations were not tested, and lower concentrations did not yield obvious changes in the FRET signal. A second exposure to 1 mM serine at the end of the experiment confirmed that the cells were still capable of responding to serine. These results indicate that the ligand-binding domain of VfcA is sufficient for recognition of serine as a chemoattractant, and that demonstrate that such chimeric MCPs can successfully be used in the FRET *in vivo* kinase assay.

The *V. fischeri vfcA* mutant exhibited altered responses to additional amino acids when examined by capillary assay (Table 3-3). Specifically, the mutant had reduced responses to threonine, alanine, and cysteine, as well as increased responses to phenylalanine, tryptophan, and tyrosine. After exposing cells expressing the VfcA-1-Tar chimera to 1 mM concentrations of the indicated amino acids, we observed FRET profiles consistent with

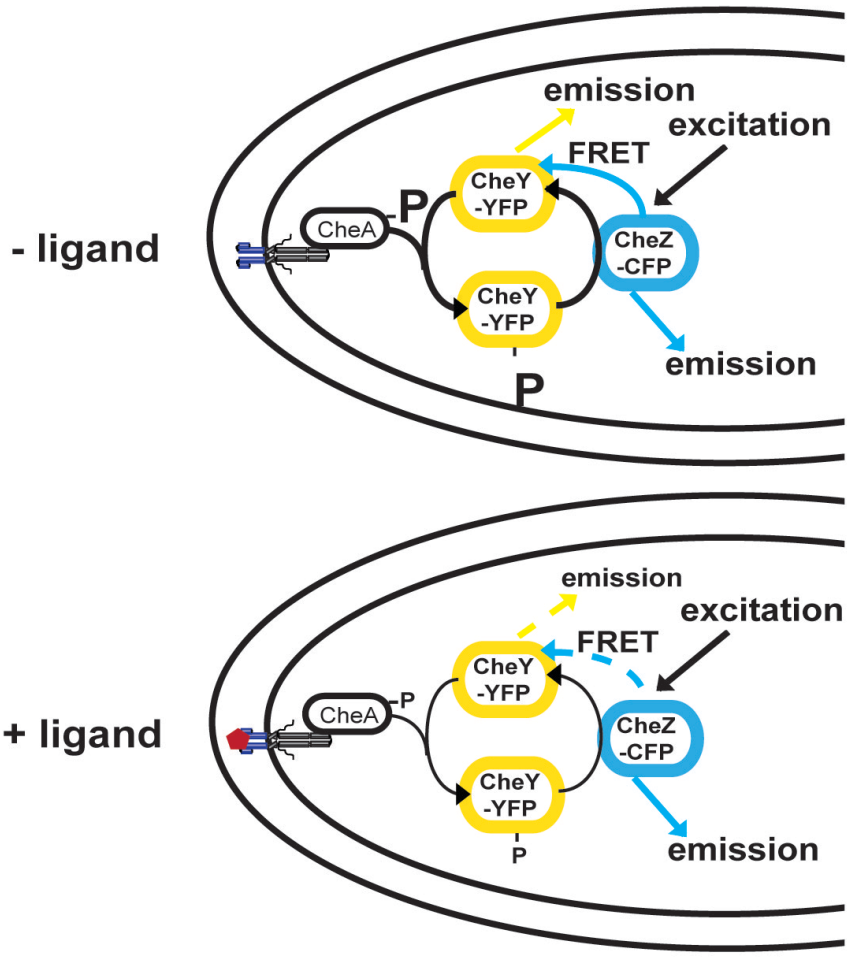

Figure 4-3. Schematic of FRET *in vivo* kinase assay in the absence or presence of a ligand. In the absence of a ligand (top), the CheA kinase is active, resulting in CheY phosphorylation and subsequent association of the phosphorylated CheY-YFP recipient with CheZ-CFP, yielding a high FRET signal. In the presence of a ligand (bottom), CheA activity is lessened, reducing both CheY-YFP association with CheZ-CFP and the subsequent FRET signal.

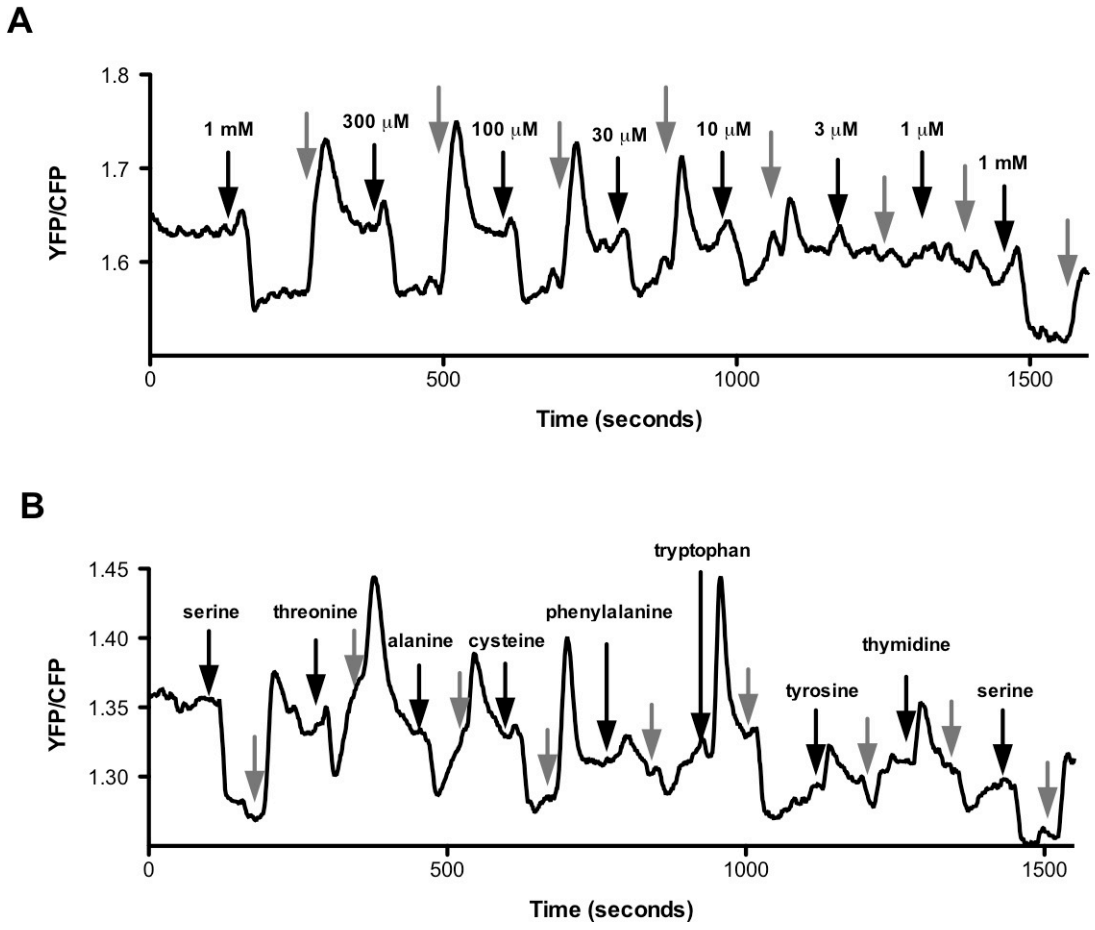

Figure 4-4. Analysis of the VfcA-1-Tar chimera by the FRET *in vivo* kinase assay.

(A) Response of the VfcA-1-Tar chimera to a gradient of serine concentrations.

(B) Response of the VfcA-1-Tar chimera to 1 mM levels of indicated amino acids. For both experiments, UU2700 was transformed with both pRZ30, harboring the FRET donor and recipient, and pCAB69, the VfcA-1-Tar expression construct. Cells were grown and prepared for FRET as described in the Materials and Methods, after induction with 2 μM NaSal and 100 μM IPTG. Black arrows indicate beginning of transient stimuli, and gray arrows mark a return to tethering buffer alone.

chemoattractant responses to threonine, alanine, and cysteine (Figure 4-4B). Phenylalanine, tryptophan, and tyrosine all elicited chemorepellent responses, with tryptophan serving as the strongest repellent at this concentration. These data indicate that the CACHE domain of VfcA is capable of directly mediating both chemoattraction and chemorepellent responses to multiple amino acids.

Probing chimeras using ligand pools

We used the FRET *in vivo* kinase assay to probe potential ligands for the remaining chimeras, in response to pools of 3-8 compounds, each at a concentration of 1 mM. The ligands were selected to represent a broad array of distinct molecules, known chemoeffectors for *V. fischeri* (DeLoney-Marino *et al.*, 2003, Mandel *et al.*, 2012), and other compounds likely found to be found in the symbiotic light-organ environment. The VF_2042-2-Tar chimera showed no responses to any tested pool (data not shown), and subsequent examination of these cells by phase contrast microscopy showed severely elongated cells. These observations suggested the induction conditions were negatively affecting cell health, so we excluded this construct from further analysis. While the cells appeared healthy, the VF_A0325-2-Tar chimera did not respond strongly to any tested pool, as the only changes in FRET signal appeared to be driven by noise or interference with the emission wavelengths (Figure 4-5). However, the VF_A0448-2-Tar chimera responded to several pools in a manner consistent with chemoattraction, most strongly to pools F, G, H, and K.

We next asked which ligands within one of these pools VF_A0448-2-Tar might specifically sense, by exposing the cells to the individual components of pool H, which

contains host-associated ligands (Figure 4-6A). The strongest chemoattractant profiles by the VF_A0448-Tar chimera were in response to *N*-acetyl-glucosamine (GlcNAc) and *N-N'*-diacetylchitobiose (chitobiose). While the FRET signal was reduced after exposure to N-acetylneuraminic acid (NANA), the behavior after being re-exposed to buffer was inconsistent with chemoattraction, so it is unlikely that VfcB senses NANA. We examined the individual components of the other targeted pools as well (F, G, and K), and observed responses consistent with a chemoattraction response after exposure to cellobiose, glucose, maltose, and mannose (data not shown). While most of the predicted VfcB ligands are PTS sugars, which have been shown to directly affect the phosphorylation state of CheA in *E. coli* (Lux et al., 1995), the FRET signature is specific to the presence of the VfcB-Tar, and is not observed when other chimeras are exposed to these compounds. These data suggest that ligand-binding domain of VF_A0448 (which we have now renamed VfcB, for *Vibrio fischeri* chemoreceptor B) might mediate recognition of severeal hexoses and di-hexoses. The basis for the response to pool K is unknown at this time.

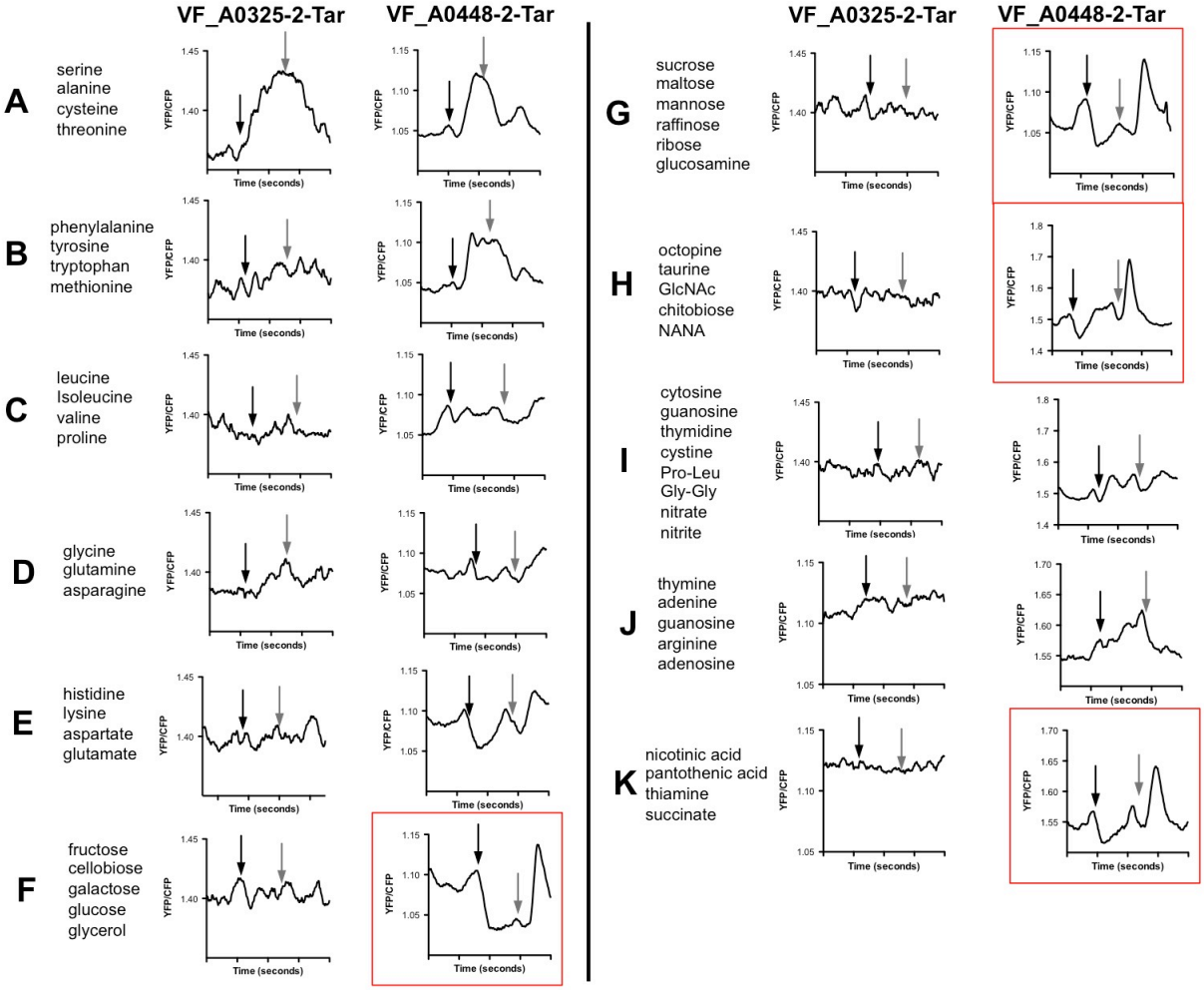
VF_A0325-2-Tar
VF_A0448-2-Tar
A
serine
alanine
cysteine
threonine
B
phenylalanine
tyrosine
tryptophan
methionine
C
leucine
Isoleucine
valine
proline
D
glycine
glutamine
asparagine
E
histidine
lysine
aspartate
glutamate
F
fructose
cellobiose
galactose
glucose
glycerol
G
sucrose
maltose
mannose
raffinose
ribose
glucosamine
H
octopine
taurine
GlcNAc
chitobiose
NANA
I
cytosine
guanosine
thymidine
cystine
Pro-Leu
Gly-Gly
nitrate
nitrite
J
thymine
adenine
guanosine
arginine
adenosine
K
nicotinic acid
pantothenic acid
thiamine
succinate
YFP/CFP
Time (seconds)

Figure 4-5. Analysis of the chimeras by the FRET *in vivo* kinase assay using ligand pools. For all experiments, UU2700 was transformed with both pRZ30, harboring the FRET donor and recipient, and the indicated chimera expression construct. Cells were grown and prepared for FRET as described in the Materials and Methods, after induction with 2 μM NaSal and either 30 μM (VF_A0325-2-Tar) or 100 μM (VF_A0448-2-Tar) IPTG. Each dash on the x-axis (time) represents 30 seconds. Black arrows indicate beginning of transient ligand flow, and gray arrows mark a return to tethering buffer alone. Pools A-K contained 1 mM concentrations of the ligands listed to the left of each row, except for NANA, which was presented at 0.01%. Red boxes mark pools that elicited a response consistent with chemoattraction.

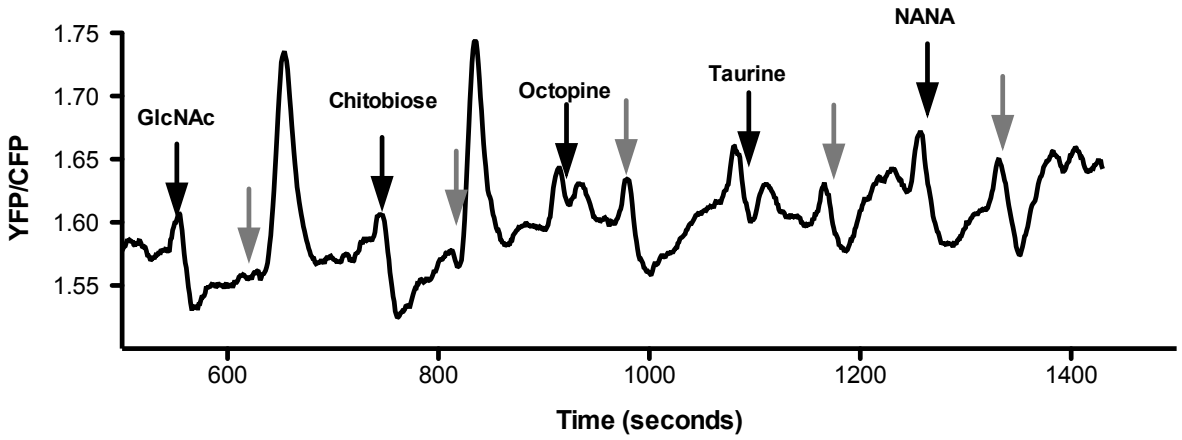

Figure 4-6. Reductive analysis of pool H using the FRET *in vivo* kinase assay. UU2700 was transformed with both pRZ30, harboring the FRET donor and recipient, and the VF_A0448-2-Tar chimera expression construct. Cells were grown and prepared for FRET as described in the Materials and Methods, after induction with 2 μM NaSal and 100 μM IPTG. Black arrows indicate beginning of transient ligand flow, and gray arrows mark a return to tethering buffer. All ligands were presented at 1 mM, except for NANA (0.01%).

DISCUSSION:

Wide-scale genome sequencing has brought the problem of understanding the complexity of MCP-ligand interactions to the forefront of the bacterial chemotaxis community. Whether due to functional redundancy or confounding behaviors like a strong energy taxis (Alvarez-Ortega and Harwood, 2007), traditional genetic, bioinformatics and physiological approaches have yet to satisfactorily enable broad characterizations of chemoreceptor-ligand pairs in the many species of bacteria with large numbers of MCPs. By combining several approaches used previously in *E. coli*, including the FRET *in vivo* kinase assay and chimeric MCPs, we have developed a technique that can be applied to most bacteria and used to address questions of chemoreceptor-ligand interactions.

As we only characterized the ligand partners for 2 MCPs out of the 12 initial targets, we recognize that the efficiency of this approach is not yet satisfactory. The limiting step of this study was generating functional chimeras. However, now that we have identified successful splice sites for several *V. fischeri* MCPs, in the future we can improve the identification of successful splice-site motifs. While it is possible that the two or more of the ligands within the same pool cancelled out an obvious response for the two chimeras that did not respond to any of the ligand pools in the FRET assay, it is more likely either that the chimeras were not well expressed under the conditions of the assay or that their ligands were not included within the pools. Again, both of these problems can be addressed and resolved in future studies. A final possibility is that the ligand sensed by these MCPs requires a periplasmic binding protein that is not conserved in *E. coli*; this concern is the hardest to

address, but the majority of characterized MCPs sense ligands directly without an adaptor protein. Nonetheless, despite these limitations, this initial study was successful in beginning to characterize a novel ligand-binding domain that mediates sugar recognition.

The ligand-binding region of VF_A0448 (now VfcB) contains no recognizable domains, as determined by MiST2 and PFAM analyses (Sonnhammer *et al.*, 1998, Ulrich and Zhulin, 2010). Therefore, by linking this domain to sugar recognition, we have begun to characterize a novel ligand-binding domain that may play an important role in both chemotaxis and other behaviors, as this region is conserved in proteins across the *Vibrionaceae*. Because we have not yet characterized whether a *vfcB* mutant in *V. fischeri* exhibits altered chemotaxis towards any of the compounds suggested by the FRET results, it is possible that the *vfcB* mutant may respond like wild type in the targeted capillary assays. This result could be due to either functional redundancy in the native *V. fischeri* background or poor expression under the conditions of the assay, as transcriptional data from another study suggest that *vfcB* expression is regulated in response to growth on GlcNAc or chitobiose (Schaefer and Ruby, personal communication). However, if this situation occurs, the FRET results could be confirmed by performing capillary assays on either the ΔMCP *E. coli* strain expressing the VfcB-Tar chimera, or a *V. fischeri* strain harboring VfcB under IPTG-inducible conditions, expecting an increase in chemotaxis towards the putative ligands in both cases.

To my knowledge, our characterization of VfcA is the first report of a CACHE domain-containing MCP directly mediating both attractant and repellent responses. Previously, we showed capillary results consistent with VfcA acting as a chemoreceptor for

both of these behaviors (Chapter 3), but those data could have resulted from indirect effects. While MCPs have recently been shown to bind multiple ligands in distinct binding pockets (Pineda-Molina *et al.*, 2012), the ability to recognize and respond distinctly to such similar molecules raises interesting biochemical questions about the CACHE domain, found in MCPs across bacterial species. These novel characterizations of VfcA and VfcB add to our overall understanding of how chemoreceptors sense ligands, not just in *V. fischeri*, but throughout bacteria, and underscore the importance of these types of studies.

ACKNOWLEDGMENTS:

We thank Julia Schwartzman, Clotilde Bongrand, and Peter Ames for experimental assistance. This work was supported by NIH grant RR12294 (to MJM-N and EGR). CAB was supported by an NIH Molecular Biosciences Training Grant and an NIH Microbes in Health and Disease Training Grant to the University of Wisconsin.

REFERENCES:

Alvarez-Ortega, C. and Harwood, C.S. (2007) Identification of a malate chemoreceptor in *Pseudomonas aeruginosa* by screening for chemotaxis defects in an energy taxis-deficient mutant. *Appl Environ Microbiol* **73**(23): p. 7793-5.

Anantharaman, V. and Aravind, L. (2000) Cache - a signaling domain common to animal Ca(2+)-channel subunits and a class of prokaryotic chemotaxis receptors. *Trends Biochem Sci* **25**(11): p. 535-7.

Briegel, A., Ortega, D.R., Tocheva, E.I., Wuichet, K., Li, Z., Chen, S., Muller, A., Iancu, C.V., Murphy, G.E., Dobro, M.J., Zhulin, I.B., and Jensen, G.J. (2009) Universal architecture of bacterial chemoreceptor arrays. *Proc Natl Acad Sci U S A* **106**(40): p. 17181-6.

Burall, L.S., Harro, J.M., Li, X., Lockatell, C.V., Himpsl, S.D., Hebel, J.R., Johnson, D.E., and Mobley, H.L. (2004) *Proteus mirabilis* genes that contribute to pathogenesis of urinary tract infection: identification of 25 signature-tagged mutants attenuated at least 100-fold. *Infect Immun* **72**(5): p. 2922-38.

Butler, S.M., Nelson, E.J., Chowdhury, N., Faruque, S.M., Calderwood, S.B., and Camilli, A. (2006) Cholera stool bacteria repress chemotaxis to increase infectivity. *Mol Microbiol* **60**(2): p. 417-26.

Camilli, A. and Mekalanos, J.J. (1995) Use of recombinase gene fusions to identify *Vibrio cholerae* genes induced during infection. *Mol Microbiol* **18**(4): p. 671-83.

DeLoney-Marino, C.R. and Visick, K.L. (2012) Role for *cheR* of *Vibrio fischeri* in the *Vibrio*-squid symbiosis. *Can J Microbiol* **58**(1): p. 29-38.

DeLoney-Marino, C.R., Wolfe, A.J., and Visick, K.L. (2003) Chemoattraction of *Vibrio fischeri* to serine, nucleosides, and N-acetylneuraminic acid, a component of squid light-organ mucus. *Appl Environ Microbiol* **69**(12): p. 7527-30.

Foynes, S., Dorrell, N., Ward, S.J., Stabler, R.A., McColm, A.A., Rycroft, A.N., and Wren, B.W. (2000) *Helicobacter pylori* possesses two CheY response regulators and a histidine kinase sensor, CheA, which are essential for chemotaxis and colonization of the gastric mucosa. *Infect Immun* **68**(4): p. 2016-23.

Herrera Seitz, M.K., Soto, D., and Studdert, C.A. (2012) A chemoreceptor from *Pseudomonas putida* forms active signalling complexes in *Escherichia coli*. *Microbiology* **158**(Pt 9): p. 2283-92.

Jones, B.D., Lee, C.A., and Falkow, S. (1992) Invasion by *Salmonella typhimurium* is affected by the direction of flagellar rotation. *Infect Immun* **60**(6): p. 2475-80.

Krell, T., Lacal, J., Munoz-Martinez, F., Reyes-Darias, J.A., Cadirci, B.H., Garcia-Fontana, C., and Ramos, J.L. (2011) Diversity at its best: bacterial taxis. *Environ Microbiol* **13**(5): p. 1115-24.

Lacal, J., Garcia-Fontana, C., Munoz-Martinez, F., Ramos, J.L., and Krell, T. (2010) Sensing of environmental signals: classification of chemoreceptors according to the size of their ligand binding regions. *Environ Microbiol* **12**(11): p. 2873-84.

Lazova, M.D., Butler, M.T., Shimizu, T.S., and Harshey, R.M. (2012) *Salmonella* chemoreceptors McpB and McpC mediate a repellent response to L-cystine: a potential mechanism to avoid oxidative conditions. *Mol Microbiol* **84**(4): p. 697-711.

Lux, R., Jahreis, K., Bettenbrock, K., Parkinson, J.S., and Lengeler, J.W. (1995) Coupling the phosphotransferase system and the methyl-accepting chemotaxis protein-dependent chemotaxis signaling pathways of *Escherichia coli*. *Proc Natl Acad Sci U S A* **92**(25): p. 11583-7.

Mandel, M.J., Schaefer, A.L., Brennan, C.A., Heath-Heckman, E.A., Deloney-Marino, C.R., McFall-Ngai, M.J., and Ruby, E.G. (2012) Squid-derived chitin oligosaccharides are a chemotactic signal during colonization by *Vibrio fischeri*. *Appl Environ Microbiol* **78**(13): p. 4620-6.

Neumann, S., Hansen, C.H., Wingreen, N.S., and Sourjik, V. (2010) Differences in signalling by directly and indirectly binding ligands in bacterial chemotaxis. *EMBO J* **29**(20): p. 3484-95.

Nyholm, S.V. and McFall-Ngai, M.J. (2004) The winnowing: establishing the squid-vibrio symbiosis. *Nat Rev Microbiol* **2**(8): p. 632-42.

Nyholm, S.V., Stabb, E.V., Ruby, E.G., and McFall-Ngai, M.J. (2000) Establishment of an animal-bacterial association: recruiting symbiotic vibrios from the environment. *Proc Natl Acad Sci U S A* **97**(18): p. 10231-5.

Osorio, C.G., Crawford, J.A., Michalski, J., Martinez-Wilson, H., Kaper, J.B., and Camilli, A. (2005) Second-generation recombination-based in vivo expression technology for large-scale screening for *Vibrio cholerae* genes induced during infection of the mouse small intestine. *Infect Immun* **73**(2): p. 972-80.

Parkinson, J.S. (2003) Bacterial chemotaxis: a new player in response regulator dephosphorylation. *J Bacteriol* **185**(5): p. 1492-4.

Parkinson, J.S., Ames, P., and Studdert, C.A. (2005) Collaborative signaling by bacterial chemoreceptors. *Curr Opin Microbiol* **8**(2): p. 116-21.

Pineda-Molina, E., Reyes-Darias, J.A., Lacal, J., Ramos, J.L., Garcia-Ruiz, J.M., Gavira, J.A., and Krell, T. (2012) Evidence for chemoreceptors with bimodular ligand-binding regions harboring two signal-binding sites. *Proc Natl Acad Sci U S A* **109**(46): p. 18926-31.

Sonnhammer, E.L., Eddy, S.R., Birney, E., Bateman, A., and Durbin, R. (1998) Pfam: multiple sequence alignments and HMM-profiles of protein domains. *Nucleic Acids Res* **26**(1): p. 320-2.

Sourjik, V. and Berg, H.C. (2002) Receptor sensitivity in bacterial chemotaxis. *Proc Natl Acad Sci U S A* **99**(1): p. 123-7.

Sourjik, V. and Wingreen, N.S. (2012) Responding to chemical gradients: bacterial chemotaxis. *Curr Opin Cell Biol* **24**(2): p. 262-8.

Stecher, B., Hapfelmeier, S., Muller, C., Kremer, M., Stallmach, T., and Hardt, W.D. (2004) Flagella and chemotaxis are required for efficient induction of *Salmonella enterica* serovar *Typhimurium* colitis in streptomycin-pretreated mice. *Infect Immun* **72**(7): p. 4138-50.

Studdert, C.A. and Parkinson, J.S. (2005) Insights into the organization and dynamics of bacterial chemoreceptor clusters through in vivo crosslinking studies. *Proc Natl Acad Sci U S A* **102**(43): p. 15623-8.

Ulrich, L.E. and Zhulin, I.B. (2005) Four-helix bundle: a ubiquitous sensory module in prokaryotic signal transduction. *Bioinformatics* **21 Suppl 3**: p. iii45-8.

Ulrich, L.E. and Zhulin, I.B. (2010) The MiST2 database: a comprehensive genomics resource on microbial signal transduction. *Nucleic Acids Res* **38**(Database issue): p. D401-7.

Wier, A.M., Nyholm, S.V., Mandel, M.J., Massengo-Tiasse, R.P., Schaefer, A.L., Koroleva, I., Splinter-Bondurant, S., Brown, B., Manzella, L., Snir, E., Almabrazi, H., Scheetz, T.E., Bonaldo Mde, F., Casavant, T.L., Soares, M.B., Cronan, J.E., Reed, J.L., Ruby, E.G., and McFall-Ngai, M.J. (2010) Transcriptional patterns in both host and bacterium underlie a daily rhythm of anatomical and metabolic change in a beneficial symbiosis. *Proc Natl Acad Sci U S A* **107**(5): p. 2259-64.

Yang, S., Perna, N.T., Cooksey, D.A., Okinaka, Y., Lindow, S.E., Ibekwe, A.M., Keen, N.T., and Yang, C.H. (2004) Genome-wide identification of plant-upregulated genes of *Erwinia chrysanthemi* 3937 using a GFP-based IVET leaf array. *Mol Plant Microbe Interact* **17**(9): p. 999-1008.

Zhou, Q., Ames, P., and Parkinson, J.S. (2011) Biphasic control logic of HAMP domain signalling in the *Escherichia coli* serine chemoreceptor. *Mol Microbiol* **80**(3): p. 596-611.

Chapter 5

Flagellar Rotation Promotes LPS Shedding and Activation of the Host Developmental Program in the Squid-Vibrio Symbiosis

PREFACE:

This chapter is in preparation for submission to *Nature* in letter format. For this thesis, I maintained the shortened length from this manuscript, but reorganized the material to better match the other chapters.

CAB, EGR, and Margaret McFall-Ngai formulated ideas and planned the experiments within this chapter. Michael A. Apicella (University of Iowa) provided additional intellectual contributions. CAB and Jason R. Hunt (University of Iowa) performed all experiments. Natacha Kramer and Benjamin C. Krasity performed additional experiments that ultimately were not included in this chapter, but enhanced our understanding of the subject matter. CAB wrote the chapter.

ABSTRACT:

Bacterial flagella provide the locomotive force used by cells to migrate through their environment. The flagella of some bacteria, including several important human pathogens, are encased in a sheath that contains both lipopolysaccharide (LPS) and membrane proteins. As such, the sheath is considered to be an extension of the outer membrane, but it serves no established function. We hypothesized that such an addition to the flagellar structure would be disrupted upon flagellar rotation, resulting in the shedding of immunogenic LPS from the cell. To test this notion, we studied the marine bacterium *Vibrio fischeri*, which expresses a tuft of sheathed flagella at one cell pole, and examined LPS release into culture supernatants by mutants lacking a functional flagellar motor. We first measured LPS indirectly using the *Limulus* amoebocyte lysate assay, and observed a reduction of LPS in the cell-free culture supernatant by approximately 50% in bacteria lacking a rotating flagellum. We observed a similar reduction when LPS was directly quantified with SDS-PAGE analysis following lipid extraction of supernatant samples. Furthermore, we examined culture supernatants from *Vibrio cholerae*, which also possesses a sheathed flagellum, and found less LPS in samples from a mutant lacking a flagellar motor. Taken together, these data support the idea that rotation of a sheathed flagellum releases LPS into the surrounding environment. We next questioned whether such a behavior could affect recognition by the host's immune response. In its symbiotic lifestyle, *V. fischeri* normally induces host epithelial apoptosis by LPS release and we observed that, in the absence of a rotating flagellum, *V. fischeri* was unable to activate this host developmental program. Our results propose a novel role for the flagellar sheath in

triggering host immune responses by promoting LPS shedding. Such a phenomenon not only has implications on the study of pathogenic bacteria with sheathed flagella, but also raises important biophysical questions of sheathed flagellar function.

INTRODUCTION:

While highly conserved at a protein level, bacterial flagella display broad diversity in morphology, number and subcellular localization. One such variation is found with the sheath surrounding the flagellar filament of several polarly-flagellated bacteria, including the important human pathogens *Vibrio cholerae*, *Helicobacter pylori*, and *Brucella melitensis* (Ferooz and Letesson, 2010, Follett and Gordon, 1963, Geis *et al.*, 1993). However, the functional role of the sheath, even as it relates to flagellar motility, remains poorly understood. Biochemical and electron microscopy studies have localized both lipopolysaccharide (LPS) and proteins to the flagellar sheath, suggesting that it is a continuation of the cellular outer membrane (Fuerst and Perry, 1988, Geis *et al.*, 1993, Hranitzky *et al.*, 1980). Further, it has been proposed that the flagellar sheath might be important in host interactions, potentially by masking the immunogenic flagellin subunits (Yoon and Mekalanos, 2008) or presenting sheath-specific protein antigens (Furuno *et al.*, 2000, Jones *et al.*, 1997, Luke and Penn, 1995). These hypotheses rely on both the stability of the sheath and its tight association with the flagellar filament. However, a physical coupling of the sheath to the flagellum has not been characterized, and, in fact, sheath-like structures have been observed in the absence of a flagellar filament (Josenhans *et al.*, 1995), suggesting that sheath formation is not strictly coupled to flagellar biogenesis. We posited that, in the absence of a tight sheath-filament interaction, flagellar rotation would affect the stability of the sheath, leading to the release of immunogenic molecules like LPS. To address this hypothesis, we examined the role of the flagellum in LPS shedding by the marine bacterium

Vibrio fischeri. *V. fischeri* serves as an ideal model to address the role of the flagellar sheath as individual cells present a tuft of 2-9 polar, sheathed flagella (Allen and Baumann, 1971), likely amplifying any flagellum-specific effects as compared to its congener *V. cholerae*, which has a single flagellum per cell.

MATERIALS AND METHODS:

Bacterial strains and growth conditions:

V. fischeri strains used in this study include: ES114 (Boettcher and Ruby, 1990); *flrA*::Tn*erm* (MB21407, Chapter 2); *motB1*::Tn*erm* (MB06357, Chapter 2); *motX*::Tn*erm* (MB12561, Chapter 2); and Δ*cheY* (this study, see below). Strains were grown at 28 °C in either Luria-Bertani salt (LBS) medium (per liter, 10 g Bacto-tryptone, 5 g yeast extract, 20 g NaCl, and 50 mL 1 M Tris buffer, pH 7.5, in distilled water) or seawater-based tryptone (SWT) medium (per liter, 5 g Bacto-tryptone, 3 g yeast extract, 3 mL glycerol, 700 mL Instant Ocean [Aquarium Systems, Inc, Mentor, OH] at a salinity of 33-35 ppt, and 300 ml distilled water). *V. cholerae* strains O395N1 and its Δ*pomAB* derivative, referred to as *motAB* within this work for consistency with *V. fischeri* naming conventions (Gosink and Hase, 2000), were grown at 37 °C in either SWT or Luria-Bertani medium (per liter, 10 g Bacto-tryptone, 5 g yeast extract, and 10 g NaCl). When appropriate, antibiotics were added to media at the following concentrations: erythromycin, 5 μg/ml; kanamycin, 100 μg/ml; and chloramphenicol, 2.5 μg/ml. Growth media were solidified with 1.5% agar as needed. Motility assays were performed as described in Chapter 2, except that plates were incubated at room temperature (23-24°C).

Construction of the *cheY* deletion mutant

Flanking DNA sequences were amplified from purified ES114 genomic DNA with

upstream primer pair cheY-1EcoRI (5'-ATAGAATTCTCGTTGAAGGCCCATATGGTGTGA-3') and cheY-2RE (5'-GCATGACCCGGGCTTCATGTTTTTATTCAAAAT-3') and downstream primer pair cheY-3RE (5'-GCATGACCCGGGCCAAATCCAAATAAATAAGC-3') and cheY-4Sph1 (5'-GCATGACCCGGGATTTTTGAACGTTTATAAGT-3'). The upstream and downstream fragments were digested with XmaI and ligated together. The resulting construct was re-amplified by PCR using primers cheY-1EcoRI and cheY-4SphI. Following restriction digest by EcoRI and SphI, this product was cloned into pKV363 and then transformed into competent cells of *Escherichia coli* B3914 competent cells using standard techniques. Conjugation of the resulting plasmid (pCAB70) into *V. fischeri* and allelic exchange were performed as previously described (Le Roux *et al.*, 2007, Shibata and Visick, 2012), to generate Δ*cheY* (CAB1535).

Construction of the *motB1* complementation:

The *motB1* open reading frame was amplified by PCR using primer pair motB1_compF (5'-GCTCTAGACTAACACACAGGAAACAGCTATGGAAGATGAAAACGACTGCA-3'), which introduces an XbaI restriction enzyme site and a ribosomal binding site, and motB1_compR (5' GCGGTACCGACCTAATCTAAGGCGCA-3'), which introduces a KpnI restriction enzyme site. The resulting product was cloned into the XbaI/KpnI-digested fragment of pVSV105 (Dunn *et al.*, 2006). Both the complementation construct (pCAB64)

and vector control were conjugated into wild-type *V. fischeri* and into the *motB1* mutant using standard techniques (Stabb *et al.*, 2001).

LPS measurement using reactive LAL assay:

Cultures were prepared by growth in SWT broth with shaking to mid-log phase, an OD_{600} of ~0.4. Cells were removed by two successive rounds of centrifugation, and the resultant supernatant was passed through a 0.22-µm pore-sized filter, yielding a purified, cell-free supernatant. Reactive LPS was detected from the purified supernatant samples using the ToxinSensor Chromogenic LAL Endotoxin Assay Kit (Genscript, Piscataway, NJ), per manufacturer's instruction. Background LPS in uninoculated media was under 50 endotoxin units per mL.

LPS measurement by silver-stained SDS-PAGE analysis:

To remove salts from 50 mL of purified supernatants (described above), samples were dialyzed agains 4 liters of distilled, deionized H2O using 3500 MWCO SnakeSkin dialysis tubing (ThermoScientific, Rockford, IL) and five water changes. The dialyzed samples were lyophilized and resuspended in 10ml DNaseI buffer (10 mM Tris-HCl, pH 7.6, 2.5 mM $MgCl_2$, 0.5 mM $CaCl_2$) and treated with 1 mg/ml DNaseI/RNaseA (Roche) overnight at 37 °C. Following the nuclease treatment, an equal volume 95% phenol at 65 °C was added. Samples were vortexed and incubated at 65 °C for 30 min, then cooled on ice and centrifuged at 3,000×*g* for 10 min at 4 °C. The aqueous layer was collected and the phenol layer was back extracted with an equal volume of deionized water pre-warmed to 65°C. The aqueous

layers were combined and residual phenol was removed by addition of one-tenth volume of 0.3 M sodium acetate, and precipitation three times with 3 volumes of absolute ethanol. The pellets were resuspended in HPLC-grade water, frozen, and again lyophilized.

Purified samples were analyzed after SDS-polyacrylamide gel electrophoresis (PAGE) using NuPAGE pre-cast 4-12% Bis-Tris polyacrylamide gels (Novex). The gels were loaded with 5 µl from each preparation, as well as known masses of purified *Vibrio fischeri* LPS for to produce a standard curve.

Following electrophoresis, gels were analyzed by silver stain. Gels were fixed overnight in 40% ethanol and 5% acetic acid. The gels were shaken in distilled water for three 10-min washes. The gels were then oxidized for 5 min in 0.7% periodic acid in 40% ethanol-5% acetic acid. After wash steps were repeated, the gels were shaken for 10 minutes in a freshly prepared staining reagent (28 mL of 0.1 N NaOH, 2 mL of concentrated ammonium hydroxide, 5 mL of 20% silver nitrate, 115 mL of distilled water). After the wash steps were repeated, the gels were developed with 25 mg of citric acid and 0.25 ml of 37% formaldehyde in 0.5 liter of distilled water. Gels were then scanned and band intensities were calculated using imageJ. A standard curve was generated based on the band intensities of the purified *V. fischeri* LPS fractions, and the concentrations of LPS in the culture supernatants were estimated from this standard curve.

Squid experiments:

Freshly hatched squid were pretreated with 100 µg/mL lysozyme-treated peptidoglycan (PGN) (Nyholm *et al.*, 2002) in 4 mL filter-sterilized Instant Ocean (FSIO) for

2 h to induce mucus shedding. As indicated in individual experiments, either bacteria, at a final concentration of ~8000 colony-forming units (CFUs) per mL, or 1 μg/mL *V. fischeri* lipid A were added to vials containing pre-treated squid in PGN-FSIO. After 10 h, squid were exposed to 0.001% acridine orange for 5 min, washed in FSIO, and anesthetized in 2% ethanol in FSIO. Squid were then ventrally dissected to expose the light organ and examined by laser-scanning confocal microscopy (LSCM). Acridine orange-positive nuclei in the ciliated epithelial field were counted for one light-organ lobe per squid as a measure of cell death induction (Delic *et al.*, 1991, Foster *et al.*, 2000).

As an estimate of bacterial colonization, the luminescence of individual squid was measured using a TD-20/20 luminometer (Turner Biosystems, Sunnyvale, CA). For experiments in which symbiont number was determined, squid were surface-sterilized by storage at -80°C. Individual squid were then homogenized, and each homogenate was diluted and plated for CFUs on LBS agar. Bacterial localization was assessed as described in Appendix B.

RESULTS AND DISCUSSION:

We first sought to measure the amount of LPS in cell-free supernatants of mid-log cultures, when cells are highly motile. In addition to wild-type *V. fischeri*, we examined four mutants disrupted in flagellar and chemotaxis genes, all of which exhibit altered motility: *flrA*, which lacks a flagellum; *motB1* and *motX*, both of which produce flagella that are unable to rotate; and *cheY*, whose flagella rotate only in one direction (Figure 5-1 and Chapter 2). This array of mutants allows us to parse out the individual roles of flagellar biogenesis, flagellar rotation and/or rotational switching in LPS release.

We used the *Limulus* amoebocyte lysate (LAL) assay (Figure 5-2) and observed significant reductions in the amount of LAL-reactive LPS produced by strains that did not produce a rotating flagellum (*flrA*, *motB1*, and *motX*). Because the LAL assay measures reactive LPS, these data suggested either that these strains shed less LPS into the media or that they release a distinct LPS with a lowered recognition by the LAL assay. To address these possibilities, we directly measured the total LPS shed from these strains using SDS-PAGE analysis, as described in the Materials and Methods and Figure 5-3A&B. By this method, we observed a similar reduction in total LPS isolated from cell-free supernatants of *flrA*, *motB1*, and *motX* cultures (Figure 5-3C). We sought to genetically complement the defect in LPS shedding observed in *motB1* mutant cultures (Figure 5-4). Expression of *motB1 in trans* only provided partial restoration of both soft-agar motility and LPS release. However, carriage of the complementing plasmid lowered the motility and shedding by wild-type cells (Figure 5-4A), suggesting full complementation should not be expected.

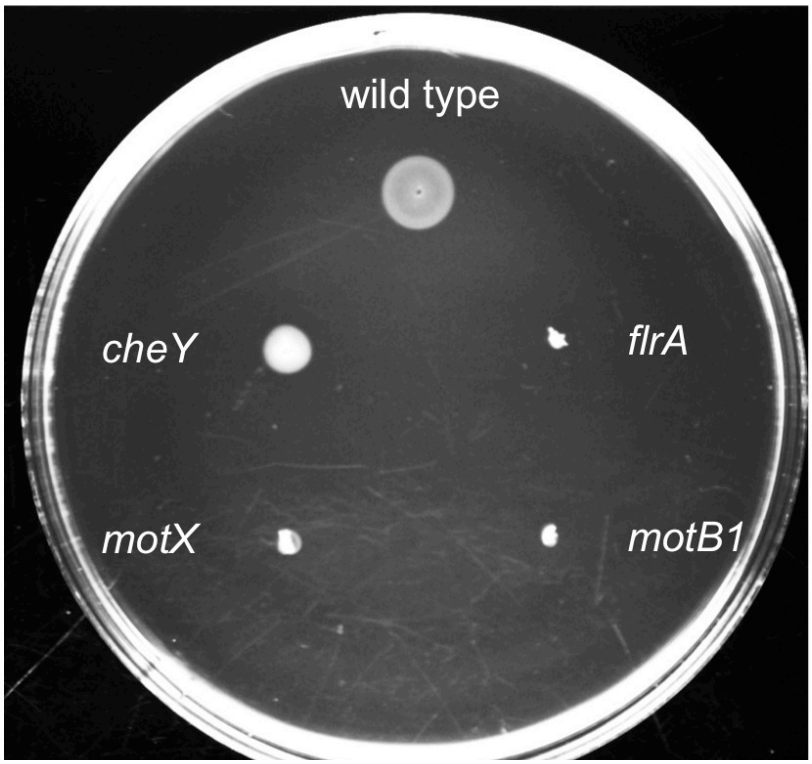

Figure 5-1. Soft-agar motility phenotypes of *V. fischeri* strains. Indicated strains were grown to mid-log phase and inoculated into SWT plates supplemented with 0.3% agar. Plates were visualized after 10 h at room temperature. The diameter of migration by the cells is a measure of their level of both flagellar motility and chemotaxis activity.

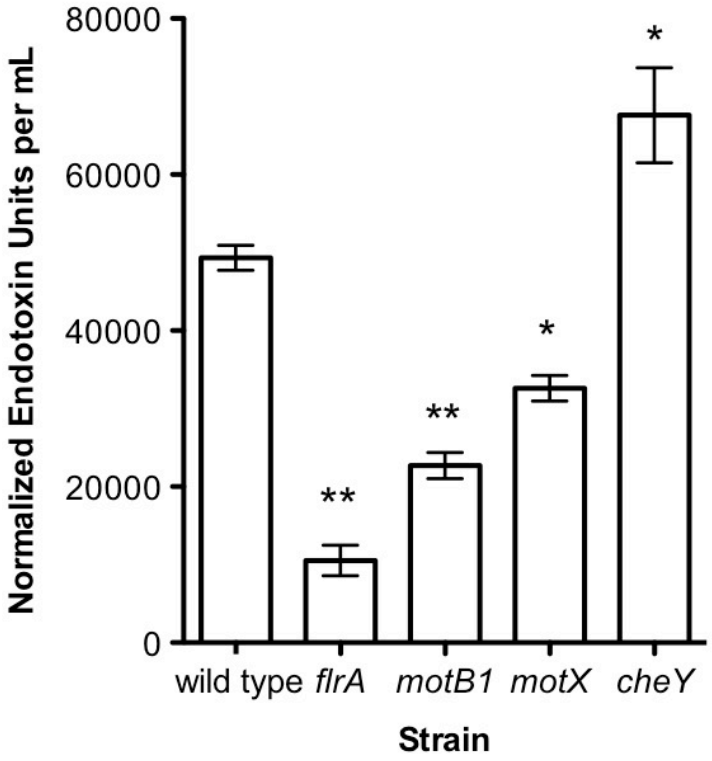

Figure 5-2. Reactive LPS in *V. fischeri* culture supernatants as measured by the LAL assay. Reactive LPS in mid-log culture supernatants of indicated strains, as measured by a chromogenic LAL assay. Single asterisk indicates $p < 0.05$ and double asterisks indicate $p<0.001$, as compared to wild type and analyzed by one-way ANOVA with a posthoc Bonferroni correction.

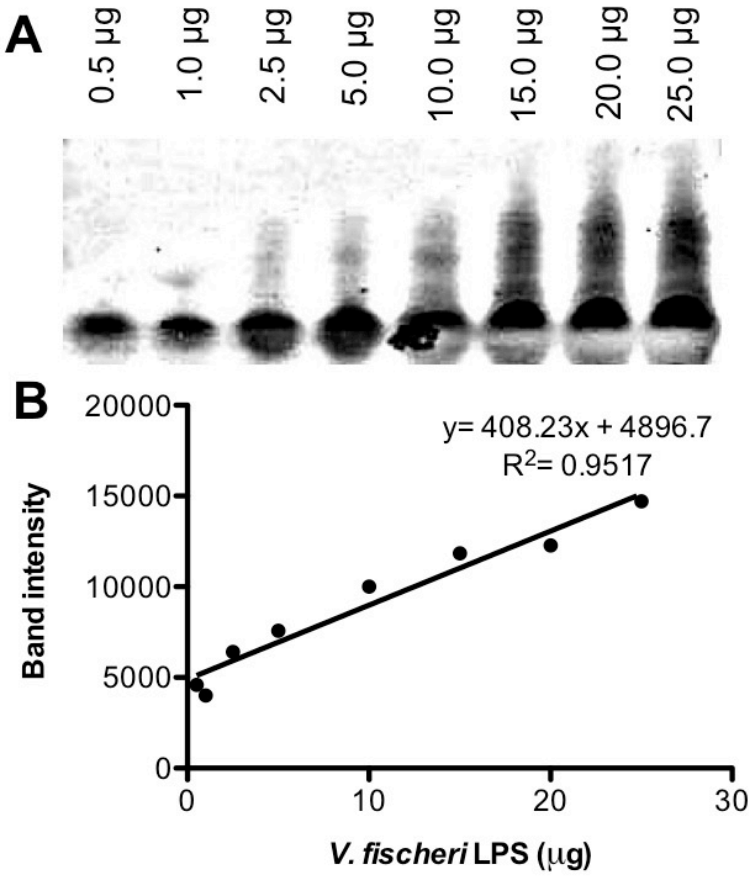

Strain	Intensity	LPS (µg)	Relative shed LPS
wild type	17822	32	1.0
flrA	6146	3	0.1
motB1	6920	5	0.2
motX	11029	15	0.5
cheY	17802	32	1.0

Figure 5-3. Quantification of total LPS in culture supernatants by SDS-PAGE analysis. (A&B). Silver-stained gel image of purified *V. fischeri* LPS analyzed by SDS-PAGE (A) and used to generate standard curve by densitometry (B). (C) Total LPS in purified lipid fractions from indicated culture supernatants, visualized by silver staining after SDS-PAGE analysis. Image has been has been modified to remove irrelevant lanes, but all samples were separated on the same gel.

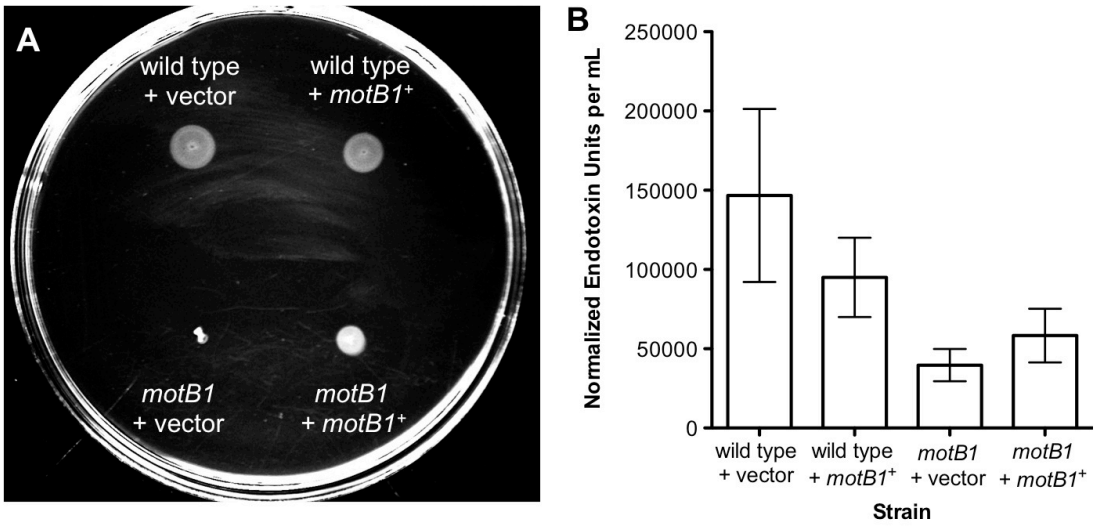

Figure 5-4. Soft-agar motility and supernatant LPS levels in genetically complemented strains. (A) Indicated strains were grown to mid-log phase and inoculated into SWT plates containing 0.3% agar. Plates were visualized after 10 h at room temperature. (B) Reactive LPS present in mid-log culture supernatants of indicated strains, as measured by a chromogenic LAL assay.

Resequencing of this plasmid identified a nonsynonymous substitution within the *motB1* open reading frame, and future construction of a corrected complementation plasmid might enable full restoration of these phenotypes. Nevertheless, as we observed reductions in LPS shedding by both the independent *motB1* and *motX* mutants, these data still support that genetic disruption of flagellar rotation reduces the amount of LPS released by *V. fischeri* cells.

The *cheY* mutant, whose flagellum rotates but does not switch direction, released at least as much LPS as wild-type, negating the possibility that the LPS is shed primarily during the switching of rotational direction. The *flrA* mutant, which does not produce a flagellum, released the least amount of LPS into culture supernatants, approximately 50% of that shed by the *motB1* mutant, as measured by both assays. These data suggest that, in addition to rotation, flagellar biogenesis itself leads to detectable levels of LPS shedding and might disrupts outer membrane stability.

We next examined if flagellar rotation-mediated LPS release is conserved within the *Vibrionaceae* or specific to *V. fischeri*. Using wild-type *V. cholerae* O395N1 and a *motAB*-deletion derivative, which lacks both of the flagellar motor proteins MotA and MotB (Gosink and Hase, 2000), we measured the amount of reactive LPS in cell-free culture supernatants by the LAL assay (Figure 5-5). In all experiments, the *motAB* supernatants contained lower levels of reactive LPS than wild type, suggesting that the phenomenon of flagellar rotation-mediated LPS shedding is conserved between *V. fischeri* and *V. cholerae*. Similar analysis of functionally analogous *Escherichia coli* mutants with non-rotating flagella showed no alteration in supernatant LPS levels (data not shown) under the conditions of our assay,

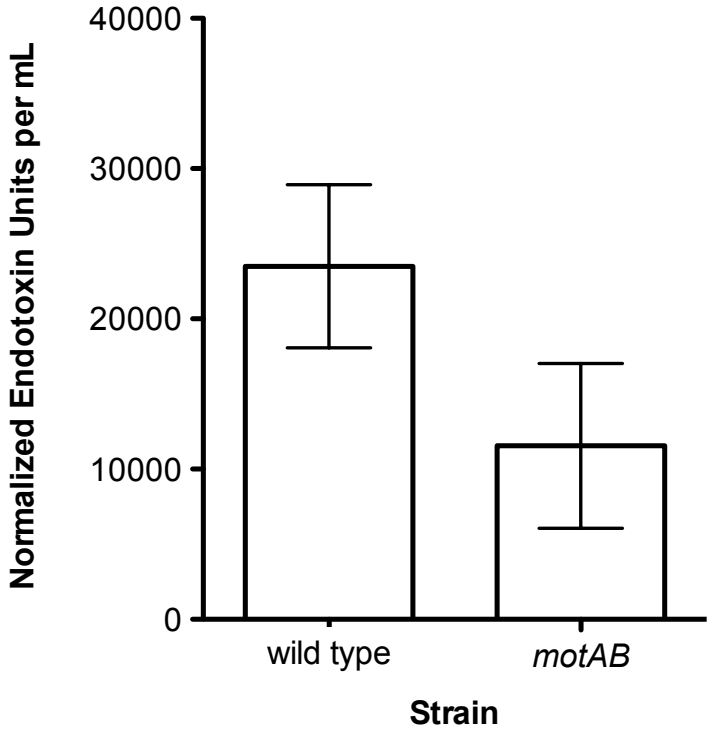

Figure 5-5. Reactive LPS in *V. cholerae* culture supernatants as measured by the LAL assay. Reactive LPS in mid-log culture supernatants of wild-type *V. cholerae* O395N1 and its *motAB* derivative grown in SWT, as measured by a chromogenic LAL assay. $p = 0.06$ by one-tailed paired T-test.

supporting that this behavior may be specific to bacteria that produce sheathed flagella, under the conditions we examined.

Because LPS is an important immunogenic molecule, we sought to ascertain if flagellar rotation-mediated LPS release plays a biological function in host recognition. In addition to its planktonic niche, *V. fischeri* colonizes a light-emitting organ within the mantle cavity of its mutualistic host, the Hawaiian bobtail squid *Euprymna scolopes*. Symbiotic initiation begins with the recruitment of *V. fischeri* cells from the surrounding seawater by each newly hatched squid. Bacterial cells aggregate near the ciliated appendages of the light organ (Figure 5-6A) and then migrate through the surfacepores, down ducts, and through antechambers to ultimately colonize the deep crypts (Nyholm and McFall-Ngai, 2004). In response to the presentation of immunogenic molecules by the colonizing *V. fischeri* cells, the light organ undergoes extensive morphogenesis, beginning with apoptosis of the ciliated epithelium of the appendages (Foster *et al.*, 2000, Koropatnick *et al.*, 2004, Montgomery and McFall-Ngai, 1994).

Early induction of apoptosis of the ciliated epithelium occurs specifically upon exposure to the lipid A component of LPS (Figure 5-7) (Foster *et al.*, 2000). We posited that the *motB1* and *flrA* mutants would be unable to induce wild-type levels of early apoptosis, as measured by the observation of acridine orange (AO)-positive nuclei. Because flagellar motility is required for symbiotic initiation (Graf *et al.*, 1994), we first determined conditions under which the amotile *flrA* and *motB1* were not yet mislocalized, and at the same numbers , as wild type at the time wild-type cells induce apoptosis (Figure 5-8). Using these conditions, we measured the number of apoptotic host cells in the absence of *V. fischeri* (apo) or after

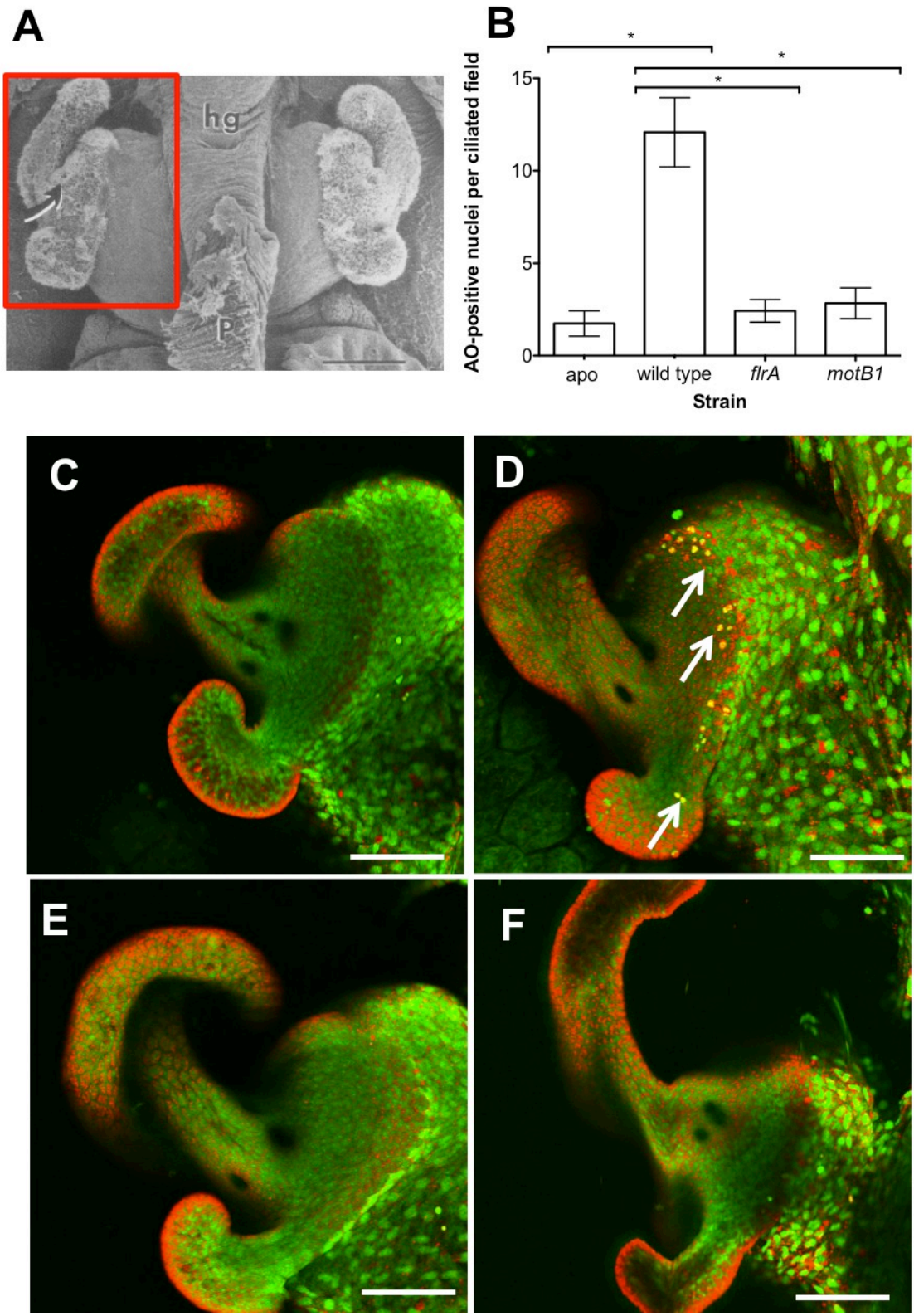
A
hg
P
B
AO-positive nuclei per ciliated field
15
10
5
0
*
*
*
apo
wild type
flrA
motB1
Strain
C
D
E
F

Figure 5-6. Acridine-orange staining of the light-organ ciliated epithlium from squid exposed to *V. fischeri* flagellar mutants.

(A) Scanning electron micrograph of the juvenile light organ, highlighting the ciliated epithelial field of one lobe. Scale bar, 100 μm. Image from (Montgomery and McFall-Ngai, 1993). (B) Acridine-orange (AO)-positive nuclei counts from 31-38 light-organ lobes per condition. Asterisks indicate significance at $p < 0.001$ by Kruskal-Wallis ANOVA, followed by Dunn's Multiple Comparison test. (C-F) Representative laser-scanning confocal microscopy images of AO-stained juvenile light organs, after exposure to either no *V. fischeri* (apo, C), wild type (D), *flrA* (E), or *motB1* (F), as described in the supplemental Materials and Methods. White arrows in (C) indicate 3 of the numerous AO-positive nuclei (yellow). All scale bars represent 100 μm.

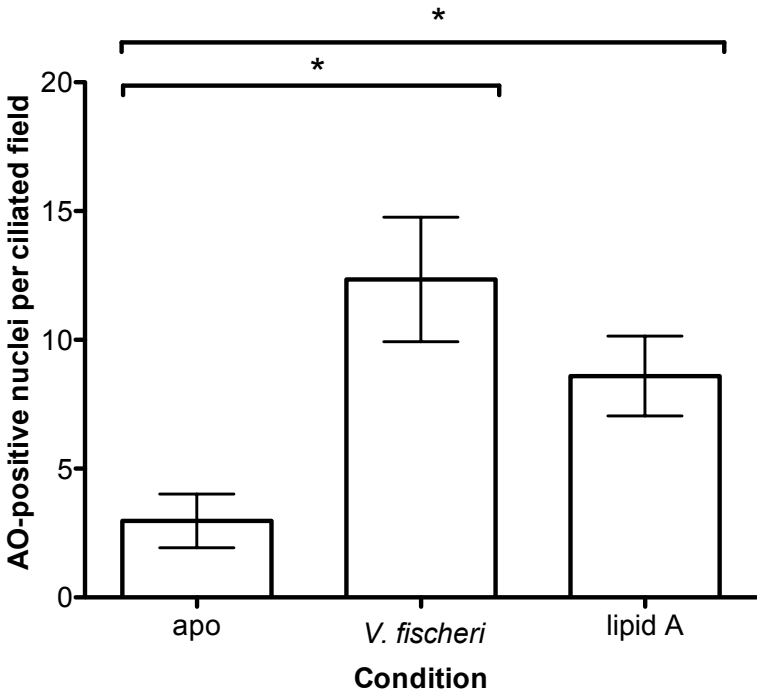

Figure 5-7. Induction of early-stage apoptosis in response to exogenous lipid A.

Squid were pretreated with PGN, as described in the supplemental M&M, and then exposed for 10 h to either no *V. fischeri* (apo), 5,000 CFU/mL wild-type *V. fischeri*, or 1 μg/mL *V. fischeri* lipid A. AO-positive nuclei were counted in the ciliated epithelial fields from 32 light-organ lobes per condition. Asterisks indicate significance at $p < 0.001$ by Kruskal-Wallis ANOVA, followed by Dunn's Multiple Comparison test.

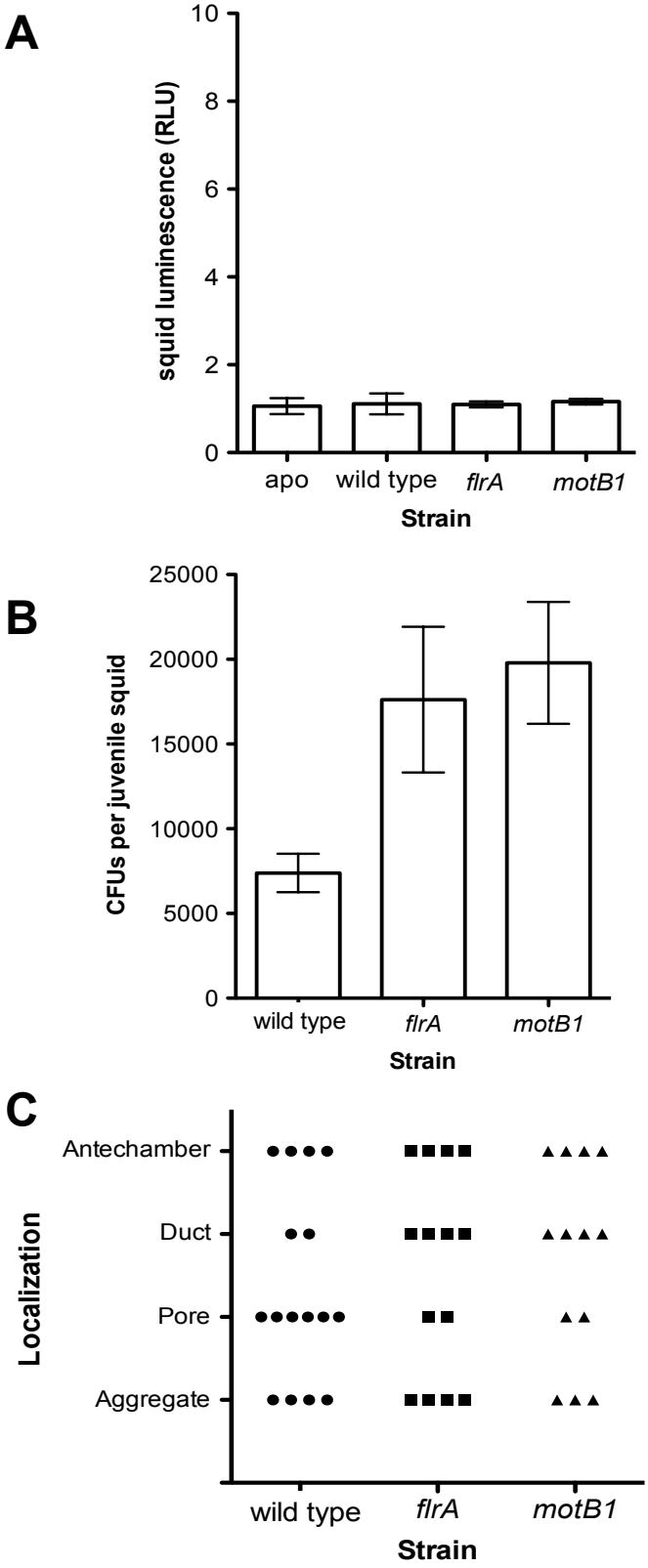
A
squid luminescence (RLU)
10
8
6
4
2
0
apo
wild type
flrA
motB1
Strain
B
CFUs per juvenile squid
25000
20000
15000
10000
5000
0
wild type
flrA
motB1
Strain
C
Localization
Antechamber
Duct
Pore
Aggregate
wild type
flrA
motB1
Strain

Figure 5-8. Bacterial colonization and localization at 10 h after PGN pretreatment are similar among wild type, *flrA* and *motB1*. (A&B) Squid were treated as described in Figure 5-6 and the supplemental Materials and Methods scored for luminescence (A), and then homogenized and plated for symbiont number (B). RLU, relative luminescence units. CFUs, colony-forming units. (C) Localization was determined by examining squid exposed to the indicated strains, genetically labeled to express GFP (Dunn *et al.*, 2006), using LSCM, after the host tissue was stained with Cell Tracker Orange. Each point represents bacterial localization for a single light-organ lobe. Light-organ morphology is described in Figure 1-1.

exposure to naturally occurring levels of wild-type, *flrA*, or *motB1* cells (Figure 5-6B-F). Exposure to wild-type *V. fischeri* induced apoptosis in an average of 12 apoptotic epithelial cells per ciliated field. Surprisingly, squid treated with the *flrA* or *motB1* mutant exhibited no apoptosis above the level observed in aposymbiotic squid, which were not exposed to *V. fischeri*. As both the *flrA* and *motB1* mutants are capable of LPS release, albeit at a reduced level (Figures 5-2 and 5-3C), the complete attenuation of apoptotic induction suggests that either (i) the threshold of LPS sensed by host cells is exquisitely calibrated to the amount of LPS shed by *V. fischeri* or (ii) the LPS released by wild-type *V. fischeri* is somehow presented in a more immunogenic manner than that released by either the *flrA* or *motB1* mutant. These results indicate that, the LPS shed by *V. fischeri* cells through flagellar rotation serves as a critical immunogenic molecule in the host's developmental program that occurs in response to symbiont exposure.

In this work, we describe a novel role for sheathed flagellar rotation in promoting both the release of the immunogenic molecule LPS and the activation of the host immune response. While characterized exclusively in *V. fischeri* and *V. cholerae*, this phenomenon may be conserved across other animal-associated bacteria that present sheathed flagella, such as *Vibrio parahaemolyticus, H. pylori* and *B. melitensis*, and may prove to similarly mediate immune recognition in these human pathogens. Further questions of this phenomenon remain, namely from where on the outer membrane and in what form is the LPS released? In a previous work, we observed small vesicle-like structures at the flagellar tip (Millikan and Ruby, 2004) that may be the source of the released LPS, but it is also possible that the LPS is released at the interface between the static outer membrane of the cell body at the site of

flagellar insertion and the rotating sheath membrane of the flagellar filament. Additionally, as we measured total LPS, we did not determine whether the LPS was released in small micelles or larger outer membrane vesicle-like structures. The biophysical properties underlying lipid interactions at a sub-micron scale, like those between the flagellar sheath and cellular outer membrane during flagellar rotation, have not been examined and such modeling would inform our understanding of this novel behavior.

ACKNOWLEDGMENTS:

We thank Claudia Häse (Oregon State University) for supplying *V. cholerae* strains and the Welch lab (UW) for providing research space. This work was supported by NIH grant RR12294 (to MJM-N and EGR). CAB was supported by an NIH Molecular Biosciences Training Grant and an NIH Microbes in Health and Disease Training Grant to the University of Wisconsin.

REFERENCES:

Allen, R.D. and Baumann, P. (1971) Structure and arrangement of flagella in species of the genus *Beneckea* and *Photobacterium fischeri*. *J Bacteriol* **107**(1): p. 295-302.

Boettcher, K.J. and Ruby, E.G. (1990) Depressed light emission by symbiotic *Vibrio fischeri* of the sepiolid squid Euprymna scolopes. *J Bacteriol* **172**(7): p. 3701-6.

Delic, J., Coppey, J., Magdelenat, H., and Coppey-Moisan, M. (1991) Impossibility of acridine orange intercalation in nuclear DNA of the living cell. *Exp Cell Res* **194**(1): p. 147-53.

Dunn, A.K., Millikan, D.S., Adin, D.M., Bose, J.L., and Stabb, E.V. (2006) New rfp- and pES213-derived tools for analyzing symbiotic *Vibrio fischeri* reveal patterns of infection and *lux* expression in situ. *Appl Environ Microbiol* **72**(1): p. 802-10.

Ferooz, J. and Letesson, J.J. (2010) Morphological analysis of the sheathed flagellum of *Brucella melitensis*. *BMC Res Notes* **3**: p. 333.

Follett, E.A. and Gordon, J. (1963) An Electron Microscope Study of *Vibrio* Flagella. *J Gen Microbiol* **32**: p. 235-9.

Foster, J.S., Apicella, M.A., and McFall-Ngai, M.J. (2000) *Vibrio fischeri* lipopolysaccharide induces developmental apoptosis, but not complete morphogenesis, of the *Euprymna scolopes* symbiotic light organ. *Dev Biol* **226**(2): p. 242-54.

Fuerst, J.A. and Perry, J.W. (1988) Demonstration of lipopolysaccharide on sheathed flagella of *Vibrio cholerae* O:1 by protein A-gold immunoelectron microscopy. *J Bacteriol* **170**(4): p. 1488-94.

Furuno, M., Sato, K., Kawagishi, I., and Homma, M. (2000) Characterization of a flagellar sheath component, PF60, and its structural gene in marine *Vibrio*. *J Biochem* **127**(1): p. 29-36.

Geis, G., Suerbaum, S., Forsthoff, B., Leying, H., and Opferkuch, W. (1993) Ultrastructure and biochemical studies of the flagellar sheath of *Helicobacter pylori*. *J Med Microbiol* **38**(5): p. 371-7.

Gosink, K.K. and Hase, C.C. (2000) Requirements for conversion of the Na(+)-driven flagellar motor of Vibrio cholerae to the H(+)-driven motor of *Escherichia coli*. *J Bacteriol* **182**(15): p. 4234-40.

Graf, J., Dunlap, P.V., and Ruby, E.G. (1994) Effect of transposon-induced motility mutations on colonization of the host light organ by *Vibrio fischeri*. *J Bacteriol* **176**(22): p. 6986-91.

Hranitzky, K.W., Mulholland, A., Larson, A.D., Eubanks, E.R., and Hart, L.T. (1980) Characterization of a flagellar sheath protein of *Vibrio cholerae*. *Infect Immun* **27**(2): p. 597-603.

Jones, A.C., Logan, R.P., Foynes, S., Cockayne, A., Wren, B.W., and Penn, C.W. (1997) A flagellar sheath protein of *Helicobacter pylori* is identical to HpaA, a putative N-acetylneuraminyllactose-binding hemagglutinin, but is not an adhesin for AGS cells. *J Bacteriol* **179**(17): p. 5643-7.

Josenhans, C., Labigne, A., and Suerbaum, S. (1995) Comparative ultrastructural and functional studies of *Helicobacter pylori* and *Helicobacter mustelae* flagellin mutants:

both flagellin subunits, FlaA and FlaB, are necessary for full motility in Helicobacter species. *J Bacteriol* **177**(11): p. 3010-20.

Koropatnick, T.A., Engle, J.T., Apicella, M.A., Stabb, E.V., Goldman, W.E., and McFall-Ngai, M.J. (2004) Microbial factor-mediated development in a host-bacterial mutualism. *Science* **306**(5699): p. 1186-8.

Le Roux, F., Binesse, J., Saulnier, D., and Mazel, D. (2007) Construction of a *Vibrio splendidus* mutant lacking the metalloprotease gene vsm by use of a novel counterselectable suicide vector. *Appl Environ Microbiol* **73**(3): p. 777-84.

Luke, C.J. and Penn, C.W. (1995) Identification of a 29 kDa flagellar sheath protein in *Helicobacter pylori* using a murine monoclonal antibody. *Microbiology* **141 (Pt 3)**: p. 597-604.

Millikan, D.S. and Ruby, E.G. (2004) *Vibrio fischeri* flagellin A is essential for normal motility and for symbiotic competence during initial squid light organ colonization. *J Bacteriol* **186**(13): p. 4315-25.

Montgomery, M.K. and McFall-Ngai, M. (1994) Bacterial symbionts induce host organ morphogenesis during early postembryonic development of the squid Euprymna scolopes. *Development* **120**(7): p. 1719-29.

Montgomery, M.K. and McFall-Ngai, M.J. (1993) Embryonic development of the light organ of the sepiolid squid *Euprymna scolopes* Berry. *Biol Bull* **184**: p. 296-308.

Nyholm, S.V., Deplancke, B., Gaskins, H.R., Apicella, M.A., and McFall-Ngai, M.J. (2002) Roles of *Vibrio fischeri* and nonsymbiotic bacteria in the dynamics of mucus secretion

during symbiont colonization of the *Euprymna scolopes* light organ. *Appl Environ Microbiol* **68**(10): p. 5113-22.

Nyholm, S.V. and McFall-Ngai, M.J. (2004) The winnowing: establishing the squid-vibrio symbiosis. *Nat Rev Microbiol* **2**(8): p. 632-42.

Shibata, S. and Visick, K.L. (2012) Sensor kinase RscS induces the production of antigenically distinct outer membrane vesicles that depend on the symbiosis polysaccharide locus in *Vibrio fischeri*. *J Bacteriol* **194**(1): p. 185-94.

Stabb, E.V., Reich, K.A., and Ruby, E.G. (2001) *Vibrio fischeri* genes hvnA and hvnB encode secreted NAD(+)-glycohydrolases. *J Bacteriol* **183**(1): p. 309-17.

Yoon, S.S. and Mekalanos, J.J. (2008) Decreased potency of the *Vibrio cholerae* sheathed flagellum to trigger host innate immunity. *Infect Immun* **76**(3): p. 1282-8.

Chapter 6

Synthesis and Future Directions

PREFACE:

CAB formulated ideas and wrote the chapter.

GENETIC BASIS OF FLAGELLAR MOTILITY AND CHEMOTAXIS:

This thesis provides a foundation for the continuing study of flagellar motility and chemotaxis in *Vibrio fischeri*. Through genetic analysis and phenotypic screening of the MB Mutant Collection, we characterized the core flagellar motility-associated genes required for normal soft-agar motility in *V. fischeri* (Chapter 2). The vast majority of the mutants we identified were disrupted in homologs of known flagellar genes, as described in other *Vibrio* species (Cameron *et al.*, 2008, McCarter, 1995), confirming the depth of our screen. These mutants also served as tools for the further examination of flagellar motility and chemotaxis in *V. fischeri* (Chapter 5 and Appendix B). Concurrently, we made a number of novel findings, such as the identification of several unexpected genes required for normal soft-agar motility and the characterization of flagellar gene paralogs.

We used two complementary approaches to identify the specific ligands sensed by chemoreceptors: reverse genetics in *V. fischeri*, and heterologous expression of chimeric MCPs in *Escherichia coli*. Using these two approaches, we have begun to clarify the chemotactic repertoire of *V. fischeri*, including the characterization of VfcA, which mediates chemotaxis towards multiple amino acids (Chapters 3 and 4), and VfcB, which senses several sugars, including the chitin-breakdown products *N*-acetyl-glucosamine and chitobiose (Chapter 4).

Taken together, these studies have defined the genetic basis of flagellar motility and chemotaxis, identified novel motility-associated genes, and characterized the first MCP-ligand

pairs in *V. fischeri*. By also developing new tools to examine these behaviors, my work has situated *V. fischeri* as a model organism for flagellar motility and chemotaxis research.

Development of new tools:

1. *V. fischeri* ES114 MB Collection

   We generated a 23,904 member transposon insertion library, a useful new tool for the study of *V. fischeri* (Chapter 2). In addition to its use within this thesis, this *V. fischeri* ES114 MB mutant collection has already been used to quickly locate mutants of interest by PCR screening of strain lysate pools (Studer *et al.*, 2008) and to isolate mutants with additional chemotactic and motility phenotypes (Post *et al.*, 2012). This library is now available to the squid-vibrio community at large, for use in additional phenotypic screens, such as siderophore production or chitin utilization.

2. Capillary chemotaxis assay

   Previous studies of chemotaxis in *V. fischeri* have relied on the use of soft-agar motility assays, which provide an indirect readout of chemotaxis (DeLoney-Marino *et al.*, 2003). Past researchers have unsuccessfully attempted to adapt capillary chemotaxis assays for use in *V. fischeri* (C. DeLoney-Marino, M. Mandel, and A. Schaefer, personal communication), thereby limiting the study of chemotaxis in this

organism. In Chapter 3, we developed a capillary assay for the quantification of chemoattraction in *V. fischeri* in liquid medium without relying on chemoattractant utilization (Parales and Harwood, 2002). While we used this technique to examine chemotaxis toward all twenty standard amino acids, this technique can now be applied to other relevant macromolecules in *V. fischeri*.

3. Chimeric MCP characterization

By expressing chimeric MCPs in *E. coli*, we were able to exploit the broad array of tools available for studying chemotaxis in this model organism and identify the chemoeffectors sensed by specific chemoreceptor ligand-binding domains (Chapter 4). Working with Sandy Parkinson at the University of Utah, we have defined a system by which to identify MCP-ligand pairs in bacteria with large numbers of predicted chemoreceptors, regardless of their genetic tractability.

Future directions:

1. How do novel motility-associated proteins contribute to flagellar motility?

In this thesis, we identified several genes of unknown function required for swimming motility: *VF_1491*, *flgO*, *flgP*, and *flgT*. It is not currently known what roles their respective gene products play in flagellar motility. As all of these proteins are

conserved in the *Vibrionaceae*, characterizing their function informs a general understanding of flagellar motility within the whole of this important family. Experiments that would clarify their role in flagellar motility include: examination of protein sub-cellular localization; characterization of protein-protein interactions by immunoprecipitation studies; and observation of mutant flagellar structures by cryotomography.

2. What is the function(s) underlying the presence of multiple flagellins in the *Vibrionaceae*?

   In our work, we isolated a mutant in *flaD*, one of the six flagellin-encoding genes in *V. fischeri*, which has been shown to be dispensable for normal motility in at least some other *Vibrio* species (Klose and Mekalanos, 1998, McGee *et al.*, 1996), suggesting that the contributions of individual flagellin homologs to flagellar function vary among these related bacteria. It is currently unknown how multiple flagellins contribute to flagellar function. In collaboration with Shin-Ichi Aizawa (Prefectural University of Hiroshima), functional and structural characterization of individual flagellin mutants will inform a model of how the six flagellins of *V. fischeri* are incorporated into flagellar filaments.

3. What *V. fischeri* chemoreceptors mediate recognition of other known chemoeffectors?

We identified ligands for two *V. fischeri* MCPs and, in doing so, also developed the tools necessary to perform these characterizations for additional chemoreceptors. Further optimization of the chimera technique and its use to examine the remaining MCPs would enhance our understanding of how chemoeffectors are sensed, and define the chemotactic repertoire of *V. fischeri*.

4. How do non-canonical MCP ligand-binding domains sense ligands?

While found in other MCPs across the *Vibrionaceae*, the ligand-binding domains of VfcA and VfcB are distinct from the well-characterized TarH domain of *E. coli* chemoreceptors and it is unknown how these domains recognize specific ligands. As additional MCP-ligand pairs are identified, we will be able to assign function to novel domains found within MCP N-terminal regions, such as the sugar-sensing mediated by VfcB. Mutagenesis of the chimeric MCPs, and subsequent screening for loss of chemoeffector recognition, would allow both identification of critical residues and initial characterization of these non-canonical ligand-binding domains.

FLAGELLAR MOTILITY AND CHEMOTAXIS IN THE SQUID-VIBRIO SYMBIOSIS:

In this thesis, I sought to expand upon the roles of flagellar motility and chemotaxis during symbiotic initiation. Using both genetic and imaging techniques, my studies characterized the physical and chemical cues to which *V. fischeri* cells respond while migrating from aggregates on the surface of the light organ to the deep crypts (Chapter 2, Chapter 3, and Appendix B). Additionally, we identified a novel role for the flagellum in promoting release of the immunogenic molecule LPS, which induces apoptosis, thereby driving the host developmental program (Chapter 5).

Integrating my work and other recent studies, I propose an updated model of symbiotic initiation, focusing on the roles of flagellar motility and chemotaxis (Figure 6-1). Upon passing through the mantle cavity, planktonic *V. fischeri* cells interact with cilia and form aggregates in the host-derived mucus (M. Altura and M. McFall-Ngai, submitted). These cells respond to environment cues and undergo transcriptional changes that prepare them for symbiotic initiation (Figure B-4) (Wang *et al.*, 2010). Aggregates then migrate to the light-organ pores, in a manner independent of flagellar motility (Figure B-1). Cells respond to a host-derived chitobiose gradient by enhancing migration through the pores of the light organ (Mandel *et al.*, 2012), on their way to the deep crypts of the light organ. While cells are undergoing symbiotic initiation, flagellar motility serves to activate host apoptosis, via rotation-mediated LPS shedding (Figure 5-6). Additional chemotactic cues likely mediate migration through the duct and bottleneck (Figures B-2 and B-3). Colonization

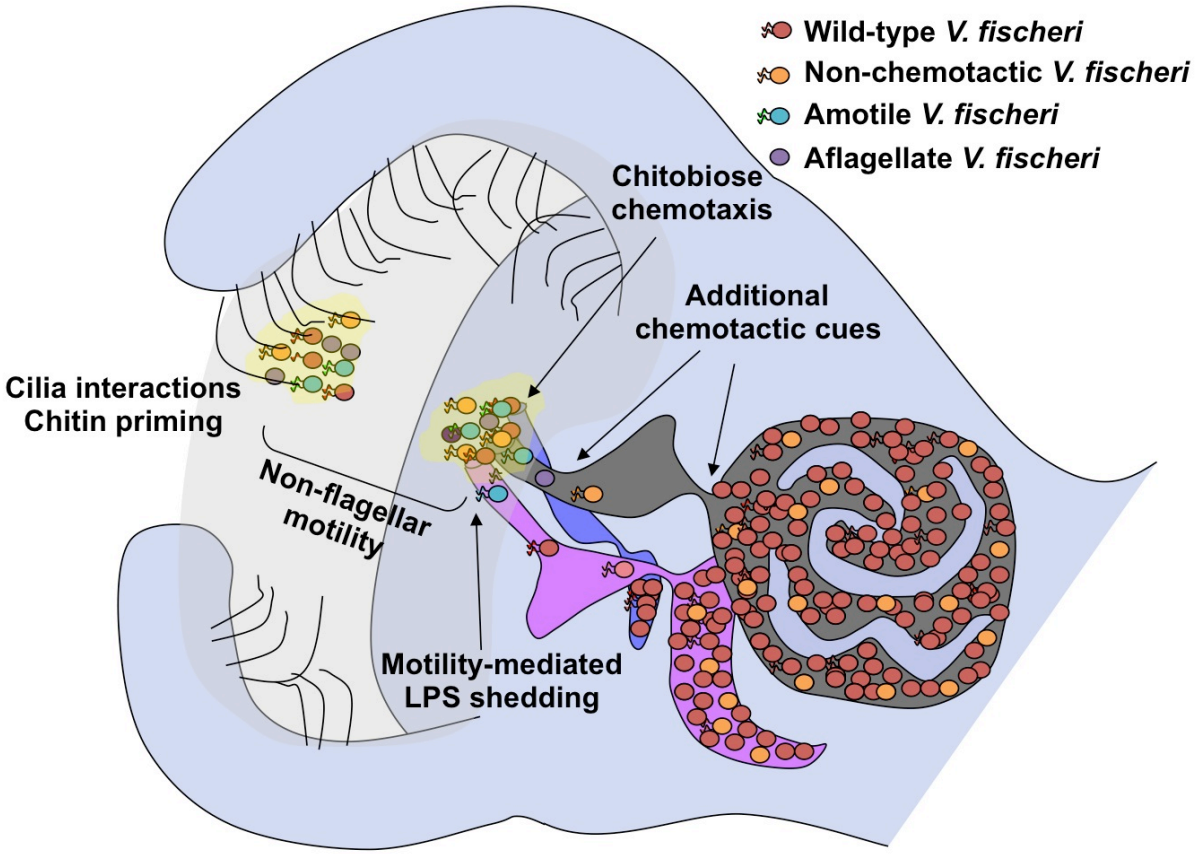

Figure 6-1. Model of motility and chemotaxis behaviors during symbiotic initiation.

of the light-organ crypts is ultimately restricted to motile, chemotactic *V. fischeri* cells and, to a lesser extent, motile, non-chemotactic *V. fischeri* cells (Figure 2-3) (DeLoney-Marino and Visick, 2012).

While it requires further testing, this model highlights the potential complexity underlying symbiotic initiation and niche specificity, even when the entire process occurs in a distance of under 100 μm. Mechanisms of natural initiation are under-studied in studies of host-microbe interactions. As such, the complexity observed during initiation of the squid-vibrio symbiosis continues to illuminate general mechanisms underlying host-microbe interactions and serve as a natural, yet experimentally tractable, mutualism model.

Future directions:

1. What additional chemotactic and motility behaviors mediate symbiotic initiation?

   As described in the model above and in Appendix B, there is evidence for multiple chemotactic signals during migration to the light-organ crypts. These cues can be clarified both by using the flooding techniques that identified the chitobiose gradient (Mandel *et al.*, 2012) and by further characterizing the MCP mutants with altered colonization abilities (Figure B-3). We also showed that flagellar motility is not required for the initial migration of aggregates to the ducts of the light organ. The behavior underlying this stage of initiation could be either host-derived (*e.g.,* driven by

ciliary interactions) or another form of bacterial motility (*e.g.*, twitching motility). This behavior is currently being addressed by another lab member (M-S. Aschtgen).

2. How is LPS released from the sheath during flagellar rotation?

We described the novel phenomenon of flagellar rotation-mediated LPS shedding in Chapter 5. However, it remains unknown whether the LPS is released in micelles or larger outer membrane vesicle (OMV)-like structures that could contain other immunogenic molecules, like flagellin monomers. Additionally, the location of LPS shedding requires clarification: while small vesicles have been observed at the flagellar tip (Millikan and Ruby, 2004), it is also possible that the LPS is released near the base of the flagellum, at the interface between the static basal membrane and the rotating sheath membrane. Microscopic examination of the flagellum, biochemical analysis of OMVs, and biophysical modeling will provide insight into this phenomenon.

3. Does flagellar-mediated LPS release play an immunogenic role in other symbioses?

Flagellar-mediated LPS release is not unique to *V. fischeri*, as we observed reductions in shed LPS from cultures of *Vibrio cholerae* motor mutants (Figure 5-2). However, the extent to which this phenomenon occurs in other bacteria with sheathed flagella, such as *Helicobacter pylori*, has not yet been characterized. The role of LPS shedding

in the host-associated lifestyles of *V. cholerae*, and other bacteria in which flagellar-mediated LPS shedding is observed, can then be studied using their respective animal and cell culture models.

REFERENCES:

Cameron, D.E., Urbach, J.M., and Mekalanos, J.J. (2008) A defined transposon mutant library and its use in identifying motility genes in *Vibrio cholerae*. *Proc Natl Acad Sci U S A* **105**(25): p. 8736-41.

DeLoney-Marino, C.R. and Visick, K.L. (2012) Role for *cheR* of *Vibrio fischeri* in the *Vibrio*-squid symbiosis. *Can J Microbiol* **58**(1): p. 29-38.

DeLoney-Marino, C.R., Wolfe, A.J., and Visick, K.L. (2003) Chemoattraction of *Vibrio fischeri* to serine, nucleosides, and N-acetylneuraminic acid, a component of squid light-organ mucus. *Appl Environ Microbiol* **69**(12): p. 7527-30.

Klose, K.E. and Mekalanos, J.J. (1998) Differential regulation of multiple flagellins in *Vibrio cholerae*. *J Bacteriol* **180**(2): p. 303-16.

Mandel, M.J., Schaefer, A.L., Brennan, C.A., Heath-Heckman, E.A., Deloney-Marino, C.R., McFall-Ngai, M.J., and Ruby, E.G. (2012) Squid-derived chitin oligosaccharides are a chemotactic signal during colonization by *Vibrio fischeri*. *Appl Environ Microbiol* **78**(13): p. 4620-6.

McCarter, L.L. (1995) Genetic and molecular characterization of the polar flagellum of *Vibrio parahaemolyticus*. *J Bacteriol* **177**(6): p. 1595-609.

McGee, K., Horstedt, P., and Milton, D.L. (1996) Identification and characterization of additional flagellin genes from *Vibrio anguillarum*. *J Bacteriol* **178**(17): p. 5188-98.

Millikan, D.S. and Ruby, E.G. (2004) *Vibrio fischeri* flagellin A is essential for normal motility and for symbiotic competence during initial squid light organ colonization. *J Bacteriol* **186**(13): p. 4315-25.

Parales, R.E. and Harwood, C.S. (2002) Bacterial chemotaxis to pollutants and plant-derived aromatic molecules. *Curr Opin Microbiol* **5**(3): p. 266-73.

Post, D.M., Yu, L., Krasity, B.C., Choudhury, B., Mandel, M.J., Brennan, C.A., Ruby, E.G., McFall-Ngai, M.J., Gibson, B.W., and Apicella, M.A. (2012) O-antigen and core carbohydrate of *Vibrio fischeri* lipopolysaccharide: composition and analysis of their role in *Euprymna scolopes* light organ colonization. *J Biol Chem* **287**(11): p. 8515-30.

Studer, S.V., Mandel, M.J., and Ruby, E.G. (2008) AinS quorum sensing regulates the *Vibrio fischeri* acetate switch. *J Bacteriol* **190**(17): p. 5915-23.

Wang, Y., Dunn, A.K., Wilneff, J., McFall-Ngai, M.J., Spiro, S., and Ruby, E.G. (2010) *Vibrio fischeri* flavohaemoglobin protects against nitric oxide during initiation of the squid-*Vibrio* symbiosis. *Mol Microbiol* **78**(4): p. 903-15.

Appendix A

Additional Scientific Contributions

In addition to the work described within this thesis, I performed research that was incorporated into the following four publications:

1. Mandel M.J., Schaefer A.L., Brennan C.A., Heath-Heckman E.A., Deloney-Marino C.R., McFall-Ngai M.J., and Ruby E.G. (2012) Squid-derived chitin oligosaccharides are a chemotactic signal during colonization by *Vibrio fischeri*. *Appl Environ Microbiol*, **78** (13): p. 4620-6.

   Contribution: Working with the *cheA* mutant isolated in Chapter 2, I performed aggregation experiments that showed that this mutant paused outside of the light-organ pore. I also did work characterizing a mutant disrupted in *chiP*, which encodes a porin involved in chitin utilization, that was not included in the paper but had a large impact on the final direction of the study.

2. Post D.M., Yu L., Krasity B.C., Choudhury B., Mandel M.J., Brennan C.A., Ruby E.G., McFall-Ngai M.J., Gibson B.W., Apicella M.A. (2012) O-antigen and core carbohydrate of *Vibrio fischeri* lipopolysaccharide: composition and analysis of their role in *Euprymna scolopes* light organ colonization. *J Biol Chem*, 2012. **287**(11): p. 8515-30.

Contribution: Along with Mark Mandel, I isolated the *waaL*::Tn*erm* mutant as part of the motility screen described in Chapter 2. I was also involved in the initial characterization of this mutant, including motility and LPS analyses.

3. Altura M.A., Heath-Heckman E.A.C., Amani Gillette A., Kremer N., Krachler A.-M., Brennan C.A., Ruby E.G., Orth K., and McFall-Ngai M.J.. First contact: Attachment of few *V. fischeri* cells during symbiosis onset demonstrates exquisite sensitivity of initial partner interactions. Submitted to *Environmental Microbiology*.

   Contribution: I constructed the Δ*mam7* mutant and performed preliminary squid experiments, in conjunction with Natacha Kremer.

4. Kremer N., Philipp E., Carpentier M.-C., Brennan C.A., Kraemer L., Altura M.A., Augustin R., Haesler R., Heath-Heckman E.A.C., Peyer S.M., Schwartzman J., Rader B., Ruby E.G., Rosenstiel P., and McFall-Ngai M.J. Bacteria on the way: molecular conversation during the initiation of the squid-vibrio symbiosis. In preparation for *Cell Host and Microbe*.

   Contribution: I characterized chitin chemotaxis using the capillary chemotaxis assay, work presented as part of Appendix B.

Appendix B

Flagellar Motility and Chemotaxis During Symbiotic Initiation

PREFACE:

CAB and EGR formulated ideas and planned the experiments. CAB performed all experiments and writing.

LOCALIZATION STUDIES:

Amotile *V. fischeri* mutants are unable to colonize the juvenile light organ (Graf *et al.*, 1994, Millikan and Ruby, 2003), suggesting that flagellar motility is required during at a least one stage of symbiotic initiation. Initial studies of bacterial aggregation reported that amotile *V. fischeri* cells were restricted at the earliest stage of initiation and remained in mucus-bound aggregates near the appendages, implicating the use of flagellar motility to migrate to the light-organ pores (Nyholm *et al.*, 2000). We sought to clarify the role of flagellar motility in initiation and observed the migration of GFP-expressing bacteria in real-time using confocal microscopy at later time-points. Surprisingly, flagellar motility mutants were observed at the pores beginning at approximately 4 hours post-inoculation (Figure B-1). Additionally, the presence of a flagellum is not required for this stage of initiation, as even the aflagellate *flrA* and *flgK* cells were able to migrate successfully to the pore, suggesting the flagellum does not serve another function (*i.e.*, as an adhesin). Migration to the light organ pore, therefore, is independent of flagellar motility. Because visualization of later stages of initiation is difficult in live squid, we did not ascertain the precise stage at which amotile mutants are later arrested during colonization. However, in independent studies examining peptidoglycan-treated squid, amotile cells were observed as far as the antechamber (Figure 5-8).

Non-chemotactic strains are able to enter into productive symbioses, achieving populations that make measurable levels of luminescence (Chapter 2). However, colonization by the *cheA* mutant only occurs in a subset of animals and requires a significantly longer exposure time (data not shown). These data suggest that chemotaxis provides a colonization

advantage to initiating *V. fischeri* cells. Because we observed *cheA* cells outside the light-organ pore (Figure B-1E), we sought to determine whether chemotaxis was important at other steps of initiation. We exposed juvenile squid to GFP-expressing *cheA* cells for 24 hours and examined the localization of the *cheA* cells, positing that they would be arrested at stage(s) where sensing of a chemotactic signal is required for migration. Rather than observing aggregate migration in real-time using live squid, as described above, the animals in this experiment were fixed and their tissues stained with rhodamine phalloidin to allow better visualization of the light organ's antechamber and deep crypts. Both wild-type cells and *cheA* cells could be visualized in the deep crypts (Figure B-2). However, we also observed *cheA* cells mislocalized near the appendages, in the duct, and at the bottleneck (Figure B-2CDE). These observations suggest there may be additional chemotactic signals that mediate symbiotic initiation, perhaps different cues at each of these locations. These experiments have revealed a greater level complexity to the model of flagellar motility and chemotaxis behaviors during initiation of the squid-vibrio symbiosis (Figure 6-1).

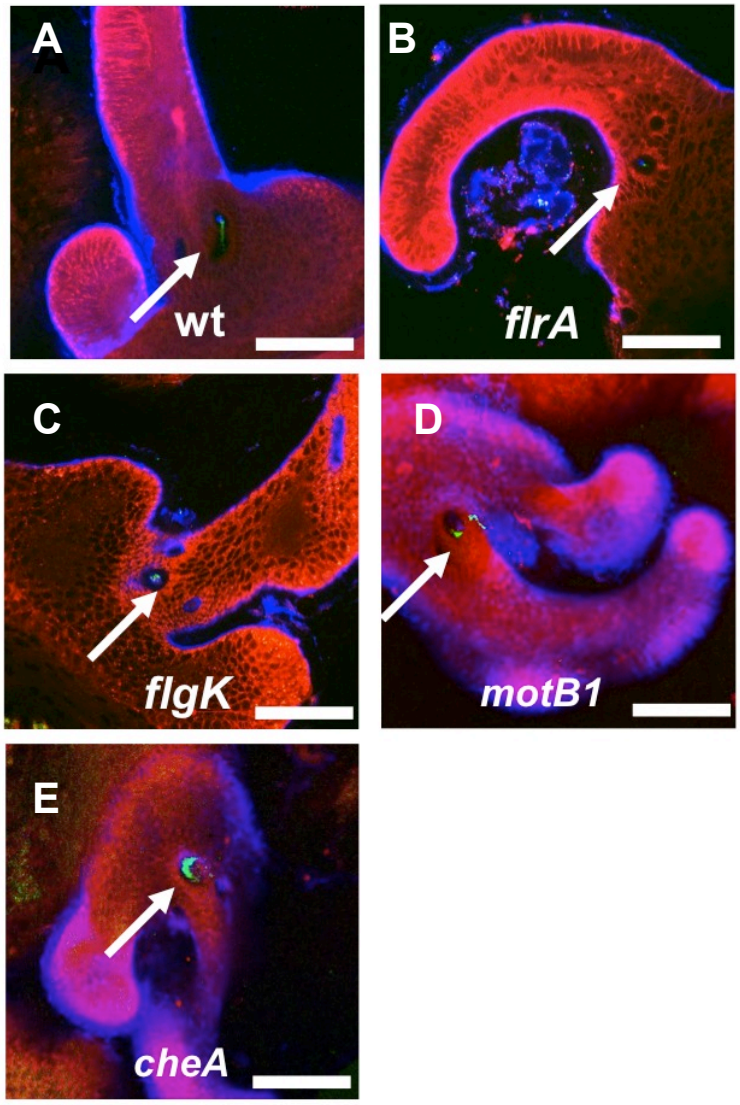

Figure B-1. Pore migration by flagellar mutants.

(A-E) Localization of indicated strains at, or beyond, the pore of the juvenile light organ. WT, wild-type *V. fischeri*. Arrows indicate pores at which aggregates can be observed. After colonization with GFP-labeled bacteria for 3-6 hours, live squid were stained with CellTracker Orange and Alexafluor633-labeled WGA, before examination by LSCM. Scale bars represent 100 μm.

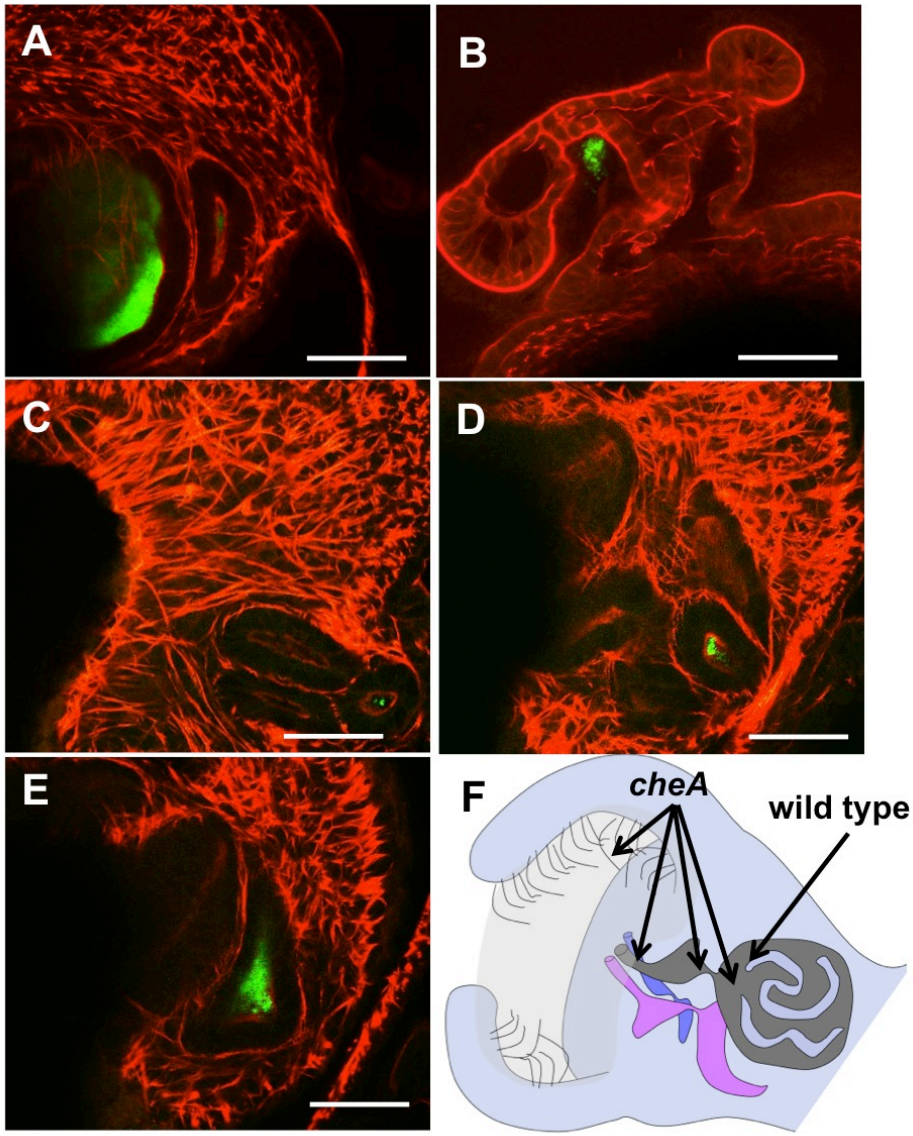

Figure B-2. Localization of the *cheA* mutant at 24 hours after colonization.

While wild-type *V. fischeri* is observed only in the crypts (A), the *cheA* mutant can be observed by the appendages (B), in the duct (C), at the bottleneck (D), as well as within the crypts (E). After colonization with GFP-expressing bacteria for 24 hours, squid were fixed and stained with rhodamine phalloidin, before examination by LSCM. Scale bars represent 50 μm. (F) Model of *cheA* mutant mislocalization.

COLONIZATION BY MCP MUTANTS:

Chemotactic wild-type *V. fischeri* colonizes the juvenile light organ more effectively than non-chemotactic mutants (Chapter 2, data not shown), suggesting that *V. fischeri* responds to specific chemotactic signals during symbiotic initiation. To determine the potential breadth of chemotaxis behavior, w examined 18 of the 19 mutants disrupted in individual MCPs that were generated in Chapter 3, excluding the *vfcA* mutant that was previously characterized (Figure 3-6). We first probed the ability of each mutant to enter into a productive symbiosis in the absence of other bacteria using restrictive colonization conditions, in which wild-type *V. fischeri* only grew to luminous levels in ~70% of squid (Figure B-3A). The *cheA* mutant did not reach luminous levels in any squid under these conditions, suggesting that chemotaxis is essentially required for colonization under these conditions. In contrast, all individual MCP mutants were, to some degree, able to enter into productive symbioses with juvenile squid. The *VF_1117* mutant exhibited the most attenuated phenotype, colonizing only 40% of squid to luminous levels.

We next examined the ability of these MCP mutants to colonize the juvenile squid in the presence of wild-type, chemotactic *V. fischeri* (Figure B-3B). We hypothesized that competitive colonization would exacerbate any defects exhibited by the MCP mutants. In this assay, several mutants were attenuated in this assay, between 3 and 10-fold as compared to wild-type *V. fischeri*: *VF_1133*, *VF_1618*, *VF_2161*, and *VF_A0325*. These mutants must be further examined to determine at what stage of colonization they each develop a competitive disadvantage. We also observed three mutants that were at a competitive advantage:

VF_1652, *VF_A0528*, and *VF_A1072*. While the advantage of these mutants was unexpected, research in *V. cholerae* has shown that, in some cases, chemotaxis behavior can confer a colonization disadvantage (Butler and Camilli, 2004). It is also possible that these MCPs mediate counter-productive chemorepellent responses and, in their absence, the bacteria migrate to the deep crypts more rapidly. These seven consequential MCPs should be further characterized to ascertain their role in symbiotic initiation, and they should also be targeted for ligand identification by the FRET *in vivo* kinase assay (Chapter 4).

As we previously described in Chapter 4, the ligand-binding domain of VfcB was sufficient for recognition of several sugars, including GlcNAc and chitobiose. Because chitobiose acts as a chemoattractant signal for migration through the pore (Mandel *et al.*, 2012), we hypothesized that the *vfcB* mutant would arrest outside the pore and therefore be attenuated in light-organ colonization. However, the *vfcB* mutant has no obvious colonization defect in either single-strain or competitive assays (Figure B-3). As we have yet to show that the *vfcB* mutant is defective in chitobiose chemotaxis in culture, one explanation for these data is that the true ligand of VfcB is not chitobiose, but rather a structurally related molecule. Another possibility is that chitobiose chemotaxis is mediated by more than one MCP, and mutation in a single MCP is not sufficient to significantly decrease chitobiose recognition.

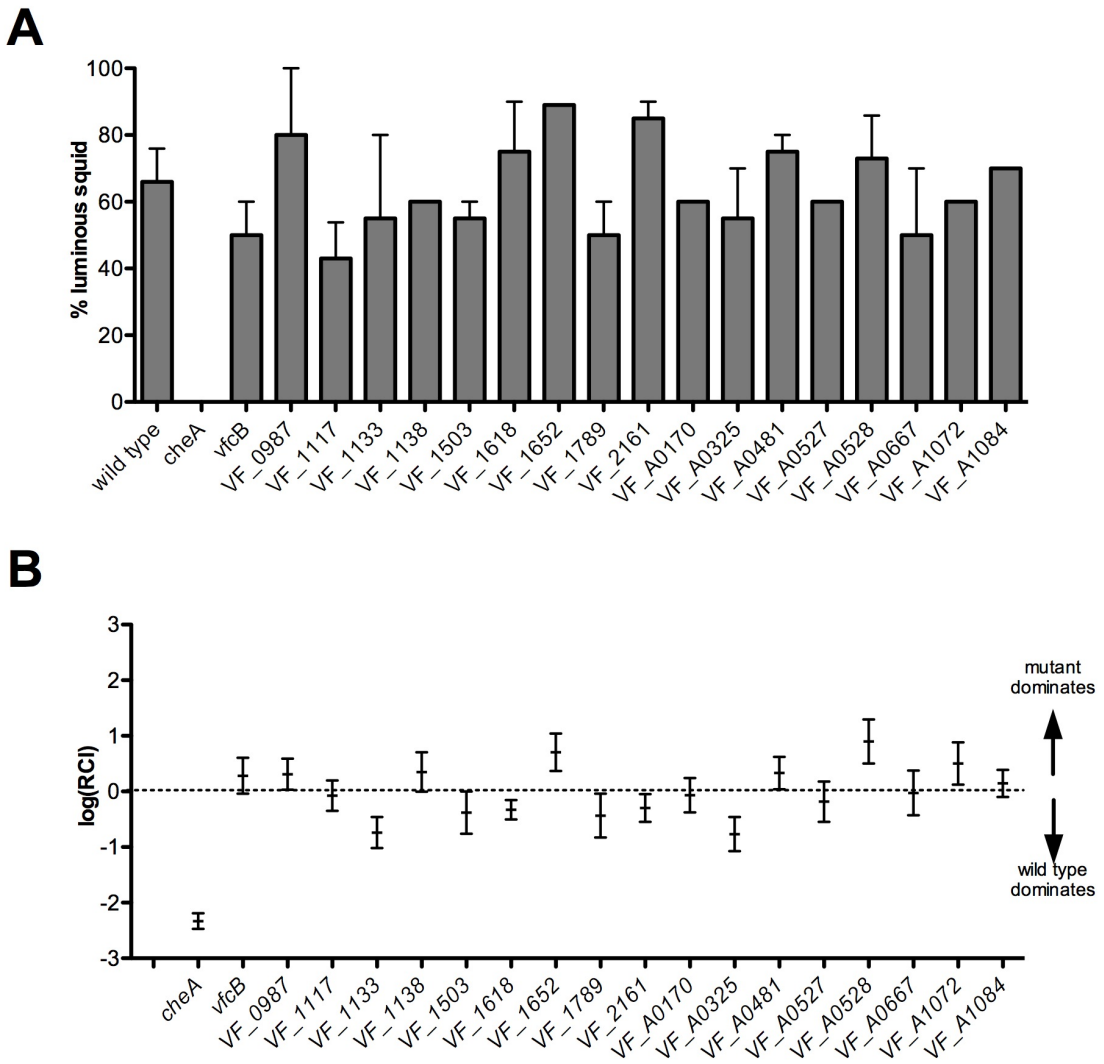

Figure B-3. Single-strain and competitive colonization of juvenile squid by MCP mutants.

(A) Single-strain colonization of juvenile squid by MCP mutants, as scored by luminescence.

(B) Competitive colonization of juvenile squid by MCP mutants. RCI is defined as the (homogenate, mutant/wild type)/(inoculum, mutant/wild type).

CHITIN CHEMOTAXIS:

Host-derived chitobiose serves as a chemotactic signal during migration through the pore of the juvenile light organ (Mandel *et al.*, 2012). However, chitobiose recognition by *V. fischeri* is poorly characterized. We used the capillary assay (Chapter 3) to examine the ability of *V. fischeri* to undergo chemotaxis towards chitobiose. Surprisingly, we found that *V. fischeri* did not respond to chitobiose under the conditions of the assay (data not shown and Figure B-4, no pretreatment). As the cells are prepared for the assay in the same manner used for inoculation of juvenile squid, these data suggest that initiating *V. fischeri* cells might not be able to sense chitobiose upon addition to seawater, and therefore would be unable to migrate through the light-organ pore.

We hypothesized that pre-exposure to chitin derivatives would prime the cells to respond to chitobiose. We examined the response of *V. fischeri* cells to 1 mM chitobiose after pretreatment with signaling levels of either GlcNAc or chitobiose (Figure B-4). While a *cheA* mutant did not respond to any condition (<2000 CFUs/capillary, data not shown), wild-type *V. fischeri* responded strongly to GlcNAc, regardless of pretreatment, but only responded to chitobiose when grown in the presence of chitobiose. While chitobiose exposure is capable of inducing chemoattraction towards chitobiose, it is likely not the only condition able to induce the cells to respond to chitobiose as a chemoattractant. Interestingly, *V. fischeri* cells pause in the host-derived mucus for over an hour before continuing to undergo symbiotic initiation (Nyholm and McFall-Ngai, 1998). We hypothesize that, during this pause, the cells may be

responding to the light-organ environment and inducing transcriptional changes, such as MCP expression, required for subsequent successful migration to the deep crypts.

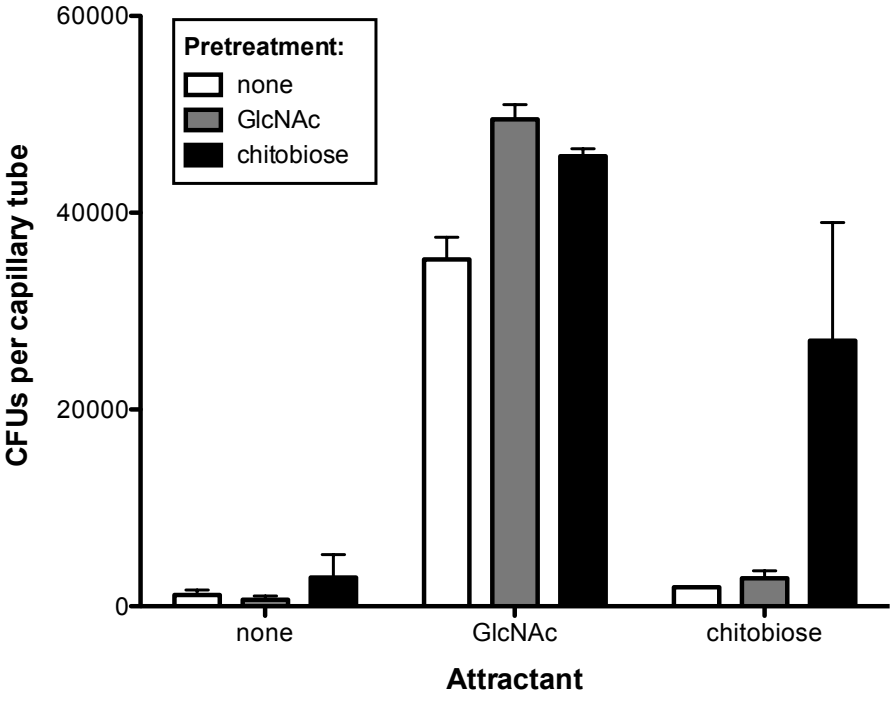

Figure B-4. Chitin chemotaxis in a capillary chemotaxis assay. Chemotactic responses of wild-type *V. fischeri* grown in the presence signaling levels (100 μM) of GlcNAc or chitobiose to 1 mM levels of GlcNAc and chitobiose.

MATERIALS AND METHODS:

Bacterial strains and growth conditions

All *V. fischeri* strains used in this appendix were described previously: *flrA*, *flgK*, *motB1*, and *cheA* in Chapter 2; and the MCP mutants in Chapter 3. Strains harbored pVSV102 (GFP) or pVSV208 (RFP) (Dunn *et al.*, 2006) to fluorescently label cells for certain experiments, as indicated below. Growth media and conditions are defined within these chapters.

Bacterial localization

To visualize the migration of GFP-expressing flagellar mutants in real-time, newly hatched squid were exposed to an inoculum of ~2 X 10^6 CFU per ml of filter-sterilized Instant Ocean (FSIO). At approximately 5 hours post-inoculation, animals were exposed to Cell Tracker Orange CMRA and Alexa Fluor633-conjugated wheat germ agglutinin (Invitrogen Molecular Probes, Carlsbad, CA) to label host tissue and host-derived mucus, respectively. Squid were then anesthetized and examined by laser-scanning confocal microscopy (LSCM) as described previously (Nyholm *et al.*, 2000, Sycuro *et al.*, 2006). Bacterial localization was determined by their expression of GFP.

To identify the stage(s) at which the *cheA* mutant was arrested, squid were exposed to 5,000 CFU/mL of the indicated strain in 100 mL FSIO for 24 hours, at which time they were anesthetized and prepared for confocal microscopy as previously described (Lee *et al.*, 2009).

Rhodamine phalloidin (Invitrogen Molecular Probes) was used to visualize host actin. Light organs were examined by LSCM and bacteria were again located by expression of GFP.

Single-strain and competitive squid colonization

Newly hatched squid were colonized by exposure to approximately 5,000 CFU/mL of the indicated strain(s) in 100 mL FSIO for 3 hours. Squid were then transferred to vials containing 4 mL uninoculated FSIO for an additional 15-18 hours, at which point they were euthanized and surface-sterilized by storage at -80°C. Individual squid were then homogenized, and each homogenate was diluted and plated for CFUs on LBS agar using standard methods (Naughton and Mandel, 2012). In competitive colonization experiments, strains were labeled with either pVSV102 or pVSV208, from which GFP or RFP, respectively, can be expressed. Colonies were then examined under a fluorescence microscopy determine the ratio of the mutant to wild type. The relative competitive index (RCI) for each individual squid was calculated as: (homogenate, mutant CFU/wild-type CFU)/(inoculum, mutant CFU/wild-type CFU).

Capillary chemotaxis assay

Strains were grown in SWT liquid medium supplemented with either 100 μM GlcNAc or chitobiose, as indicated, to an optical density of OD_{600}~0.3, pelleted gently for 5 min at 800 x *g*, and resuspended in H-ASW (100 mM $MgSO_4$, 20 mM $CaCl_2$, 20 mM KCl, 400 mM NaCl, and 50 mM HEPES, pH 7.5). One microliter capillary tubes were sealed at one end, filled with either H-ASW alone or H-ASW containing the indicated attractant, and inserted

into microcentrifuge tubes containing the cell suspension. The tubes were incubated on their side for 5 minutes at room temperature (23-24°C), after which the capillary tubes were removed from the cell suspension and washed. The contents were expelled into 150 μL H-ASW and dilutions were plated for CFUs on LBS plates.

REFERENCES:

Butler, S.M. and Camilli, A. (2004) Both chemotaxis and net motility greatly influence the infectivity of *Vibrio cholerae*. *Proc Natl Acad Sci U S A* **101**(14): p. 5018-23.

Dunn, A.K., Millikan, D.S., Adin, D.M., Bose, J.L., and Stabb, E.V. (2006) New rfp- and pES213-derived tools for analyzing symbiotic *Vibrio fischeri* reveal patterns of infection and *lux* expression in situ. *Appl Environ Microbiol* **72**(1): p. 802-10.

Graf, J., Dunlap, P.V., and Ruby, E.G. (1994) Effect of transposon-induced motility mutations on colonization of the host light organ by *Vibrio fischeri*. *J Bacteriol* **176**(22): p. 6986-91.

Lee, P.N., McFall-Ngai, M.J., Callaerts, P., and de Couet, H.G. (2009) The Hawaiian bobtail squid (*Euprymna scolopes*): a model to study the molecular basis of eukaryote-prokaryote mutualism and the development and evolution of morphological novelties in cephalopods. *Cold Spring Harb Protoc* **2009**(11): p. pdb emo135.

Mandel, M.J., Schaefer, A.L., Brennan, C.A., Heath-Heckman, E.A., Deloney-Marino, C.R., McFall-Ngai, M.J., and Ruby, E.G. (2012) Squid-derived chitin oligosaccharides are a chemotactic signal during colonization by *Vibrio fischeri*. *Appl Environ Microbiol* **78**(13): p. 4620-6.

Millikan, D.S. and Ruby, E.G. (2003) FlrA, a σ^{54}-dependent transcriptional activator in *Vibrio fischeri*, is required for motility and symbiotic light-organ colonization. *J Bacteriol* **185**(12): p. 3547-57.

Naughton, L.M. and Mandel, M.J. (2012) Colonization of *Euprymna scolopes* Squid by *Vibrio fischeri. J Vis Exp* (61).

Nyholm, S.V. and McFall-Ngai, M.J. (1998) Sampling the light-organ microenvironment of *Euprymna scolopes*: description of a population of host cells in association with the bacterial symbiont *Vibrio fischeri*. *Biol Bull* **195**(2): p. 89-97.

Nyholm, S.V., Stabb, E.V., Ruby, E.G., and McFall-Ngai, M.J. (2000) Establishment of an animal-bacterial association: recruiting symbiotic vibrios from the environment. *Proc Natl Acad Sci U S A* **97**(18): p. 10231-5.

Sycuro, L.K., Ruby, E.G., and McFall-Ngai, M. (2006) Confocal microscopy of the light organ crypts in juvenile *Euprymna scolopes* reveals their morphological complexity and dynamic function in symbiosis. *J Morphol* **267**(5): p. 555-68.